Nuclear structure of ^{166}Ho studied in neutron-capture, (d,p), and $(d,^3\mathrm{He})$ reactions

P. Prokofjevs, L. I. Simonova, M. Balodis, J. Bērziņš, and V. Bondarenko
Nuclear Research Center, LV 2169 Salaspils, Latvia

H. F. Wirth, T. von Egidy, C. Doll, J. Ott, and W. Schauer
Technical University of Munich, D-85748 Garching, Germany

R. W. Hoff
Lawrence Livermore National Laboratory, Livermore, California 94550

R. F. Casten
Yale University, New Haven, Connecticut 06520
and Brookhaven National Laboratory, Upton, New York 11973

R. L. Gill
Brookhaven National Laboratory, Upton, New York 11973

J. Honzátko and I. Tomandl
Nuclear Physics Institute, 25068 Řež, Czech Republic

S. Boneva, V. A. Khitrov, and A. M. Sukhovoj
Joint Institute of Nuclear Research, Dubna, Russia

D. G. Burke
Department of Physics and Astronomy, McMaster University, Hamilton, Ontario, Canada L8S 4M1

J. Kvasil and A. Macková
Department of Nuclear Physics, Charles University, V Holešovičkách 2, CS-18000 Praha 8, Czech Republic
(Received 12 August 1999; published 1 March 2000)

The nucleus ^{166}Ho was studied with thermal and average resonance neutron capture and with (d,p) and $(d,^3\mathrm{He})$ reactions. We have devoted a large effort to the measurements of $\gamma\gamma$-coincidence spectra in the broad energy interval 50–6243 keV. From these data and those of previous studies, the level scheme has been developed containing levels grouped into 23 rotational bands below 1 MeV. Of these, six bands are new and several others, known previously, have been modified and expanded based upon our experimental data. In all, 32 new levels have been identified. Of particular note has been the identification of two rotational bands whose underlying structure consists of γ-vibrational states built upon the two lowest energy quasiparticle states in ^{166}Ho. Two new Gallagher-Moszkowski matrix elements were determined: $E_{\mathrm{GM}}(p7/2^-[523]\pm n5/2^-[523]) = -108.5$ keV and $E_{\mathrm{GM}}\{(p7/2^-[523]\pm n7/2^+[633])\mp Q_{22}\} = +138.2$ keV. The resultant level scheme is in good agreement with semiempirical and quasiparticle phonon models where residual interactions have been taken into account. Suggestions are given for further experimentation on ^{166}Ho level structure using existing technology.

PACS number(s): 21.10.−k, 23.20.Lv, 25.40.Hs, 27.70.+q

I. INTRODUCTION

Doubly odd, deformed nuclei offer the unique possibility to obtain information on the proton-neutron interaction at low excitation energies. Two manifestations of this interaction can be observed in the level structure of these nuclei, namely the Gallagher-Moszkowski (GM) energy splitting of spin doublets $K=|\Omega_p\pm\Omega_n|$, where K and Ω are projections of quantum numbers of the total spin and of the odd-particle spin, respectively, and the odd-even energy shifts in the levels of $K=0$ rotational bands (Newby shifts) [1,2]. Over the past several decades, a considerable body of experimental data has been accumulated, especially concerning level structure in the deformed nuclei of the rare-earth region [3]. By assuming appropriate forms for the proton-neutron interaction, one can also calculate values for these matrix elements, E_{GM} and E_N [4]. Comprehensive studies have been made of the parameters that describe the force between unpaired, unlike nucleons in odd-odd deformed nuclei with the goal of optimizing the fit for the matrix elements between theory and experiment [4–6]. Qualitatively, one can say that we have not reached a stage where the theoretical treatments of this problem produce predictive results that can be considered reliable [7]. Thus, it is still important to experimentally determine *n-p* interaction matrix elements by identifying new pairs of GM bands, making these identifications as accu-

rately as possible in order to produce a reliable body of data. Experimental studies need to focus on questions of configuration mixing, both that which occurs among single-particle states and that which occurs between these states and vibrational excitations. Most of the configurations assigned to states in odd-odd nuclei have been of two-quasiparticle nature. A few γ-vibrational states have been observed (e.g., in ^{176}Lu and ^{188}Re) with limited confidence. A comprehensive review of all aspects of the nuclear structure of odd-odd nuclei in the rare-earth region ($144 \leqslant A \leqslant 194$) has been published recently [8].

Excitations of the ^{166}Ho nucleus have been studied previously in a series of measurements involving thermal neutron-capture reactions [9,10] and single-nucleon transfer reactions, i.e., (d,p) [11] and (t,α) [12]. Additional studies have involved averaged-resonance neutron capture [13], polarized neutron capture in polarized targets [14], and conversion-electron measurements following neutron capture [15]. Some data have been derived from β-decay measurements [16,17]. Delayed radiation following the decay of a 185-ms 3^+ isomer of ^{166}Ho at 190.90 keV, which was produced by the ^{165}Ho(d,p) reaction, has been studied [18]. The results of these studies are summarized in previous publications [3,19]. For example, the Nuclear Data Sheets compilation lists 17 rotational bands with assigned configurations in ^{166}Ho. During the past decade or so, several papers have appeared in which the known experimental data for level structure in ^{166}Ho have been subjected to further analysis [15,20–22]. This has resulted in both revised and new configuration assignments, some of which are conflicting and need resolution. The present paper is the first comprehensive report of new experimental measurements of the ^{166}Ho level scheme since those of Kennett, Islam, and Prestwich, published in 1984 [10]. Preliminary reports of some of the data presented in the present paper appeared in Refs. [15,23–25]. Also, the quasiparticle-phonon model calculations of ^{166}Ho, described in Sec. V of this paper, were published in preliminary form in 1992 [26].

A significant part of the present experimental program has been coincidence measurements of γ rays from thermal neutron capture over a broad energy interval, from 50 keV to the neutron binding energy (6243 keV). The $\gamma\gamma$-coincidence spectra were measured in thermal neutron capture reactions at the NRC reactor, Salaspils, Latvia ($E_\gamma = 50$–760 keV), at the NRI reactor, Řež, Czech Republic ($E_\gamma = 100$–6243 keV), and at the JINR reactor, Dubna, Russia (two-step cascades for final levels 0–548 keV). The coincidence data have enabled us to make reliable placements of γ transitions in the ^{166}Ho decay scheme. Previously, all such placements relied upon the Ritz combination principle, a technique whose reliability was somewhat reduced in this case because the ^{166}Ho neutron-capture γ rays, having been measured in the 1960s, were more uncertain than some of the more modern data sets, especially among the higher energy transitions. The level scheme has also been studied via primary γ-ray measurements with averaged-resonance neutron capture at the Brookhaven National Laboratory (BNL) research reactor. In this instance, our new measurements corroborate those of Bollinger and Thomas [13] in virtually every detail. The ^{166}Ho levels were studied with the (d,p) and $(d,^3\mathrm{He})$ reactions at the Tandem Accelerator of the University and Technical University of Munich, Germany, with two times better resolution than in previous (d,p) measurements [11].

As a result of the present measurements, new insights into the band structure of ^{166}Ho have been obtained. We find agreement with an appreciable fraction of the previous measurements, but we also differ significantly on the placement of certain rotational bands and the existence of new levels in the decay scheme.

II. EXPERIMENTS AND RESULTS

A. Averaged resonance neutron capture (ARC) measurements

Primary γ rays following averaged resonance neutron capture (ARC) have been measured with a three-crystal pair spectrometer [27,28] at the Brookhaven High-Flux Beam Reactor. The target consisted of 60 g of Ho_2O_3. Measurements were provided with a neutron beam of 2 keV average energy that was produced by transmission through a scandium filter. Typical γ-ray energy resolution was FWHM $=5.5$ keV at 6.5 MeV. Although it was usual to calibrate the spectrometer with capture lines from a chlorine standard, experimental circumstances did not allow the calibration to be made this way. Instead, the pattern of capture lines to a small number of well-established low- lying levels in ^{166}Ho was identified in the γ spectrum and this match, along with the experimentally known neutron binding energy, 6243.69 ± 0.11 keV [29], allowed calibration of the primary γ rays. The energies and relative intensities of the observed transitions are listed in Table I. All levels from the table are consistent with those reported by Bollinger and Thomas [13] who measured γ rays emitted by an internal Ho target surrounded by a boron absorber in the Argonne National Laboratory $CP-5$ reactor. The boron absorber caused the target to see a $1/E$ neutron spectrum. A large fraction of the levels listed in Table I correspond to levels also defined by secondary γ transitions that depopulate them. In a couple of instances, we were unable to resolve multiplets in the spectrum, those centered at 598 and 660 keV. In a few cases, evidence for an indicated level has not yet been identified in the spectrum of secondary γ rays, e.g., for peaks at 781.6 and 947.1 keV (each energy is uncertain to about ± 1 keV). Peaks at these energies have been identified in our ARC spectrum and in that of Bollinger and Thomas.

The ARC data are analyzed further by plotting the results in the form of reduced γ-ray intensities (I_γ / E_γ^5) versus excitation energy (Fig. 1). Since the ground state of ^{165}Ho has $I^\pi = 7/2^-$, s-wave neutron capture, which is predominant in 2 keV neutron interactions, will populate (capture) states with $I^\pi = 3^-$ or 4^-. The energy width of the neutron beam is sufficient (45%) that capture is spread over at least 100 capture states. Thus, because of statistical averaging, the reduced intensities of primary γ rays of a given multipolarity are found to be more or less equal. The $E1$ γ transitions that dominate the ARC spectrum show greater intensity compared to the $M1$ transitions by a factor of approximately 6. In this experiment, we lack sufficient sensitivity to detect γ

TABLE I. Primary γ rays from 2-keV ARC measurements and level energies in ^{166}Ho derived therefrom.

Adopted values		2-keV ARC data			Indicated spin
E_{lvl} (keV)[a]	I^{π}	E_{γ} (keV)	E_{lvl} (keV)[b]	I_{γ} (rel)[c]	and/or parity
54.2388(7)	2^-	6189.8(4)	53.8(4)	17(2)	$\pi=-$
171.0726(12)	3^-	6072.9(5)	170.8(5)	23(3)	$\pi=-$
180.4686(28)	4^-	6063.4(7)	180.3(7)	20(3)	$\pi=-$
190.9038(20)	3^+	6052.5(2)	191.2(2)	122(5)	$3^+,4^+$
260.6653(23)	4^+	5983.0(1)	260.7(1)	112(6)	$3^+,4^+$
263.7895(23)	5^+	5979.9(1)	263.8(1)	45(6)	$2^+,5^+$
329.777(4)	5^-	5914.0(5)	329.6(5)	24(4)	$\pi=-$
348.2617(26)	5^+	5895.3(2)	348.4(2)	75(5)	$2^+,5^+$
371.9878(25)	4^+	5871.9(2)	371.8(1)	124(5)	$3^+,4^+$
416.016(5)	2^-	5827.6(1)	416.1(0)	13(2)	$\pi=-$
430.040(4)	2^+	5813.5(2)	430.2(2)	72(4)	$2^+,5^+$
431.240(5)	5^-				
464.558(6)	2^+	5779.3(4)	464.4(4)	63(6)	$2^+,5^+$
470.8433(27)	5^+	5772.8(1)	470.8(0)	66(8)	$2^+,5^+$
475.736(7)	3^-	5768.0(1)	475.7(0)	28(8)	$\pi=-$ or $2^+,5^+$
481.854(4)	3^+	5762.0(3)	481.6(3)	83(5)	$2^+,5^+$ or $3^+,4^+$
522.045(5)	3^+	5721.9(2)	521.8(2)	110(7)	$3^+,4^+$
543.684(4)	2^-	5700.0(1)	543.7(0)	18(5)	$\pi=-$
547.934(5)	4^+	5695.7(1)	548.0(0)	71(7)	$2^+,5^+$
558.579(4)	4^+	5685.7(6)	558.0(6)	96(13)	$3^+,4^+$
562.859(7)	4^-	5681.1(10)	562.6(10)	25(13)	$\pi=-$
592.460(9)	3^+	5651.2(2)	592.5(2)	139(8)	$3^+,4^+$
597.027(4)	3^-				
598.511(6)	4^+	5645.2(1)	598.5(0)	106(10)	$3^+,4^+$
605.109(6)	2^+	5638.1(4)	605.6(4)	59(5)	$2^+,5^+$
628.435(12)	2^-	5615.3(1)	628.4(0)	12(8)	$\pi=-$
634.329(4)	5^+	5610.1(6)	633.6(6)	68(9)	$2^+,5^+$
638.229(9)	2^-	5605.5(1)	638.2(0)	20(9)	$\pi=-$
654.802(11)	5^+	5588.8(5)	654.9(5)	54(8)	$2^+,5^+$
658.086(10)	5^-		658.1(15)[d]		$\pi=-$
662.235(7)	3^+	5581.8(9)	661.9(9)	95(13)	$3^+,4^+$
668.019(6)	4^-	5576.2(10)	667.5(10)	25(12)	$\pi=-$
671.750(12)	4^+	5571.5(7)	672.2(7)	84(13)	$2^+,5^+$ or $3^+,4^+$
683.810(5)	3^-	5562.4(9)	681.3(9)	26(4)	$\pi=-$
693.701(6)	5^+	5550.4(3)	693.2(3)	78(5)	$2^+,5^+$
704.947(9)	3^-	5538.2(10)	705.5(10)	14(4)	$\pi=-$
719.44(4)	4^+	5524.0(3)	719.7(3)	99(7)	$3^+,4^+$
725.586(12)	2^-		725.8(15)[d]		$\pi=-$
736.495(8)	4^+	5507.2(3)	736.5(3)	87(6)	$2^+,5^+$ or $3^+,4^+$
742.08(8)	4^-	5501.6(1)	742.1(0)	32(6)	$2^+,5^+$ or $\pi=-$
757.588(10)	5^-	5486.0(1)	757.6(0)	22(11)	$\pi=-$
760.375(7)	3^-	5484.2(1)	759.5(0)	17(11)	$\pi=-$
769.375(7)	5^+	5473.8(3)	769.9(3)	72(6)	$2^+,5^+$
		5462.1(10)	781.6(10)	13(5)	$\pi=-$
		5455.2(7)	788.5(7)	32(8)	$2^+,5^+$ or $\pi=-$
792.98(2)	4^-	5450.7(1)	793.0(0)	30(9)	$\pi=-$ or $2^+,5^+$
806.68(18)	5^+	5437.8(4)	805.9(4)	53(5)	$2^+,5^+$
815.133(9)	3^+	5428.7(2)	814.9(2)	106(6)	$3^+,4^+$
824.58(2)	3^-	5419.1(1)	824.6(0)	32(6)	$2^+,5^+$ or $\pi=-$
832.264(9)	5^+	5411.8(7)	831.9(7)	67(12)	$2^+,5^+$
837.734(8)	4^-	5406.7(13)	837.0(13)	29(12)	$\pi=-$ or $2^+,5^+$
860.55(2)		5383.4(8)	860.3(8)	36(5)	$2^+,5^+$ or $\pi=-$

TABLE I. (*Continued.*)

Adopted values		2-keV ARC data			Indicated spin
$E_{\rm lvl}$ (keV)[a]	I^{π}	E_{γ} (keV)	$E_{\rm lvl}$ (keV)[b]	I_{γ} (red)[c]	and/or parity
868.27(15)	4^-	5374.2(5)	869.5(5)	59(6)	$2^+,5^+$
881.089(19)	3^-	5363.5(1)	880.2(1)	39(6)	$2^+,5^+$ or $\pi=-$
885.39(17)		5358.8(1)	884.9(0)	39(9)	$2^+,5^+$
890.988(12)	4^+	5352.9(3)	890.7(3)	119(8)	$3^+,4^+$
905.60(1)	2^+	5338.5(3)	905.2(3)	83(6)	$2^+,5^+$
925.51(3)	5^+	5318.5(4)	925.1(4)	71(6)	$2^+,5^+$
		5296.6(5)	947.1(5)	51(6)	$2^+,5^+$
961.23(16)	$3+$	5282.5(3)	961.2(3)	96(8)	$3^+,4^+$
978.55(24)		5265.1(5)	978.6(5)	91(10)	$3^+,4^+$
985.15(4)	5^+	5258.8(6)	984.9(6)	63(10)	$2^+,5^+$

[a]The adopted energies and spin-parity assignments listed in columns 1 and 2 were taken from Table II and Nuclear Data Sheets [19].

[b]$I_{\gamma}(\text{red})=I_{\gamma}(\text{reduced})=I_{\gamma}/(E_{\gamma}^5)$; units are arbitrary.

[c]An uncertainty of zero indicates that in the fitting procedure the level energy was fixed at the adopted value in order to derive the best possible intensity.

[d]Peak not resolved in the present data; energy listed taken from Ref. [13].

rays of higher multipole order. Therefore, the 2 keV ARC measurement is expected to populate most strongly states with $I^{\pi}=3^+$ and 4^+, states with $I^{\pi}=2^+$ and 5^+ about a factor of 2 less, and states with $I^{\pi}=(2-5)^-$ about a factor of 6 below the most intense group. The experimental intensities are compared with a calculation based upon a Monte Carlo simulation of the averaging process [30] in Fig. 1.

B. The $\gamma\gamma$-coincidence measurements

The $\gamma\gamma$-coincidence spectra from the ^{165}Ho$(n,\gamma)^{166}$Ho reaction were measured at the IRT reactor of the Nuclear Research Center of the Latvian Academy of Sciences. The thermal neutron beam from the tangential experimental channel was transmitted through a 52 cm thick Si filter. The collimated neutron flux (1×1 cm^2) at the target was 5×10^6 n cm^{-2} s^{-1}. The target material consisting of 0.9 g Ho metal (99% purity) was contained in a thin polyethylene bag. The $\gamma\gamma$ coincidences were recorded using one x-ray Ge detector (10 cm^3) in the energy range 20 to 465 keV and another one of 78 cm^3 in the energy range 59 to 760 keV with the resolutions (FWHM) at 304.6 keV energy of 1.39 keV and of 2.2 keV, respectively. The prompt resolving time was about 23 ns in a wide energy range of 20–1500 keV. The gates were set on the x-ray detector. Two sections of $\gamma\gamma$-coincidence spectra gated on the 116 and 149 keV γ rays are shown in Fig. 2.

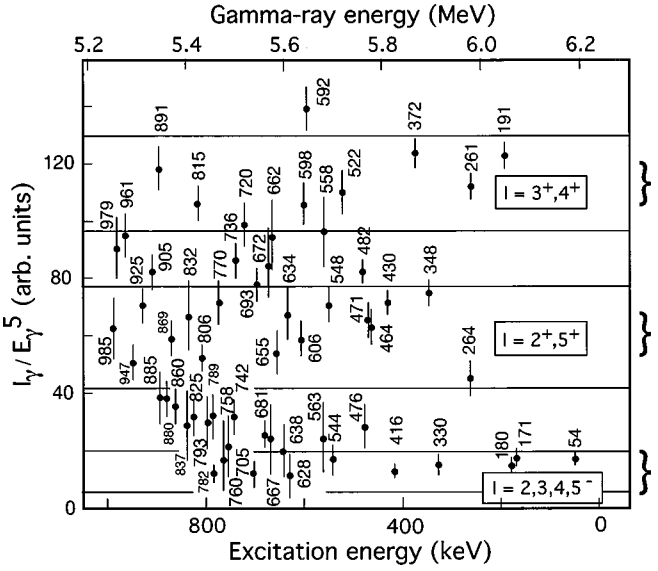

FIG. 1. Reduced γ-ray intensities from 2-keV averaged resonance capture (ARC) measurements (versus excitation energy).

An additional $\gamma\gamma$-coincidence measurement has been carried out at the Nuclear Physics Institute in Řež, Czech Republic, using large Ge-detectors and a neutron guide facility at the 15 MW light-water LVR-15 reactor. The target consisted of 0.464 g Ho_2O_3 (99.99% purity). The spectra were recorded in the range of 100–6243 keV with a 22% HpGe and a 12% Ge(Li) detector. The energy resolutions at 1332 keV were 1.9 and 2.1 keV, respectively. More details about the experimental setup and the data acquisition system are given elsewhere [31]. One section of $\gamma\gamma$- coincidence spectrum for the 239 keV gate is shown on Fig. 3. The results obtained are listed as footnoted entries in Table II that summarizes all of the assigned rotational bands in ^{166}Ho, their component level energies, and the γ transitions that depopulate these levels.

C. Two-step cascades in the (n,γ) reaction

The coincidence technique with pulse-amplitude summation of two-step cascades following thermal neutron capture is a source of information about high-energy and low-energy γ-ray coincidences. Measurements were performed at the IBR-30 pulsed reactor in JINR, Dubna, Russia. Thermal neutron capture was selected by the time-of-flight method. The ^{165}Ho target mass was 4 g. Data acquisition took about 400

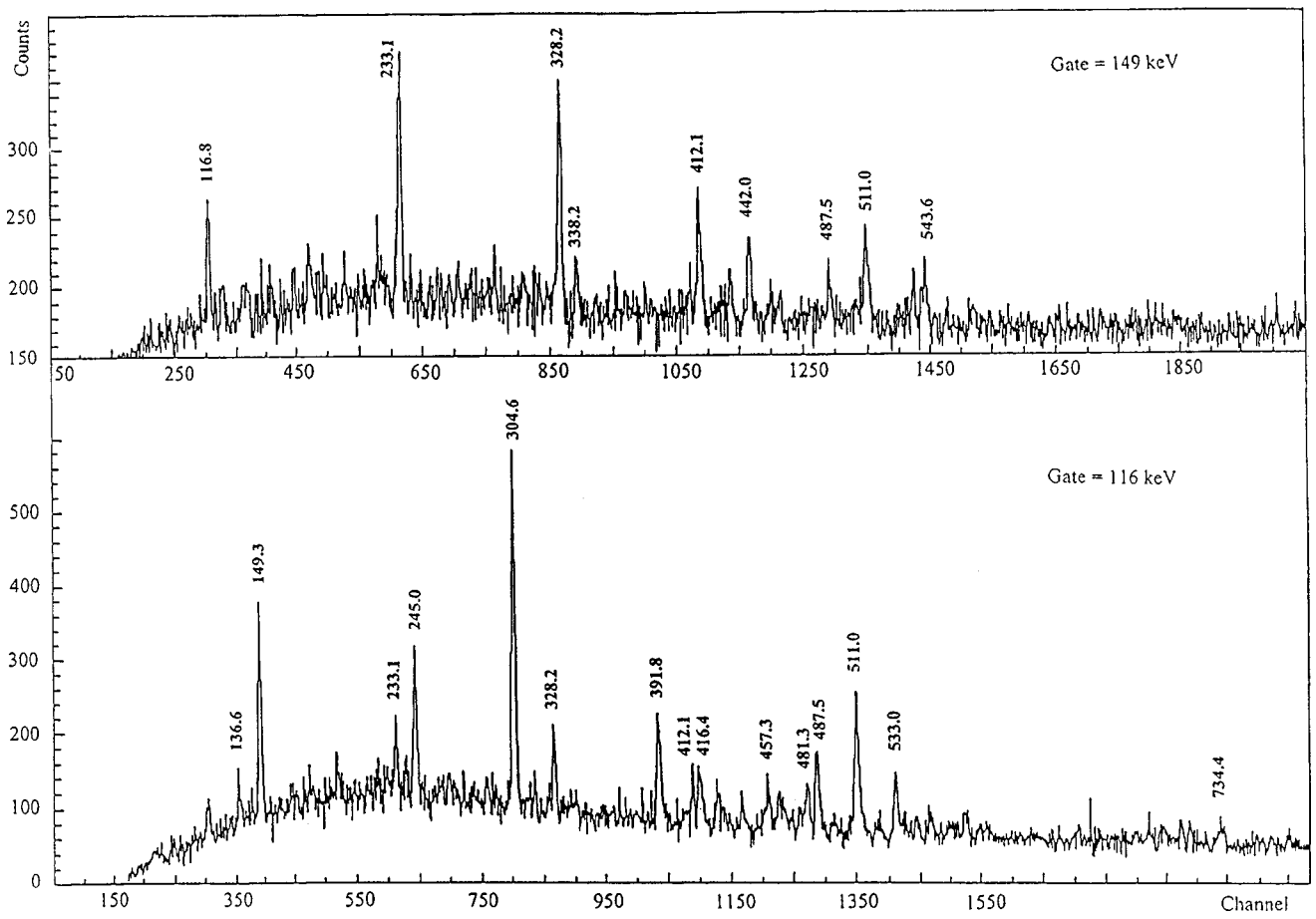

FIG. 2. $\gamma\gamma$-coincidence spectra from gates on the 116 and 149 keV transitions.

h. The spectrometer consisted of a 15% efficient HPGe detector and a 10% efficient Ge(Li) detector with 3–4 keV energy resolution at 1332 keV. The time resolution was 10–12 ns with a ^{60}Co source. To avoid the backscattered gamma quanta a 2.5 g/cm^2 thick lead filter was used. The experimental method and processing procedure have already been described [32,33]. The data processing included off-line construction of spectra of coincidence pulses after summation of their amplitudes. This spectrum (Fig. 4) has peaks, corresponding to all two-step gamma cascades between the compound state and certain low-lying levels. Events selected in each peak on Fig. 4 represent the distribution for two-step cascades which de-excite the compound state via many intermediate states to certain final levels (Fig. 5). The results of these $\gamma\gamma$-coincidence measurements are listed as footnoted entries in Table II. The listed transitions are limited to those two-step cascades that finished at the following final levels (0, 54.3, 82.6, 171.1, 180.5, 191.7, 262.1, 329.9, 348.4, 372.1, 416.2, 430.1, 453.9, 476.1, 522.2, 548.1 keV). The spin difference between the initial and final level of detected cascades is $|J_\lambda - J_f| \leqslant 2$. Only $E1$, $M1$, and $E2$ transitions were detected. Cascade intensities were normalized so that the area of the experimental distribution in interval 520 keV $\leqslant E_\gamma \leqslant (E_{\text{cascade}} - 520$ keV) was 100% for each level where $E_{\text{cascade}} = E_1 + E_2 = B_n - E_{\text{final}}$.

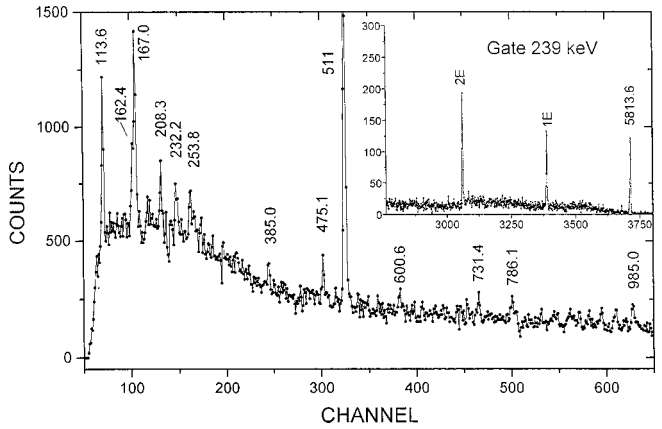

FIG. 3. $\gamma\gamma$-coincidence spectrum from a gate on the 239 keV transition.

D. (d,p) and $(d,^3\text{He})$ reaction measurements

The reaction ^{165}Ho$(d,p)^{166}$Ho was measured with the Q3D spectrograph [34] at the Tandem Accelerator of the University and Technical University of Munich. The ^{165}Ho target had dimensions 0.5 mm×4 mm and thickness 40 μg/cm^2 on a 4 μg/cm^2 thick carbon backing. Spectra were measured at a deuteron energy of 17 MeV at angles of $\Theta_{\text{lab}} = 15°$, 30°, and 45° up to an excitation energy of 1.8 MeV. Altogether twelve overlapping spectra with an energy range

TABLE II. Rotational bands of ^{166}Ho and their depopulating γ rays.

I^π	$E_{\rm lev}(\Delta E)$	$E_\gamma(\Delta E)$	$I_\gamma(\Delta I)$	Mult.	E_f	I^π
		0^- $(7/2^-[523]-7/2^+[633])$ AZ				
0^-	0					
2^-	54.2388(7)	54.2392(7)[c]	2.5(3)	$E2+<20\%M1$	0.0	0^-
1^-	82.4709(19)	82.470(2)[c]	0.97(9)	$M1(+E2)$	0.0	0^-
		28.249(9)	0.040(8)		54.23	2^-
3^-	171.0726(12)	116.835(10)[c]	15.8(15)	$M1+<3\%E2$	54.23	2^-
		88.60(3)	0.03(1)		82.47	1^-
4^-	180.4686(28)	126.228(3)[c]	1.06(10)	$E2(+M1)$	54.23	2^-
		(9.39)[a]			171.07	3^-
5^-	329.777(4)	158.702(9)[c]	0.06(1)		171.07	3^-
		149.307(3)[c]	4.25(42)	$M1(+E2)$	180.46	4^-
6^-	377.808(4)	197.339(8)[c]	0.32(5)	$M1,E2$	180.46	4^-
		48.0315(7)[f]	0.17(3)		329.77	5^-
7^-	557.690(5)	227.88(7)	0.020(4)		329.77	5^-
		179.882(4)[c,d]	0.15(5)[b]	$M1(+E2)$	377.80	6^-
		7^- $(7/2^-[523]+7/2^+[633])$ AZ				
7^-	5.971(12)					
8^-	137.731(13)	131.759(5)	0.14(2)		5.97	7^-
9^-	286.96(10)	280.99(10)	0.03(1)		5.97	7^-
		1^- $(3/2^+[411]-1/2^-[521])$ BY				
1^-	373.158(6)	290.61(3)[c]	1.7(2)	$M1(+E2)$	82.47	1^-
		201.95(3)	0.05(1)		171.07	3^-
2^-	416.016(5)	333.62(2)[c]	1.6(2)	$M1(+E2)$	82.47	1^-
		245.007(7)[c]	1.04(10)	$M1(+E2)$	171.07	3^-
		(43.08)[a]			373.15	1^-
3^-	475.736(7)	420.7(6)[s]	0.16(5)[b]		54.23	2^-
		304.60(2)[c,e]	2.6(2)	$M1(+E2)$	171.07	3^-
		102.55(4)[f]	0.016(3)		373.15	1^-
		(59.62)[a]			416.01	2^-
4^-	562.859(7)	508.4(8)[s]	0.28(8)[b]		54.23	2^-
		391.89(4)[c,e]	1.13(11)		171.07	3^-
		382.8(2)	0.05(1)		180.46	4^-
		233.112(14)[c]	0.63(6)	$M1(+E2)$	329.77	5^-
		146.808(8)[c]	0.09(2)		416.01	2^-
		87.193(15)	0.04(1)		475.73	3^-
5^-	658.086(10)	477.4(3)[c,e]	0.20(5)		180.46	4^-
		328.245(15)[c,e]	0.73(7)		329.77	5^-
		182.302(16)[c]	0.10(1)		475.73	3^-
6^-	788.610(12)	458.74(22)[c]	0.09(3)[b]		329.77	5^-
		225.722(9)	0.070(14)		562.85	4^-
		130.641(16)	0.010(2)		658.08	5^-
		2^- $(3/2^+[411]+1/2^-[521])$ BY				
2^-	638.229(9)	467.3(3)[c]	0.30(10)		171.07	3^-
		265.12(5)[c]	0.18(4)		373.15	1^-
		208.34(4)[c]	0.065(10)		430.04	$2+$
		173.47(12)[c]	0.020(4)		464.55	2^+
		116.197(13)[c]	0.06(1)		522.04	3^+
		94.643(11)[c]	0.20(3)		543.68	2^-

TABLE II. (*Continued*).

I^π	$E_{\rm lev}(\Delta E)$	$E_\gamma(\Delta E)$	$I_\gamma(\Delta I)$	Mult.	E_f	I^π
3^-	704.947(9)	533.5(3)[c]	0.60(20)		171.07	3^-
		288.60(7)[c]	0.12(2)		416.01	2^-
		274.77(7)[c]	0.13(3)		430.04	2^+
		229.00(7)[g]	0.05(2)		475.73	3^-
		161.42(2)	0.030(4)		543.68	2^-
		107.71(3)	0.030(8)		597.02	3^-
		109.241(12)	0.030(6)		595.84	1^-
		99.584(16)	0.020(5)		605.10	2^+
4^-	792.98(2)	612.0(5)	0.30(6)		180.46	4^-
		376.91(14)[c]	0.12(2)		416.01	2^-
		317.28(3)[c]	0.22(4)		475.73	3^-
		230.11(5)[g]	0.030(6)		562.85	4^-
		195.687(14)[c]	0.08(1)		597.02	3^-
		154.71(3)	0.025(5)		638.22	2^-
		5^- $\{(7/2^-[523]+7/2^+[633])-Q_{22}\}$ AZg				
5^-	431.240(5)	425.30(3)	1.3(3)		5.97	7^-
		167.450(5)[c]	0.95(9)	$E1$	263.78	5^+
6^-	529.817(8)	524.2(3)	0.5(1)		5.97	7^-
		266.03(5)[c]	0.28(3)		263.78	5^+
		234.79(5)[c]	0.05(1)		295.08	6^+
		150.268(8)[c]	0.11(2)		379.54	6^+
		98.572(16)	0.04(1)		431.24	5^-
7^-	644.29(6)	506.8(3)	0.20(4)		137.73	8^-
		213.04(6)	0.010(2)		431.24	5^-
		114.50(3)[g]	0.010(2)		529.81	6^-
		2^- $\{(7/2^-[523]-7/2^+[633])+Q_{22}\}$ AZg				
2^-	543.684(4)	543.66(20)[c,e]	2.4(6)		0.0	0^-
		489.39(5)[c,e]	2.0(6)[b]	$E2,M1$	54.23	2^-
		363.10(30)	0.05(1)		180.46	4^-
		170.584(15)[c]	0.05(1)		373.15	1^-
		113.644(4)[c]	0.15(2)		430.04	2^+
3^-	597.027(4)	542.86(20)[c,e]	3.5(9)		54.23	2^-
		425.99(3)[c,d]	0.24(7)[b]		171.07	3^-
		416.47(5)[c]	0.80(16)		180.46	4^-
		224.01(15)	0.010(2)		373.15	1^-
		181.086(5)[c]	0.10(3)[b]		416.01	2^-
		166.983(5)[c]	0.17(2)		430.04	2^+
		132.472(17)[f]	0.030(6)		464.55	2^+
		121.48(3)[f]	0.010(2)		475.73	3^-
		115.167(4)[f]	0.090(1)		481.85	3^+
		53.3434(7)	0.09(1)		543.68	2^-
4^-	668.019(6)	613.8(4)[c,e]	0.7(2)		54.23	2^-
		496.9(2)[c]	0.3(1)		171.07	3^-
		487.58(6)[c,e]	1.3(2)	$M1(+E2)$	180.46	4^-
		338.20(4)[c]	0.15(2)		329.77	5^-
		295.99(8)	0.04(1)		371.98	4^+
		197.11(5)	0.030(6)		470.84	5^+
		192.33(2)[c]	0.07(1)		475.73	3^-
		186.147(6)[c]	0.12(2)		481.85	3^+
		124.350(15)	0.040(8)		543.68	2^-
		120.36(3)	0.010(2)		547.93	4^+
		70.988(10)	0.18(4)		597.02	3^-

TABLE II. (*Continued*).

I^π	$E_{\rm lev}(\Delta E)$	$E_\gamma(\Delta E)$	$I_\gamma(\Delta I)$	Mult.	E_f	I^π
5^-	757.588(10)	577.0(3)[c,e]	0.70(14)		180.46	4^-
		386.3(3)	0.048(8)		371.98	4^+
		380.1(2)	0.05(2)		377.80	6^-
		209.69(4)	0.020(6)		547.93	4^+
		160.63(2)	0.040(8)		597.02	3^-
		99.584(16)[g]	0.020(5)		658.08	5^-
		1^- $(1/2^+[411]+1/2^-[521])$ CY				
1^-	595.841(5)	593.8(7)	0.080(16)		0	0^-
		512.7(3)	0.80(16)		82.47	1^-
		179.882(4)[c,d]	0.10(3)[b]		416.01	2^-
		120.06(2)	0.020(3)		475.73	3^-
2^-	628.435(12)	457.37(7)[c]	0.6(1)		171.07	3^-
		437.3(3)	0.06(1)		190.90	3^+
		255.37(3)[c]	0.09(2)		373.15	1^-
		212.30(6)[g]	0.040(8)		416.01	2^-
		198.31(5)	0.030(6)		430.04	2^+
		152.71(3)	0.025(5)		475.73	3^-
		84.742(14)	0.04(1)		543.68	2^-
3^-	683.810(5)	423.39(18)	0.16(3)		260.66	4^+
		267.82(9)[c]	0.11(2)		416.01	2^-
		253.78(3)[c]	0.12(2)		430.04	2^+
		219.44(6)	0.08(16)		464.55	2^+
		201.95(3)[g]	0.05(1)		481.84	3^+
		140.117(5)[c]	0.35(4)		543.68	2^-
		135.883(4)	0.10(2)		547.93	4^+
		86.765(11)	0.10(2)		597.02	3^-
4^-	742.08(8)	481.31(8)	0.85(17)		260.66	4^+
		412.1(2)[c,d]	0.40(12)[b]		329.77	5^-
		266.53(5)[c]	0.24(5)		475.73	3^-
		198.31(5)[g]	0.03(1)		543.68	2^-
		145.00(3)[c]	0.020(4)		597.02	3^-
		113.644(4)[g]	0.15(2)		628.43	2^-
		$0^-(1/2^+[411]-1/2^-[521])$ CY				
$(0^-$	658.99(3)	285.81(8)[g]	0.06(2)		373.15	$1^-)$
2^-	725.586(12)	643.1(8)	0.4(1)		82.47	1^-
		554.3(4)[c,d]	0.45(14)[b]		171.07	3^-
		352.28(12)[c]	0.130(26)		373.15	1^-
		309.59(6)[c]	0.10(5)		416.01	2^-
		182.04(4)	0.20(4)		543.68	2^-
		97.253(20)	0.0150(3)		628.43	2^-
1^-	774.516(15)	401.31(10)[c]	0.11(3)[b]		373.15	1^-
		358.4(3)[c]	0.05(1)		416.01	2^-
		115.51(3)	0.010(2)		658.99	0^-
		90.720(15)	0.04(1)		683.81	3^-
4^-	868.27(15)	538.6(4)[c]	0.20(6)		329.77	5^-
		392.2(5)[c]	0.11(3)		475.73	3^-
		305.36(15)[c]	0.14(4)		562.85	4^-
3^-	881.089(19)	827.1(3)[e]	0.19(6)		54.23	2^-
		798.6(4)[e]	0.26(8)		82.47	1^-
		709.6(6)[c,e]	0.14(4)		171.07	3^-
		404.7(6)[c]	0.05(2)		475.73	3^-
		242.90(2)	0.17(3)		638.22	2^-

TABLE II. (*Continued*).

I^π	$E_{\rm lev}(\Delta E)$	$E_\gamma(\Delta E)$	$I_\gamma(\Delta I)$	Mult.	E_f	I^π
		155.42(3)[g]	0.025(5)		725.59	2^-
		$3^-(1/2^-[541]-7/2^+[633])$EZ or $(1/2^+[411]+5/2^-[512])$CX				
3^-	760.375(7)	579.9(7)	0.5(3)		180.46	4^-
		570.0(3)	0.20(4)		190.90	3^+
		499.5(4)	0.10		260.66	4^+
		430.31(18)[c]	0.13(3)		329.77	5^-
		216.85(6)	0.040(8)		543.68	2^-
		163.352(7)[c]	0.51(5)		597.02	3^-
		92.355(13)	0.05(1)		668.01	4^-
4^-	837.734(8)	577.0(3)[g]	0.70(14)		260.66	4^+
		169.712(5)[c]	0.240(24)		668.01	4^-
5^-	935.047(17)	174.77(4)	0.020(4)		760.37	3^-
		97.253(20)	0.015(3)		837.73	4^-
		3^+ $(7/2^-[523]-1/2^-[521])$ AY				
3^+	190.9038(20)	136.662(2)[c]	27.5(27)	$E1+<0.3\%M2$	54.23	2^-
		19.840(6)	1.09(5)	$(E1)$	171.07	3^-
		10.43(2)	0.052(5)		180.47	4^-
4^+	260.6653(23)	89.599(13)[c]	0.10(1)		171.07	3^-
		69.7604(14)[c]	2.8(28)	$M1+<30\%E2$	190.90	3^+
5^+	348.2617(26)	157.344(8)[c]	0.21		190.90	3^+
		87.5946(16)[c]	1.24(12)	$M1+<30\%E2$	260.66	4^+
		(18.49)[a]			329.77	5^-
6^+	453.773(4)	193.107(6)[c]	0.19(2)		260.66	4^+
		105.517(4)[c]	0.52(5)	$M1+<30\%E2$	348.26	5^+
7^+	577.216(6)	313.48(6)[g]	0.12(6)		263.78	5^+
		229.00(7)	0.05(1)		348.26	5^+
		123.437(5)[c]	0.10(2)		453.77	6^+
		4^+ $(7/2^-[523]+1/2^-[521])$ AY				
4^+	371.9878(25)	181.086(5)[c]	1.27(13)	$M1(+E2)$	190.90	3^+
		111.324(2)[c]	0.63(6)	$M1(+E2)$	260.66	4^+
		108.199(2)[c]	0.85(8)	$M1(+E2)$	263.78	5^+
5^+	470.8433(27)	279.79(10)	0.03(1)		190.90	3^+
		207.04(2)	0.04(1)		263.78	5^+
		175.73(4)	0.03(1)		295.08	6^+
		122.577(4)	0.09(2)		348.26	5^+
		98.8572(15)	0.56(5)	$E2,M1$	371.98	4^+
		91.286(13)	0.07(2)		379.54	6^+
6^+	588.104(4)	216.160(5)	0.02(1)		371.98	4^+
		134.34(3)	0.02(1)		453.77	6^+
		117.264(3)[d]	0.20(2)		470.84	5^+
7^+	723.256(18)	208.90(4)[g]	0.030(6)		514.36	7^+
		135.15(2)	0.040(7)		588.10	6^+
		5^+ $(3/2^+[411]+7/2^+[633])$BZ+$(7/2^-[523]+3/2^-[521])$AU				
5^+	263.7895(23)	257.81(2)	0.26(4)	$M2(+E1)$	5.97	7^-
		72.8859(15)	0.20(4)	$E2+M1$	190.90	3^+
		3.13[a]	0.01[b]		260.66	4^+
6^+	379.549(4)	373.47(7)	0.45(7)		5.97	7^-
		115.759(3)	0.34(5)		263.78	5^+
		84.468(10)[f]	0.13(3)		295.08	6^+
7^+	514.363(7)	250.49(9)	0.07(2)		263.78	5^+
		134.815(6)	0.06(1)		379.54	6^+

TABLE II. (*Continued*).

I^π	$E_{\rm lev}(\Delta E)$	$E_\gamma(\Delta E)$	$I_\gamma(\Delta I)$	Mult.	E_f	I^π
		$2^+(7/2^-[523]-3/2^-[521])$AU+$(3/2^+[411]-7/2^+[633])$ BZ				
2^+	430.040(4)	239.140(11)[c,e]	4.2(4)	$M1(+E2)$	190.90	3^+
		169.45(3)	0.020(4)		260.66	4^+
3^+	481.854(4)	291.04(8)	0.12(2)		190.90	3^+
		221.174(9)[c,e]	3.9(4)	$M1(+E2)$	260.66	4^+
		109.887(18)	0.020(5)		371.98	4^+
		51.8155(7)	0.23(3)		430.04	2^+
4^+	547.934(5)	357.04(4)	0.29(6)		190.90	3^+
		287.24(3)[c]	0.17(2)		260.66	4^+
		199.71(8)[c]	0.80(8)	$M1(+E2)$	348.26	5^+
		175.98(2)	0.07(1)		371.98	4^+
		66.103(7)[f]	0.20(4)		481.85	3^+
5^+	634.329(4)	180.545(5)[c]	0.20(3)	$M1(+E2)$	453.77	6^+
		152.45(3)	0.016(5)		481.85	3^+
		86.359(11)	0.10(3)		547.93	4^+
		75.753(16)	0.07(2)		558.57	4^+
		46.232(4)	0.020(4)		588.10	6^+
6^+	732.549(14)	278.69(10)	0.06(2)		453.77	6^+
		155.42(3)	0.025(5)		577.21	7^+
		98.200(15)[c]	0.030(10)		634.32	5^+
		6^+ $(7/2^-[523]+5/2^-[512])$ AX				
6^+	295.088(9)	289.120(15)[c]	2.3(2)	$E1$	5.97	7^-
7^+	423.654(10)	285.81(8)	0.06(2)		137.73	8^-
		159.89(3)	0.010(1)		263.78	5^+
		128.566(5)[c]	0.14(2)		295.08	6^+
		1^+ $(7/2^-[523]-5/2^-[512])$ AX				
1^+	426.090(5)	425.99(3)[c,d]	3.5(1.0)[b]		0.0	0^-
		371.75(3)[c]	3.0(3)	$E1$	54.23	2^-
		343.51(3)	0.39(8)		82.47	1^-
2^+	464.558(6)	410.27(2)[c]	1.36(26)		54.23	2^-
		293.42(8)	0.07(1)		171.07	3^-
		273.64(7)	0.16(3)		190.90	3^+
		48.303(4)[f]	0.030(6)		416.01	2^-
		38.493(6)[f]	0.03(1)	$M1(+E2)$	426.09	1^+
3^+	522.045(5)	341.57(3)	0.28(6)		180.46	4^-
		261.31(7)	0.04(1)		260.66	4^+
		95.953(2)[f]	0.12(1)		426.09	1^+
		57.517(8)[f]	0.32(6)		464.55	2^+
4^+	598.511(6)	427.0(2)[c,d,e]	0.27(8)[b]		171.07	3^-
		418.08(18)[c,e]	0.20(6)		180.46	4^-
		268.15(9)[c]	0.07(2)		329.77	5^-
		134.00(3)	0.010(2)		464.55	2^+
		76.4663(14)	0.34(3)		522.04	3^+
5^+	693.701(6)	512.7(3)[e]	0.03[b]		180.46	4^-
		171.67(3)	0.030(6)		522.04	3^+
		95.190(3)[c]	0.25(4)		598.51	4^+
6^+	807.074(10)	113.373(3)	0.12(2)		693.70	5^+
		4^+ $(7/2^-[523]+1/2^-[510])$ AT				
4^+	558.579(4)	367.54(16)	0.07		190.90	3^+
		297.90(3)[c]	0.39(8)	$M1(+E2)$	260.66	4^+
		263.36(5)	0.12(2)		295.08	6^+
		210.300(6)	0.30(5)		348.26	5^+

TABLE II. (*Continued*).

I^π	$E_{\rm lev}(\Delta E)$	$E_\gamma(\Delta E)$	$I_\gamma(\Delta I)$	Mult.	E_f	I^π
		186.582(6)[c]	0.28(3)		371.98	4^+
		83.049(14)[f]	0.05(4)		475.73	3^-
		76.7258(14)[f]	0.19(3)		481.85	3^+
5^+	654.802(11)	463.9(3)	0.6(1)		190.90	3^+
		394.50(20)	0.10(2)		260.66	4^+
		359.7(2)	0.08(2)		295.08	6^+
		306.49(3)[c]	0.24(5)		348.26	5^+
		282.80(8)	0.06(2)		371.98	4^+
		201.08(3)	0.040(8)		453.77	6^+
		183.96(4)	0.050(7)		470.84	5^+
		96.265(20)	0.020(6)		558.57	4^+
6^+	771.77(8)	442.17(8)[c]	0.25(7)[b]		329.77	5^-
		423.39(18)[c,g]	0.16(3)		348.26	5^+
		117.264(3)[c,d]	0.20(2)		654.80	5^+
		3^+ $(7/2^-[523]-1/2^-[510])$ AT				
3^+	815.072(10)	624.0(4)[c,e]	0.6(2)		190.90	3^+
		554.3(3)[e,g]	0.15(5)[b]		260.66	4^+
		442.9(3)[c,e]	0.4(1)		371.98	4^+
		388.8(3)[c]	0.08(3)[b]		426.09	1^+
		385.0(2)[c]	0.040(8)		430.04	2^+
		350.61(12)[c]	0.07(1)		464.55	2^+
		267.19(5)[c]	0.28(6)		547.93	4^+
		256.60(2)[c]	0.26(4)	$M1(+E2)$	558.57	4^+
		222.634(7)[c]	0.22(2)		592.46	3^+
4^+	890.988(12)	236.31(8)[c,g]	0.03(1)		654.80	5^+
		75.985(8)	0.07(2)		815.07	3^+
5^+	985.15(4)	313.48(6)[g]	0.12(6)		671.75	4^+
		215.44(9)	0.010(2)		769.54	5^+
		170.09(3)	0.030(6)		815.07	3^+
6^+	1098.61(21)	(d,p) data; no γ transitions identified				
		1^+ $(7/2^-[523]-5/2^-[523])$ AV				
1^+	567.654(6)	194.529(10)[c]	0.13(2)		373.15	1^-
		151.533(9)[c]	0.08(1)		416.01	2^-
		141.599(7)[c]	0.13(1)		426.09	1^+
		(137.51(2))	0.020(7)		430.04	2^+
		103.116(15)	0.050(7)		464.55	2^+
2^+	605.109(6)	433.92(18)[c]	0.17(3)		171.07	3^-
		231.957(14)[c]	0.24(5)		373.15	1^-
		188.98(3)[c]	0.07(1)		416.01	2^-
		179.032(6)[c]	0.25(4)		426.09	1^+
		140.544(10)[c]	0.090(9)		464.55	2^+
		129.353(7)[c]	0.08(2)		475.73	3^-
		83.049(14)	0.05(1)		522.04	3^+
3^+	662.235(7)	607.7(7)	0.11(2)		54.23	2^-
		472.2(5)	0.14(3)		190.90	3^+
		246.07(2)[c]	0.20(4)		416.01	2^-
		236.31(8)[g]	0.03(1)		426.09	1^+
		232.286(9)[c]	0.06(3)[b]		430.04	2^+
		197.677(10)[c]	0.20(3)		464.55	2^+
		118.49(2)	0.030(6)		543.68	2^-
		94.529(11)	0.04(1)		567.65	1^+
		57.19(1)	0.16(3)		605.10	2^+

TABLE II. (*Continued*).

I^π	$E_{\rm lev}(\Delta E)$	$E_\gamma(\Delta E)$	$I_\gamma(\Delta I)$	Mult.	E_f	I^π
4^+	736.495(8)	564.8(3)[g]	0.20(4)		171.07	3^-
		475.8(3)	0.15(3)		260.66	4^+
		406.83(16)[c]	0.13(3)		329.77	5^-
		260.75(2)[c]	0.16(2)		475.73	3^-
		214.442(9)[c]	0.22(4)		522.04	3^+
		137.99(4)	0.007(1)		598.51	4^+
		131.41(3)	0.010(2)		605.10	2^+
		74.261(16)	0.09(3)		662.23	3^+
5^+	832.264(9)	284.26(12)[c]	0.08(3)		547.93	4^+
		233.79(5)[c]	0.12(2)		598.51	4^+
		170.09(3)	0.010(2)		662.23	3^+
		95.767(3)[c]	0.090(9)		736.49	4^+
6^+	942.605(13)	206.15(2)[g]	0.050(7)		736.49	4^+
		110.327(12)	0.040(8)		832.26	5^+
		$6^+(7/2^-[523]+5/2^-[523])$ AV				
6^+	722.00(15)	426.89(15)[c]	0.13(4)[b]		295.08	6^+
7^+	848.49(21)	553.37(21)[c]	0.07(2)[b]		295.08	6^+
		3^+ $(1/2^+[411]-7/2^+[633])$ CZ				
3^+	592.460(9)	412.1(2)[c,d,e]	0.20(6)[b]		180.46	4^-
		401.56(6)[c,e]	2.1(3)	$(M1,E2)$	190.90	3^+
		331.88(3)[c]	0.27(4)		260.66	4^+
		162.452(10)[c]	0.06(1)		430.04	2^+
4^+	671.750(12)	411.09(3)[c]	0.75(25)		260.66	4^+
		323.42(7)	0.12(2)		348.26	5^+
		299.88(17)	0.030(6)		371.98	4^+
		241.76(5)	0.05(1)		430.04	2^+
		218.00(6)	0.040(8)		453.77	6^+
		189.89(5)	0.010(2)		481.85	3^+
		123.81(2)	0.010(2)		547.93	4^+
		113.17(2)	0.020(4)		558.57	4^+
		16.97[a]	0.013		654.80	5^+
5^+	769.549(16)	509.0(2)[c]	0.50(15)[b]		260.66	4^+
		(421.13(5)[c,e]	0.28(8)[b]		348.26	5^+)
		390.0(2)	0.18(4)		379.54	6^+
		316.10(9)[g]	0.090(18)		453.77	6^+
		247.68(9)	0.03(1)		522.04	3^+
6^+	884.055(14)	212.30(6)[g]	0.040(8)		671.75	4^+
		164.570(40)	0.02(0)		719.44	4^+
		114.50(3)[g]	0.010(2)		769.54	5^+
		4^+ $(1/2^+[411]+7/2^+[633])$ CZ				
4^+	719.44(4)	455.60(6)[c,e]	0.50(25)[b]	$M1(+E2)$	263.78	5^+
		347.24(8)[c]	0.20(4)		371.98	4^+
		248.77(9)	0.06(1)		470.84	5^+
5^+	806.68(18)	546.0(5)[e]	0.020(6)		260.66	4^+
		433.9(9)[e]	0.015(5)		371.98	4^+
		335.61(8)	0.62(12)		470.84	5^+
		324.74(7)	0.11(2)		481.85	3^+
(6^+	911.40(4)	191.961(11)	0.13(2)		719.44	4^+)

TABLE II. (*Continued*).

I^π	$E_{\rm lev}(\Delta E)$	$E_\gamma(\Delta E)$	$I_\gamma(\Delta I)$	Mult.	E_f	I^π
		$2^+(7/2^-[523]-3/2^-[521])$ AU				
2^+	905.60(1)	733.94(21)[c,e]	0.024(7)		171.07	3^-
		714.7(2)[c,e]	0.26(8)		190.90	3^+
		475.8(3)[c]	0.15(3)		430.04	2^+
		312.90(8)[c]	0.12(6)		592.46	3^+
		145.228(7)	0.140(14)		760.37	3^-
3^+	961.23(16)	700.8(3)[e]	0.06(2)		260.66	4^+
		542.8(8)[e]	0.006(2)		416.01	2^-
		534.9(4)[c]	0.30(6)		426.09	1^+
4^+	1030.47(23)	858.0(5)[c,e]	0.04(1)		171.07	3^-
		849.5(7)[e]	0.015(5)		180.46	4^-
		839.9(7)[e]	0.13(4)		190.90	3^+
		770.5(4)[e]	0.06(2)		260.66	4^+
		701.1(5)[c,e]	0.016(5)		329.77	5^-
		600.8(7)[c,e]	0.024(6)		430.04	2^+
		5^+ $(7/2^-[523]+3/2^-[521])$ AU				
5^+	925.51(3)	661.0(6)[g]	0.6(2)		263.78	5^+
		206.15(2)[c]	0.050(7)		719.44	4^+
6^+	1038.43(20)	(d,p) data; no γ transitions identified				

[a]Transition not observed; placement suggested by $\gamma\gamma$-coincidence data.
[b]I_γ estimated by taking into account coincidence data.
[c]Low-energy $\gamma\gamma$ coincidence.
[d]Doublet.
[e]High-energy $\gamma\gamma$ coincidence.
[f]γ-transition intermediate between coincident $\gamma\gamma$ transitions.
[g]Multiply placed γ transition.

of nearly 700 keV in each case were taken. The data recorded at different angles were normalized to the number of deuteron elastic-scattered events counted by a monitor detector mounted in the target chamber. An energy resolution of approximately 5 keV FWHM was obtained. A representative spectrum taken at $\Theta_{\rm lab}=30°$ is shown in Fig. 6. The decomposition of multiple peaks at 426 keV in the (d,p) spectrum is shown in Fig. 7. For the measurements a proportional chamber with cathode strip read-out and a scintillator [35] were used to record the spectrum. For high resolution each cathode strip is connected to its own preamplifier and ADC. The energy scale was calibrated with level energies from the Nuclear Data Sheets [19]. The experimental relative intensities in Table III are listed in arbitrary units.

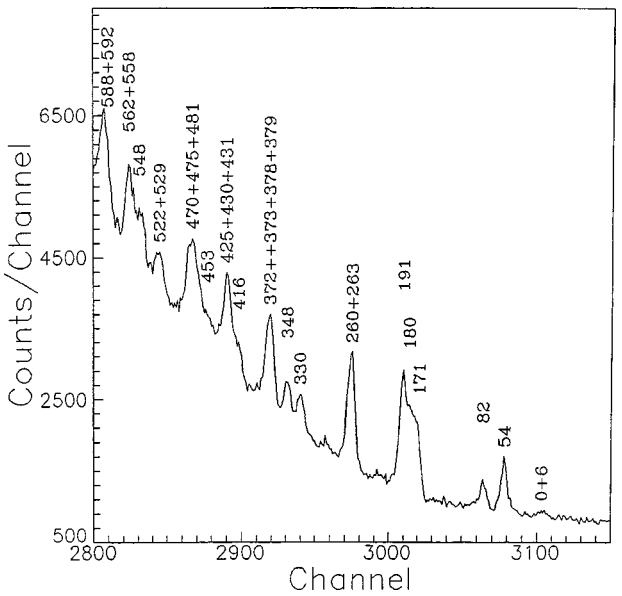

FIG. 4. Spectrum of coincident pulses after their amplitude summation in the high-energy-low-energy coincidence measurements.

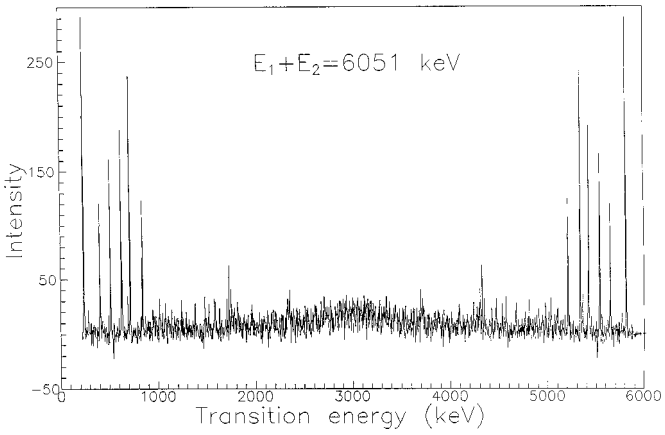

FIG. 5. Spectrum of γ rays with the condition that the two-step gamma-ray cascades go to the level at 190.9 keV.

TABLE III. Spectroscopy of ^{166}Ho via the (d,p) reaction ($E=17$ MeV).

			Intensity I_p (rel)[b]						Intensity I_p (rel)[b]		
J^{π} [a]	E_{lev} (keV)[a]	E_{expt} (keV)	15°	30°	45°	J^{π} [a]	E_{lev} (keV)[a]	E_{expt} (keV)	15°	30°	45°
7^-	5.971(12)	6.21(25)	5.0(7)	17.0(41)	6.1(8)	5^+	806.68(18)				
2^-	54.2388(7)	54.3(4)	2.4(6)		3.3(7)	6^+	807.32(5)	807.01(16)	10.1(18)	10.4(12)	6.9(12)
1^-	82.4709(19)	82.6(11)	1.2(4)			3^+	815.072(10)	814.86(27)	213(5)[g]	133(4)[g]	99(5)[g]
8^-	137.731(13)	138.02(16)	8.4(11)	21.1(18)	20.7(18)	6^+	820.65(2)	819.06(20)	19(4)[g]	17(3)[g]	17(2)[g]
3^-	171.0726(12)	171.42(26)	3.2(8)	9.0(11)	5.2(8)	3^-	824.550(16)	824.6(4)	8.3(14)		
4^-	180.4686(28)	180.62(19)	5.8(11)	12.9(18)	9.8(9)	5^+	832.264(9)	831.44(23)	3.9(8)	4.6(11)	5.9(11)
3^+	190.9038(20)	190.87(8)	373(11)	267(60)	126(4)		836.7[h]	837.9(3)	3.3(8)	3.0(9)	3.5(10)
4^+	260.6653(23)	260.67(11)	152(6)[c]	122(9)[c]	80(7)[c]	7^+	848.49(21)	848.46(16)	5.1(18)	13.7(18)	7.7(9)
5^+	263.7895(23)	264.65(27)	21(5)[c]	39(6)[c]	23(6)[c]	6^+	884.055(14)	884.0(6)			3.6(8)
9^-	286.96(10)	287.5(5)	7.4(28)	8.7(18)	12.9(32)	4^+	890.988(12)	890.64(17)	140(5)	126(10)	82(3)
6^+	295.088(9)	295.42(11)	92(5)	137(6)	69(4)			895.5(6)	12(3)	12(3)	10.5(18)
5^-	329.777(4)	329.83(24)	3.4(10)	9.2(18)	22.5(30)	2^+	905.60(1)	904.64(13)	36(3)	54(4)	23(1)
5^+	348.2617(26)	348.28(10)	41(2)	58(4)	65(4)	6^+	911.40(4)	911.40(28)		6.2(11)	4.7(8)
4^+	371.9878(25)	372.1(4)	540(8)	400(9)	213(4)	$2^+,5^+$	925.51(3)	925.21(16)		46(4)	22(1)
6^-	377.808(4)					3^+	961.23(16)	961.23(16)		26(2)	11.6(12)
		378.90(20)	88(4)	110(5)	77(3)	$3^+,4^+$	979.542(27)	978.55(24)	32(2)	37(3)	20(2)
6^+	379.549(4)					5^+	985.14(15)	985.74(18)	46(3)	49(5)	38(2)
		384.23(16)	12(3)	18(4)	12.4(18)	$3^+,4^+$	1004.82(5)	1003.8(6)		4.5(9)	1.8(8)
7^+	423.654(10)	423.58(20)	120(7)[d]	144(7)[d]	70(4)[d]	$2^+,5^+$	1010.66(3)	1009.8(4)	3.9(9)	6.3(10)	3.8(9)
1^+	426.090(5)	426.04(20)	15(6)[d]	49(6)[d]	35(4)[d]	4	1030.47(23)	1030.3(2)	16.1(14)	14.3(13)	8.8(10)
2^+	430.040(4)	430.5(5)	29(4)[e]	22(3)	15.6(18)			1038.4(3)	13.3(14)	19.8(18)	12.3(11)
6^+	453.77(4)	453.77(10)	19(5)[e]	36(3)	28(2)	$2^+,5^+$	1054.83(22)	1055.4(4)	15.6(23)		9.9(10)
2^+	464.558(6)	464.50(13)	56(5)	109(6)	54(3)	3	1087.87(5)	1088.6(7)	14.4(12)		2.3(7)
5^+	470.8433(27)	470.88(25)	111(7)	135(6)	72(3)	6^+	1097.43(6)	1098.6(7)	8.9(12)		8.2(10)
3^-	475.736(7)	476.5(4)			12(2)[e]	3,5	1114.647(20)	1114.7(8)	4.5(11)		3.3(8)
3^+	481.854(4)	482.2(6)			4.6(14)[e]		1131.0(3)	1130.4(10)	3.3(10)		6.5(6)
7^+	514.363(7)	514.42(15)	54(3)	84(4)	48(3)		1137.75(14)	1138.4(10)	5.4(12)	8.4(13)	8.3(6)
3^+	522.045(5)	522.1(4)	84(4)	139(5)	80(3)	1^+	1150	1148.5(11)	6.9(13)	7.5(12)	6.0(8)
6^-	529.817(8)	529.01(24)	10(2)	11(2)	11(2)	4^+	1161.30(4)	1161.1(11)	2.2(11)		1.9(5)
4^+	547.934(5)	547.96(5)	83(4)	58(3)	38(2)			1168.4(11)	3.7(13)	8.7(2)	4.7(6)
4^+	558.579(4)	558.55(9)	114(4)[f]	86(4)[f]	62(3)[f]		1174.9(6)	1174.0(11)	23(2)	26(2)	14.7(9)
4^-	562.859(7)	562.6(4)	16(4)[f]				1190.09(5)	1190.1(14)	8.3(14)	10.6(13)	4.9(5)
1^+	567.654(6)	567.92(21)	7.4(13)	12(2)	10.9(11)		1202.07(16)	1202.3(13)	12.4(18)	15.6(18)	10.7(7)
7^+	577.216(6)	576.5(4)	2.3(18)[e]	7.5(13)	6.2(9)		1208.57(9)	1209.6(14)	14.7(18)[e]	5.7(13)	2.5(5)
6^+	588.104(4)	588.13(8)	45(4)	62(6)	42(3)		1217.21(31)	1216.6(14)	19.8(28)[e]	8.0(12)	4.1(5)
3^+	592.460(9)	592.52(18)	74(2)	58(1)	35(1)			1226.9(15)		5.7(9)	2.9(6)
4^+	598.511(6)	598.36(22)	64(3)	86(4)	64(3)		1240.66(8)	1240.4(15)	29(3)	17.0(18)	8.4(9)
2^+	605.109(6)	604.88(12)	15(2)	19(2)	15(2)		1244.2(1)	1245.1(16)	23(3)	10.1(18)	7.2(9)
5^+	634.329(4)	634.91(19)	45(3)	37(4)	22(2)		1263.8(6)	1264.9(18)	2.8(13)	4.0(11)	
7^-	644.29(6)	644.0(4)	11(2)	14(3)	7.5(13)		1271.4(2)	1271.2(17)	25(2)	35(2)	19.0(11)
5^+	654.802(11)	655.13(11)	74(4)	73(5)	46(2)			1280.7(18)	16(2)	29(2)	17.3(11)
3^+	662.235(7)	662.5(5)	11(2)	22(5)	15(2)		1289.25(12)	1290.9(18)	17(2)	23(2)	16.7(12)
4^+	671.750(12)	671.31(24)	12(1)	23(20	13(1)		1298.41(11)	1297.1(19)	17(2)	20(2)	15.5(12)
5^+	693.701(6)	694.06(29)	22(2)	30(2)	23(3)	4^+	1304.76(14)	1303.7(19)	5.5(9)	7.3(13)	7.5(11)
4^+	719.44(4)						1327.50(22)	1326.9(21)	5.5(18)	6.3(10)	
7^+	723.256(18)	722.95(18)	16(3)	22(2)	10.3(12)			1334.5(21)	11(2)	18(4)	15(2)
2^-	725.586(12)							1341.7(21)	19(2)	20(2)	13(2)
4^+	736.495(8)	737.21(18)	20(2)	28(2)	20(1)		1349.87(7)	1350.2(22)	23(2)	28(3)	13.8(12)
5^+	769.549(16)							1358.8(22)	30(2)	39(3)	29(2)
		769.72(10)	21(2)	32(2)	18(1)		1367.26(17)	1367.1(23)	49(3)	61(4)	45(2)
6+	771.77(8)						1376.76(9)	1376.6(24)	17(2)	21(2)	17(2)

TABLE III. (*Continued*).

			Intensity I_p (rel)[b]						Intensity I_p (rel)[b]		
J^π [a]	E_{lev} (keV)[a]	E_{expt} (keV)	15°	30°	45°	J^π [a]	E_{lev} (keV)[a]	E_{expt} (keV)	15°	30°	45°
		1382.6(24)			9.3(12)			1601(4)			8(2)
	1387.70(7)	1388.4(25)			10.4(11)		1603.8(2)	1605(4)			5(2)
	1396.72(8)	1397.2(25)	10(3)	12(4)	3.0(7)		1616.0(3)	1615(4)			8(1)
7^+	1417(3)	1417(3)	22(2)	35(3)	17.6(9)			1623(4)			10(1)
		1426(3)	75(4)	92(5)	38.5(13)		1635.5(1)	1636(4)			9(1)
		1432(3)	56(4)	45(4)	24.3(12)		1644.4(2)	1643(4)			6(1)
	1439(2)	1440(3)	24(2)	33(3)	15.0(9)		1655.0(6)	1654(4)			8(1)
		1445(3)	4.1(14)	8(3)	3.8(7)		1676.6(1)	1677(4)	11(2)		5(1)
	1458.8(5)	1458(3)	4.1(13)	6.0(18)	3.9(6)		1687.3(5)	1686(4)	12(3)		4(1)
	1463.9(2)	1465(3)		8.7(18)	5.2(6)	7^-	1692(4)	1692(4)	89(6)		38(2)
	1471.7(4)	1471(3)		8.7(18)	3.5(6)			1687(4)	13(3)		12(1)
	1487.1(1)	1487(3)		5.8(13)	4.8(6)			1702(4)	11(3)		5(1)
	1498.1(4)	1499(3)		17(2)	7.3(6)		1716.6(2)	1717(4)	27(3)	18(4)	10(1)
		1508(3)		15(2)	8.6(11)		1723.8(6)	1723(5)	20(2)	12(3)	8(1)
		1513(3)		70(4)	31(2)		1731.1(1)	1731(5)	44(3)	32(4)	20(1)
	1526.8(2)	1528(3)		24(3)	12.0(11)			1745(5)	47(3)	33(5)	27(2)
	1532.1(1)	1533(3)		22(3)	14(2)		1752.4(3)	1753(5)	25(30)	17(2)	16(1)
	1537.6(1)	1537(3)		29(3)	10(2)			1759(5)	18(3)	21(30)	14(10)
	1547.5(2)	1547(3)		2.5(12)	2.3(9)			1765(5)	85(40)	71(4)	54(20)
	1558.9(2)	1558(3)		15(2)	10(1)			1779(5)	47(40)	40(6)	22(3)
	1570.7(1)	1569(4)		4.6(12)	4.7(7)			1784(5)	53(6)	38(6)	21(3)
	1576.9(1)	1577(4)		13(2)	10(1)			1788(5)	47(7)	36(7)	35(3)
	1592.4(2)	1593(4)		4.0(11)	3.8(8)						

[a]Energy levels from Table II and Nuclear Data Sheets [19].

[b]The experimental relative intensities have been normalized so that the total, summed over the three angles, for the spin 3 to 7 members of the strongly populated $K^\pi=3^+$ band at 190 keV is equal to the corresponding sum of cross sections (in μb/sr) for a 60% component of the $p7/2^-[523]-n1/2^-[521]$ two-quasiparticle state. The value of 60% is used because the QPM predicts there is a 60% $p7/2^-[523]-n1/2^-[521]$ component in this band. Table X shows that this choice of normalization also causes the summed spin 4 to 6 intensity of the $K^\pi=4^+$ band at 372 keV to be essentially equal to 70% of that expected for a pure $p7/2^-[523]+n1/2^-[521]$ configuration, compared with a QPM prediction of 70% for this component.

[c]The peak at 265 keV is not well resolved from the large peak at 261 keV.

[d]The peak at 426 keV is not well resolved from the large peak at 424 keV.

[e]Intensity questionable.

[f]The peak at 563 keV is not well resolved from the large peak at 559 keV.

[g]The peak at 819 keV is not well resolved from the large peak at 815 keV.

[h]Identification questionable.

The reaction ^{167}Er$(d,^3$He$)^{166}$Ho was also measured in Munich with the equipment described above. The Er target was enriched to 95.6% ^{167}Er. It had dimensions 1 mm$\times$4 mm and thickness 40 μg/cm^2 on a 4 μg/cm^2 thick carbon backing. Spectra were measured at a deuteron energy of 27 MeV at angles of $\Theta_{lab}=30°$, 40°, and 50° up to an excitation energy of 1.2 MeV. Four spectra with an energy resolution of approximately 9 keV FWHM were recorded. A representative spectrum taken at $\Theta_{lab}=50°$ is shown in Fig. 8. The energy scale was calibrated with level energies from the Nuclear Data Sheets [19]. Relative intensities are listed in arbitrary units in Table IV. Due to difficulties with the monitor counter described above, relative intensities at different angles were not obtained experimentally, and the results for each angle are normalized separately as explained in a footnote to Table IV.

III. CALCULATED (d,p) AND $(d,^3$He$)$ CROSS SECTIONS

The experimental (d,p) and $(d,^3$He$)$ cross sections are compared with values calculated using Nilsson model wave functions and standard reaction theory. The formalism has been described in several review articles [36] and the method has been widely used for studies of heavy odd-odd deformed nuclides [8,37,38]. The cross section for transfer of a single nucleon, starting from the ground state of an odd-mass target

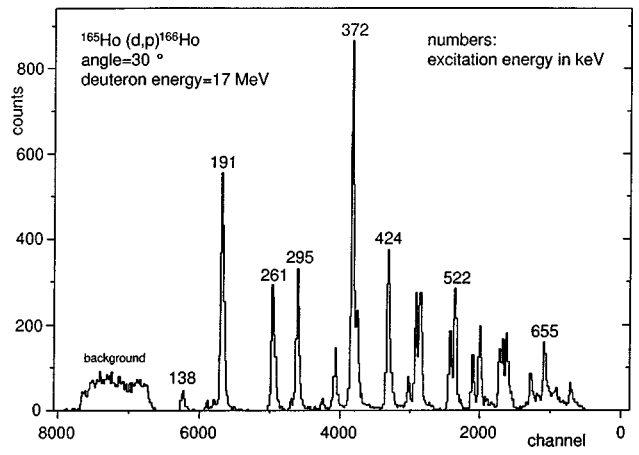

FIG. 6. A portion of the proton spectrum from the ^{165}Ho$(d,p)^{166}$Ho reaction with 17 MeV deuterons at $\Theta=30°$.

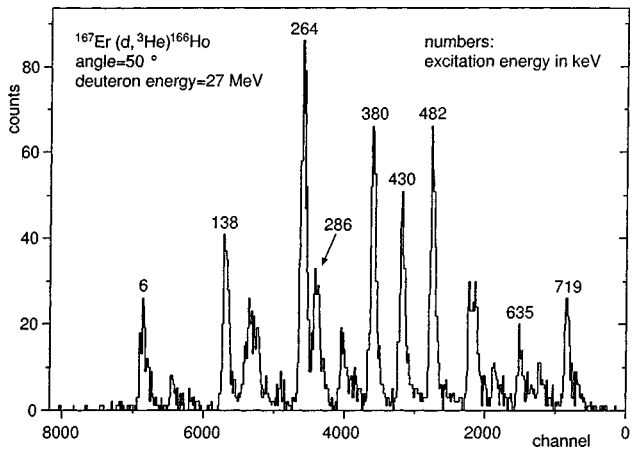

FIG. 8. A portion of the spectrum from the ^{167}Er$(d,^{3}$He$)^{166}$Ho reaction with 27 MeV deuterons at $\Theta=50°$.

nucleus with I_0,K_0 and leading to a rotational band member of spin I_f,K_f in an odd-odd deformed nucleus is

$$\frac{d\sigma}{d\Omega}=N\sum_{j,l}\left[\sum_i a_i(C_{jl})_i P_i\langle I_0K_0j\Delta K|I_fK_f\rangle\right]^2 \times\left(\frac{d\sigma}{d\Omega}\right)_{\mathrm{DW}}. \quad (1)$$

Intrinsic cross sections for the single-nucleon transfer process are obtained from distorted wave Born approximation (DWBA) calculations as $(d\sigma/d\Omega)_{\mathrm{DW}}$, and N is a normalization constant for these cross sections. The C_{jl} values are expansion coefficients describing the Nilsson orbital of the transferred nucleon. The quantity P_i^2 is a pairing factor, which for a pickup reaction is V_i^2, the occupation probability in the target for the transferred nucleon. For a stripping reaction $P_i^2=U_i^2=1-V_i^2$ is the ''emptiness'' probability. In the derivation of Eq. (1) the final state was assumed to be a Coriolis-mixed configuration, with amplitudes a_i for the various Nilsson orbitals for the transferred nucleon.

For the present work DWBA calculations were performed with the computer program DWUCK4 [39], using optical model parameters which have been successfully employed in this mass region. For the ^{165}Ho$(d,p)^{166}$Ho reaction optical parameters were obtained from global fits to deuteron and proton scattering data. The deuteron parameters used were from set B of Perey and Perey [40], and those for protons were from Becchetti and Greenlees [41]. Actual values used for the parameters are listed in Table V. (The symbols are defined in Ref. [41].) Calculations for the ^{167}Er$(d,^{3}$He$)^{166}$Ho reactions were made with parameters established by Lu and Alford [42] and widely used for $(^{3}\mathrm{He},d)$ reactions in the rare earth region. Actual values are presented in Table VI. For all calculations the radial integration was performed with no lower cutoff. As recommended by Kunz [39], finite range parameters of 0.621 and 0.77 were used for the (d,p) and $(d,^{3}\mathrm{He})$ reactions, respectively.

Nilsson model calculations were performed for a quadrupole deformation of $\delta=0.30$. For neutron orbitals the Nilsson parameters were $\kappa=0.0637$ and $\mu=0.42$ while for the proton orbitals they were $\kappa=0.0637$ and $\mu=0.60$, as recommended by Lamm [43]. Values of U^2 and V^2 factors for various orbitals in the target ground states were estimated from BCS pairing considerations. Coriolis mixing effects have not been included for these calculations.

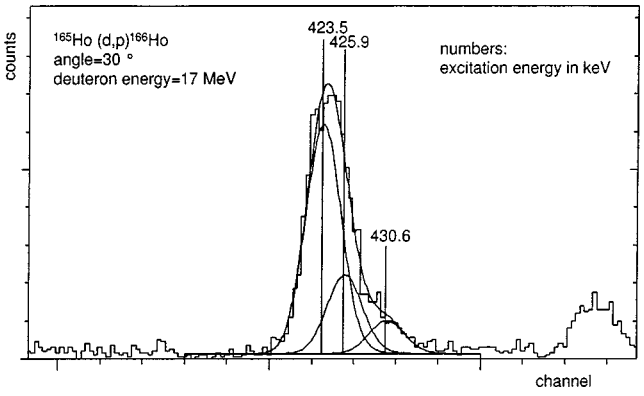

FIG. 7. Decomposition of the (d,p) peaks at 426 keV.

IV. SEMIEMPIRICAL PREDICTION OF THE LEVEL STRUCTURE

The technique used here for modeling excited levels in ^{166}Ho is a semiempirical method that has been applied to odd-odd deformed nuclei for many years and that was first described by Struble *et al.* [11] and Motz *et al.* [9]. The excitations of the quasiparticle states in an odd-odd nucleus are deduced by summing separate contributions from the two unpaired nucleons whose excitations have been observed experimentally in neighboring odd-A nuclei. Estimates are made of the effect of the n-p interaction either through theoretical calculation, e.g., see Boisson *et al.* [4], or, when data are available, from experimental evidence in a previously studied odd-odd nucleus. Rotational parameters are estimated using a parallel concept, i.e., the summing of contributions to the moment of inertia from the unpaired nucleons. Details of such calculations have been discussed previously [44]. When the experimental data for quasiparticle excita-

TABLE IV. Spectroscopy of ^{166}Ho via the $(d,^3\mathrm{He})$ reaction ($E=27$ MeV).

J^{π} [a]	E_{lev} (keV)[a]	E_{expt} (keV)	Intensity I_p (rel)[b] 30°	40°	50°
7^-	5.971(12)	5.7(3)	8.5(10)	4.8(6)	5.2(6)
	impurity[c]	14.2(8)	2.5(6)	1.9(4)	1.6(5)
2^-	54.2388(7)	54.3(9)	1.1(5)	1.3(3)	1.5(3)
1^-	82.4709(19)	84.5(28)			0.4(2)[d]
8^-	137.731(13)	138.21(24)	10.0(11)	8.2(7)	9.6(7)
3^-	171.0762(12)	171.6(7)	2.8(8)	3.1(6)	2.0(6)
4^-	180.4686(28)	180.2(6)	7.8(11)	4.0(7)	4.5(6)
3^+	190.9038(20)	190.8(6)	3.9(9)	2.8(6)	3.8(5)
	impurity[c]	227.5(14)	1.4(6)	0.7(3)	
5^+	263.7895(23)	263.76(18)	33.0(18)	22.2(11)	16.2(13)
		273.1(16)	2.8(8)	2.2(6)	4.8(9)
9^-	286.96(10)	286.5(6)	7.5(10)	5.1(7)	6.9(6)
6^+	295.088(9)	296.8(12)			2.0(5)
5^-	329.777(4)	330.8(7)	3.9(8)	2.2(4)	3.0(5)
5^+	348.2617(26)	347.7(9)	2.0(6)	1.2(3)	
6^+	379.549(4)	380.2(5)	21.8(16)	12.4(9)	14.0(8)
	impurity[c]	390.9(9)	3.8(9)	1.8(6)	2.1(5)
2^+	430.040(4)	430.14(22)	17.0(15)	11.1(11)	9.0(8)
	impurity[c,e]	439.1(8)	2.5(8)	2.5(8)	1.8(5)
6^+	453.77(4)	454.5(13)	1.4(6)	0.7(4)[d]	
3^+	481.854(4)	481.65(20)	22.0(19)	12.1(11)	10.7(9)
	impurity[f]	489.6(7)	5.9(13)	3.0(8)	2.7(6)
4^+	547.934(5)	548.1(4)	8.3(11)	5.6(7)	4.7(6)
4^+	558.579(4)	558.5(4)	7.9(8)	4.0(7)	4.8(6)
3^+	592.460(9)	591.7(6)	3.6(8)	2.0(6)	1.5(3)
5^+	634.329(4)	635.1(6)	2.8(9)	2.4(6)	2.8(5)
5^+	654.802(11)[e]	651.9(14)		1.6(4)	
4^+	671.750(12)	670.8(6)	2.9(9)	1.6(4)	1.7(3)
4^+	719.44(4)	719.1(4)	7.3(11)	3.8(6)	4.7(6)
6^+	732.549(14)	729.6(30)	2.1(8)	1.2(4)	
0^+	803.36(10)				
		805.0(11)		2.0(6)	
5^+	806.68(18)				
	820.65(2)	820.7(13)		1.8(4)	
	885.39(8)	884.8(16)		1.2(4)	
$2^+,5^+$	925.51(3)	926.5(13)		1.9(4)	
$2^+,5^+$	1010.66(3)	1010.2(22)		0.8(4)	
		1093.7(19)		0.4(2)	
		1142.2(21)		0.6(2)	

[a]From the Table II and Nuclear Data Sheets [19].

[b]For the results at each angle the values are normalized so that the sum of intensities for the spin 2, 3, and 4 members of the $K^{\pi}=2^+$ band at 430 keV plus the spin 5 and 6 members of the $K^{\pi}=5^+$ band at 263 keV is equal to the corresponding sum of cross sections (in μb/sr) predicted assuming these bands contain 55% admixtures of $p3/2^+[411]\pm n7/2^+[633]$ configurations. These five levels have the strongest peaks in the experimental spectra. The value of 55% is the average of 50% and 60% predicted by the QPM for the admixtures of these two-quasiparticle states in the $K^{\pi}=2^+$ and $K^{\pi}=5^+$ bands, respectively (see Table IX). Experimental justification for this choice is that the ratio of summed (t,α) cross sections measured [12] to that predicted, summed for the same five levels, is 53%.

[c]Peak belongs to the ^{165}Ho isotope.

[d]Intensity questionable.

[e]Identification questionable.

[f]Peak belongs to the ^{167}Ho isotope.

TABLE V. Optical model parameters for ^{165}Ho$(d,p)^{166}$Ho calculations at $E_d=17$ MeV.

	V (MeV)	r_r (fm)	a_r (fm)	W (MeV)	$4a_iW_D$ (MeV)	r_i (fm)	a_i (fm)	r_c (fm)	V_{so} (MeV)	r_{so} (fm)	a_{so} (fm)	Nonlocal param.
d	−101.7	1.15	0.81		50.3	1.34	0.68	1.30				0.54
p	−56.8	1.17	0.75	−1.81	22.9	1.32	0.64	1.25	6.2	1.0l	0.75	0.85
n	(a)	1.25	0.65									

[a]Adjusted to fit separation energy.

tions are well determined in the odd-A neighboring nuclei, a rather extensive set of two-quasiparticle states can be calculated for the subject odd-odd nucleus. In the case of ^{166}Ho, eight proton configurations and eight neutron configurations were taken from the odd-A observations (Table VII) resulting in 128 possible parallel and antiparallel couplings of odd-particle momenta.

While excitations that are predominantly vibrational are not excluded in this modeling technique, the lower lying states in the odd-A nuclei tend to be largely of quasiparticle character. Exceptions to this generality include a $K^\pi=\frac{3}{2}^-$ proton state observed at approximately 540 keV in ^{165}Ho and ^{167}Ho that is mostly of gamma vibrational character, built upon the $7/2^-[523]$ ground state of these nuclei, and a $K^\pi=\frac{3}{2}^+$ neutron state observed at approximately 535 keV in ^{165}Dy and ^{167}Er that is also of gamma vibrational character, built upon the $7/2^+[633]$ ground state of these nuclei.

The results of the model calculation of ^{166}Ho levels are given in Table VIII. Listed are band energies for all GM configuration pairs with $K\leqslant 7$ where the lower member lies within the energy range 0–950 keV. These comprise a total of 45 bands. The remaining bands whose energies can be calculated with this modeling technique lie above 950 keV and thus are beyond the scope of the present investigation.

V. THE QUASIPARTICLE-PHONON MODEL (QPM) CALCULATIONS

Low-lying states in odd-odd deformed nuclei have been extensively theoretically investigated for a long time (see, e.g., [1,2,4,9,11,19,22,45–48]). The most attention has been paid to the Gallagher-Mozskowski splitting [1] and Newby shift [2], which are directly connected with the neutron-proton interaction and provide a good possibility for its investigation. In most papers the neutron-proton interaction was introduced as some effective force with parameters fitted to the available experimental data (see, e.g., [22,46]). The only exception is the paper [47] where the effective n-p interaction was obtained in a self-consistent way from the Hartree-Fock-Bogoliubov average field. The rotational degrees of freedom of odd-odd nuclei were usually treated in the framework of the rotor-plus-two-quasiparticle approach (see, e.g., [4,47–49]). The coupling of external nucleons with even-even core vibrations was neglected in most papers and the collectivity of the low-lying states in odd-odd nuclei was not investigated.

The first paper studying the coupling of quasiparticle and vibrational degrees of freedom in odd-odd nuclei was that of Soloviev [45]. In this paper the n-p interaction was not taken into account. The coupling of quasiparticle and vibrational degrees of freedom leads to the appearance of collective vibrational (phonon) components in the low-lying states. The importance of vibrational admixtures in low-lying states of odd-A nuclei for the description of energy spectra and transition probabilities was demonstrated in numerous calculations in the framework of the quasiparticle-plus-phonon model (see, e.g., [50,51]). Phenomenological models [52–56] also confirmed the important role of collective vibrational admixtures in the description of the low-lying states in odd-odd nuclei. Therefore in Ref. [26] the quasiparticle-plus-phonon model was generalized also for the case of odd-odd nuclei and the n-p residual interaction as well as the coupling of odd nucleons with a vibrating even-even core were treated on the same microscopic footing. In the framework of this approach it was shown that low-lying states in odd-odd deformed nuclei have two-quasiparticle character with small collective components not exceeding 20–30 % (see [57]).

The theoretical interpretation of the data on ^{166}Ho was performed in the framework of the standard rotor model where the intrinsic nonrotating degrees of freedom were described by the modified quasiparticle-plus-phonon model [26]. Since this approach is discussed in detail in [26], we present here only the basic ideas.

The low-lying states in odd-odd deformed nuclei can be described within the adiabatic approximation of the separation of intrinsic nonrotating degrees of freedom and the rotational ones with the corresponding nuclear Hamiltonian:

TABLE VI. Optical model parameters for ^{167}Er$(d,^3$He$)^{166}$Ho calculations at $E_d=27$ MeV.

	V (MeV)	r_r (fm)	a_r (fm)	W (MeV)	$4a_iW_D$ (MeV)	r_i (fm)	a_i (fm)	r_c (fm)	V_{so} (MeV)	r_{so} (fm)	a_{so} (fm)	Nonlocal param.
d	−111	1.05	0.859		56.2	1.24	0.794	1.25				0.54
^{3}He	−175	1.14	0.723	−17.5		1.60	0.81	1.4				0.25
p	(a)	1.25	0.65						8.0			0.85

[a]Adjusted to fit separation energy.

TABLE VII. Band energies for quasiparticle excitations in odd-mass nuclei adjacent to ^{166}Ho; rotational parameters in adjacent odd-mass and even-even nuclei. [Even-even nuclei: $\hbar^2/2J(^{166}\mathrm{Dy})=12.76$ keV; $\hbar^2/2J(^{166}\mathrm{Er})=13.43$ keV.]

Odd proton states Average of data from ^{165}Ho and ^{167}Ho[a]			Odd neutron states Average of data from ^{165}Dy and ^{167}Er[a]		
Proton orbital	$E(K)$ (keV)	$\hbar^2/2J$ (keV)	Neutron orbital	$E(K)$ (keV)	$\hbar^2/2J$ (keV)
A $7/2^-[523]$	0	10.81	Z $7/2^+[633]$	0	9.04
B $3/2^+[411]$	311(51)	11.83	Y $1/2^-[521]$	158(50)	10.91
C $1/2^+[411]$	411(18)	12.29	X $5/2^-[512]$	265(81)	11.49
D $3/2^-\{A-Q_{22}\}$	543(27)	10.26	W $3/2^+\{Z-Q_{22}\}$[b]	535(4)	8.78
E $1/2^-[541]$[c]	681(0)	9.50	V $5/2^-[523]$	601(67)	10.83
F $7/2^+[404]$	845(129)	11.64	U $3/2^-[521]$[d]	663(90)	11.26
G $5/2^+[413]$	1038(43)	12.13	T $1/2^-[510]$[e]	667(97)	11.35
H $5/2^+[402]$	1229(174)	12.09	S $5/2^+[642]$[f]	813	8.79

[a]Data taken from Ref. [62].
[b]According to calculations by Michaelis *et al.* [74], these states have a large vibrational admixture (40–70 %); other calculations [75,76] show vibrational mixtures of 10–12 %, with the larger part of the wave function being $3/2^+[651]$.
[c]Data available for ^{165}Ho only.
[d]Calculations [74] indicate some admixture of $(1/2^-[521]\otimes 2^+)$ in this state.
[e]Calculations [74,75] indicate approximately equal amounts of single-particle character, as listed here, and a vibrational state$(5/2^-[512]\otimes 2^+)$.
[f]Data available for ^{167}Er only.

$$H=H_{\mathrm{intr}}+H_{\mathrm{rot}}, \tag{2}$$

with the intrinsic part H_{intr} and rotational part H_{rot}. For an axially symmetric rotor, with rotational axis perpendicular to the symmetry axis of the deformed average field, the rotational part of the Hamiltonian is [26,49]

$$\begin{aligned} H_{\mathrm{rot}} &= \frac{\hbar^2}{2J}\sum_{i=1,2}(\hat{I}_i-\hat{j}_i)^2 \\ &= \frac{\hbar^2}{2J}(\hat{I}^2-\hat{I}_3^2)+\frac{\hbar^2}{2J}(\hat{I}_+\hat{j}_-+\hat{I}_-\hat{j}_+) \\ &\quad +\frac{\hbar^2}{2J}(\hat{j}_+\hat{j}_-+\hat{j}_-\hat{j}_+), \end{aligned} \tag{3}$$

where the first term on the right-hand side (RHS) of Eq. (3) is a pure rotational term, the second term represents the Coriolis interaction and the last one stands for the centrifugal interaction. In Eq. (3) J is the moment of inertia of the odd-odd nucleus, $\hat{I}_3$ and $\hat{j}_3$ are projection operators of the total $(\vec{I})$ and of the intrinsic angular momenta $(\vec{j}=\vec{j}_n+\vec{j}_p)$ onto the nuclear symmetry axis, respectively, and $\hat{I}_\pm$ and $\hat{j}_\pm$ are defined as $\hat{I}_\pm=\hat{I}_1\pm i\hat{I}_2$, $\hat{j}_\pm=\hat{j}_1\pm i\hat{j}_2$, respectively.

The wave functions of the Hamiltonian (2) have the form

$$|I^\pi M\xi\rangle=\sum_{\varrho K} b^{I\xi}_{\varrho K}|I^\pi MK\varrho\rangle, \tag{4}$$

where $b^{I\xi}_{\varrho K}$ are the Coriolis mixing coefficients, M and K are the angular momentum projections in the laboratory and the intrinsic systems, respectively, and ξ and ϱ are additional quantum numbers characterizing a given state. The symbol $|I^\pi MK\varrho\rangle$ represents the symmetrized product of the Wigner functions D^I_{MK} and the intrinsic wave function $|\psi(K^\pi)\rangle$ (see, e.g., [58])

$$\begin{aligned} |I^\pi MK\varrho\rangle &= \sqrt{\frac{2I+1}{16\pi^2(1+\delta_{0K})}} \\ &\quad\times[D^I_{MK}+(-1)^I D^I_{M-K}\hat{R}_1]|\psi_\varrho(K^\pi)\rangle, \end{aligned} \tag{5}$$

where $|\psi(K^\pi)\rangle$ is the eigenvector of H_{intr} with corresponding intrinsic energy η_ϱ,

$$H_{\mathrm{intr}}|\psi_\varrho(K^\pi)\rangle=\eta_{\varrho K}|\psi_\varrho(K^\pi)\rangle \tag{6}$$

and $\hat{R}_1$ is the rotation operator (angle π) around the first intrinsic axis of the fixed-body frame (we suppose that ^{166}Ho is an R-symmetric nucleus).

The Coriolis mixing amplitudes $b^{I\xi}_{K\varrho}$ in Eq. (4) can be obtained by the diagonalization of the matrix of the total Hamiltonian (2) constructed in the basis of the function (5). The expressions for the matrix elements of individual terms of the Hamiltonian (2) can be found in many papers (see, e.g., [49]). Therefore we do not give them here. The operator $\hat{R}_1$ in Eq. (5) changes the sign of K for the intrinsic state $|\psi_\varrho(K^\pi)\rangle$. Special care has to be given to the $K=0$ case for which we have (see, e.g., [58])

$$R_1|\psi_{\varrho\,\gamma}(K=0)\rangle=\gamma|\psi_{\varrho\,\gamma}(K=0)\rangle, \tag{7}$$

where $\gamma=\pm 1$. In order that $|IMK=0\varrho\rangle$ does not vanish, one has the following condition:

$$\gamma=(-1)^I. \tag{8}$$

So, the intrinsic wave function $|\psi_{\varrho\gamma}(K^\pi=0)\rangle$ is the eigenvector of the operator R_1 with eigenvalue γ. Therefore for the case of $K=0$ we should ascribe the additional index γ to the intrinsic wave function. Following Eq. (8) each rotational band with $K=0$ splits into two bands. One of them, with $\gamma=+1$, can involve only states with even values of I, while the band with $\gamma=-1$ can have only odd values of I.

The intrinsic degrees of freedom are described in our approach by the generalized quasiparticle-plus-phonon model (QPM). In this model the intrinsic part $H_{\rm intr}$ of the nuclear Hamiltonian (2) is given by a deformed, in the case of ^{166}Ho, axially R-symmetric, average field $H_{\rm sp}$, a short-range residual interaction $H_{\rm pair}$ (pairing) and a long-range residual interaction, $H_{\rm res}$ [26]:

$$H_{\rm intr}=H_{\rm sp}+H_{\rm pair}+H_{\rm res}. \tag{9}$$

In our approach the single-particle average field $H_{\rm sp}$ is approximated by the Nilsson Hamiltonian with its standard parametrization (see [59]). The pairing interaction $H_{\rm pair}$ has the form of a monopole term (see [26,58]) and long-range residual interactions are taken in the form of the isoscalar and isovector multipole decomposition (see [26,51,58]):

$$H_{\rm res}=-1/2\sum_{\lambda\mu\geqslant 0}\sum_{\tau\tau'}(\kappa_0^{(\lambda\mu)}+\tau\tau'\kappa_1^{(\lambda\mu)})Q_{\lambda\mu}^{(\tau)}Q_{\lambda-\mu}^{(\tau')}, \tag{10}$$

where $Q_{\lambda\mu}^{(\tau)}$ is the residual nonaverage part of the symmetrized multipole operator with the given multipolarity λ and the multipolarity projection μ (see [26,60] for details). The index τ represents the neutron and proton systems for which $\tau=-1$ and $+1$, respectively.

After the Valatin-Bogoliubov transformation from single-particle operators (a_ν,a_ν^+) to the quasiparticle ones $(\alpha_\nu,\alpha_\nu^+)$ and using the random phase approximation (RPA) equations for one-phonon vibrational excitations of the even-even core, the intrinsic Hamiltonian (2) can be schematically rewritten in the form (see [26,51] for details)

$$H_{\rm intr}=H_{\rm core}+H_{nQ}+H_{pQ}+H_{np}, \tag{11}$$

where $H_{\rm core}$ generates quasiparticle and phonon (vibrational) excitations of the doubly-even core, H_{nQ} and H_{pQ} represent the coupling of odd neutron and proton quasiparticles with the vibrating doubly-even core, respectively. H_{np} stands for the interaction between the odd neutron and proton. The explicit expressions for each of the terms involved in Eq. (11) are given in [26], where one can find also their microscopic origin.

The search for the eigenvectors $|\psi_\varrho(K^\pi)\rangle$ and eigenvalues $\eta_{\varrho K}$ of the intrinsic Hamiltonian $H_{\rm intr}$ [see Eq. (6)] is usually performed in two steps. In the first step the RPA is used for the determination of the structure and energy of the two quasi-particle phonons $Q_{\lambda\mu}^+$ with corresponding multipolarity λ and multipolarity projection μ from the RPA equation (see, e.g., [51,58])

$$[H_{\rm core},Q_{\lambda\mu}^+]=\hbar\omega_{\lambda\mu}Q_{\lambda\mu}^+,\quad [H_{\rm core},Q_{\lambda\mu}]=-\hbar\omega_{\lambda\mu}Q_{\lambda\mu},$$

$$[Q_{\lambda\mu},Q_{\lambda'\mu'}^+]=\delta_{\lambda'\lambda}\delta_{\mu\mu'}. \tag{12}$$

The one-phonon states $Q_{\lambda\mu}^+|\rangle$ describe the low-lying vibrational states in the even-even core.

In the second step the interactions H_{nQ} and H_{pQ} [see Eq. (11)] between odd particles and the vibrating even-even core as well as the interaction H_{np} between odd particles are involved and in terms of the variational principle we can obtain the amplitudes $C_{\nu_n\nu_p}^{\varrho}$ of neutron-proton two-quasiparticle components, $\alpha_{\nu_n}^+\alpha_{\nu_p}^+|\rangle$, and the amplitudes $D_{\lambda\mu\nu_n\nu_p}^{\varrho}$ of two-quasiparticle components, $\alpha_{\nu_n}^+\alpha_{\nu_p}^+Q_{\lambda\mu}^+|\rangle$, in the odd-odd nucleus intrinsic wave function $|\psi_\varrho(K^\pi)\rangle$:

$$|\psi_\varrho(K^\pi)\rangle=\Bigg(\sum_{\nu_n\nu_p}C_{\nu_n\nu_p}^{K\varrho}\alpha_{\nu_n}^+\alpha_{\nu_p}^+ + \sum_{\nu_n\nu_p\lambda\mu}D_{\lambda\mu\nu_n\nu_p}^{\varrho}\alpha_{\nu_n}^+\alpha_{\nu_p}^+Q_{\lambda\mu}^+\Bigg)\Bigg|\Bigg\rangle, \tag{13}$$

with the intrinsic energy $\eta_{\varrho K}$.

It should be noted that usually in the low-lying intrinsic states $|\psi_\varrho(K)\rangle$ one two-quasiparticle component, say $\alpha_{\varrho_n}^+\alpha_{\varrho_p}^+|\rangle$, predominates with the corresponding angular momentum projection $K=|K_{\varrho_n}\pm K_{\varrho_p}|$. Two intrinsic states $|\psi_{\varrho=\varrho_n\varrho_p}(K)|\rangle$ with $K=K_{\varrho_n}+K_{\varrho_p}$ and $K=|K_{\varrho_n}-K_{\varrho_p}|$ have a similar structure (that means amplitudes $C_{\nu_n\nu_p}^{\varrho K}$ and $D_{\lambda\mu\nu_n\nu_p}^{\varrho K}$) and they form the well known Gallagher-Mozskowski (GM) doublet with the corresponding GM splitting energy:

$$\Delta E_{\varrho=\varrho_n\varrho_p}^{(\rm GM)}=\eta_{\varrho K=|K_{\varrho_n}-K_{\varrho_p}|}-\eta_{\varrho K=K_{\varrho_n}+K_{\varrho_p}}. \tag{14}$$

Moreover, for the case of $K=0$ one can define the Newby shift

$$\Delta E_{\varrho K=0}^{(N)}=\eta_{\varrho K=0\,\gamma=-1}-\eta_{\varrho K=0\,\gamma=+1}, \tag{15}$$

which determines the energy shift between two rotational $K=0$ bands with the same internal structure differing only by the quantum number $\gamma=\pm 1$. The GM splitting energies and Newby shifts are usually calculated in the framework of the model of independent quasiparticles (see, e.g., [46–48]), where they can be directly related to the two-particle matrix elements of the *n-p* interaction H_{np}. The QPM approach presented in [26] and in this paper takes these quantities into account as well as the vibrational degrees of freedom of the even-even core.

The interpretation of the experimental levels given in the present investigation is based on the calculation of the energies and the structure of the low-lying intrinsic states of ^{166}Ho. This calculation represents the generalization of that given in [26]. Here we again start with the average field $H_{\rm sp}$ approximated by the Nilsson Hamiltonian, whose parameters (including deformation) were taken from [49,61]. Since the isovector part of the long-range residual interaction $H_{\rm res}$ [see Eq. (10)] has no substantial influence on the low-lying intrinsic states in deformed nuclei (see, e.g., [58]) in our calcula-

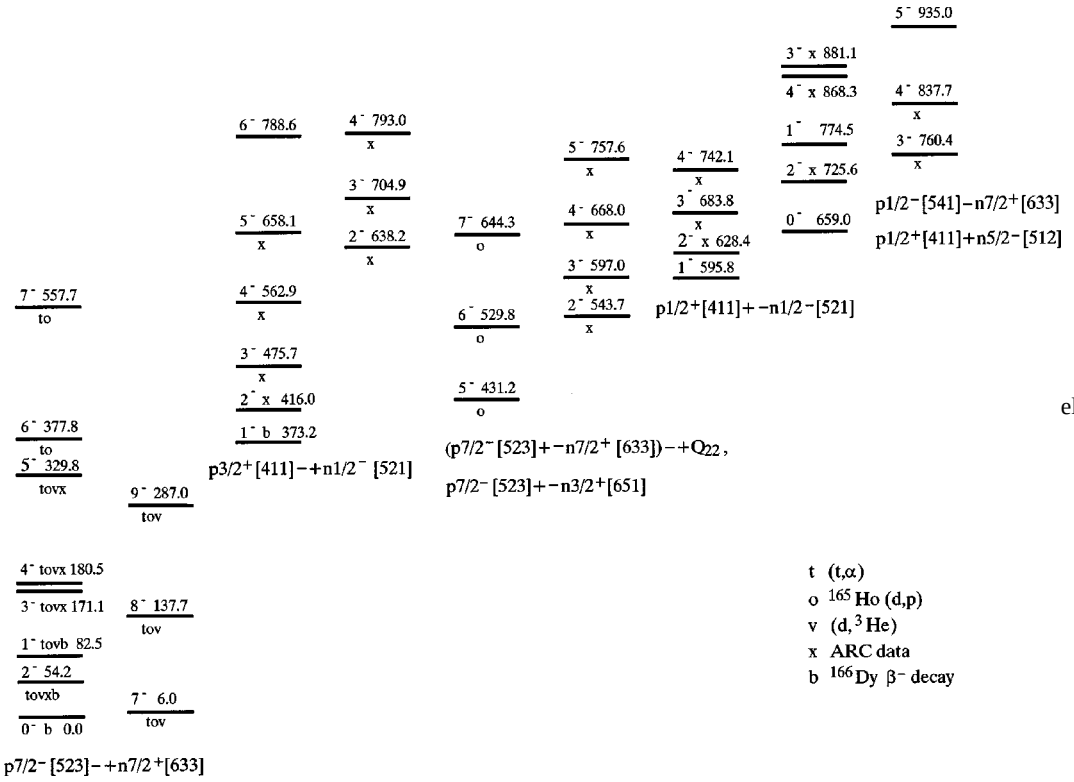

FIG. 9. Negative parity levels of ^{166}Ho.

tions, we restrict ourselves only to the isoscalar part ($\kappa_1^{(\lambda\mu)}=0$). We did not optimize any model parameter. QPM parameters (pairing strength constants and long-range residual interaction constants $\kappa_0^{(\lambda\mu)}$ for $\lambda=2,3$) were determined in [58] by the properties of the even-even core (needed experimental values of the lowest quadrupole and octupole one-phonon energies were taken from [50]). A standard δ-force dependence of the *n-p* interaction H_{np} [46] was used. The parameters of H_{np} were taken from [46] where they were obtained by a least square fit to all GM splitting energies and Newby shifts known at that time.

In order to improve the agreement of the experimental and theoretical bandhead energies, we shifted some Nilsson orbits with respect to the values used in [26]. Aside from these shell shifts, we used the same model parameters as in [26].

The structures and energies of the low-lying intrinsic states below 1 MeV in ^{166}Ho are shown in Table IX. The first and second columns of this table contain the components and the percentages with which they enter the structure of the corresponding intrinsic state (13) ($|C^{\varrho K\gamma}_{\nu_n\nu_p}|^2$ for two-quasiparticle components and $|D^{\varrho K\gamma}_{\lambda\mu\nu_n\nu_p}|^2$ for two-quasiparticle plus phonon components). The difference of the calculated intrinsic energy for a given state, $\eta_{\varrho K\gamma}$, and the calculated intrinsic energy for the ground state, $\eta_{\varrho_0 K_0\gamma_0}$, is given in the third column of this table. The fourth column contains the energy of the first member of the rotational band built on the corresponding intrinsic state. These values were obtained by means of the standard $I(I+1)$ formula without an inclusion of Coriolis coupling (i.e., $E(I,K\varrho)=\eta_{\varrho K\gamma}-\eta_{\varrho_0 K_0\gamma_0}+(\hbar^2/2J)[I(I+1)-K^2]_{I=K}-(\hbar^2/2J)[I(I+1)-K^2]_{I=K_0}$). The inertial parameters were assumed to be $\hbar^2/2J\sim 9$ keV for all bands. The last column contains the experimental energies of the first level of the rotational band of the corresponding intrinsic state. The individual GM doublets are separated by the double-line. The GM splitting energies (14) can be deduced from the third column for each GM doublet. When $K=0$, the third column also contains the Newby shifts (15).

VI. LEVEL SCHEME AND ROTATIONAL BANDS

A. Interpretation of experimental results

The present experimental data for ^{166}Ho have been interpreted in terms of single-particle configuration assignments to unpaired nucleons in the states upon which rotational bands are built. Assignments are made by considering the specific nature of each experimental measurement and with guidance from the predictions of a semiempirical model (Sec. IV) and a more formal quasiparticle-phonon model (QPM) (Sec. V). Mixing among configurations with identical K quantum numbers is a feature of this interpretation; predictions are obtained from the QPM studies. Included in our considerations is the possibility that vibrational excitations play a role in the level structure of ^{166}Ho, in a manner analogous to that found in the neighboring odd-mass nuclei. The results are summarized in Figs. 9, 10(a), and 10(b) and Tables II, VIII, and IX. Table II lists all of the experimental levels in ^{166}Ho proposed by the authors plus γ rays from the decay of each level. Most of the γ-transition data (energies, intensities, and multipolarities) are taken from Ref. [9]. Some γ energies and intensities are newly determined in our

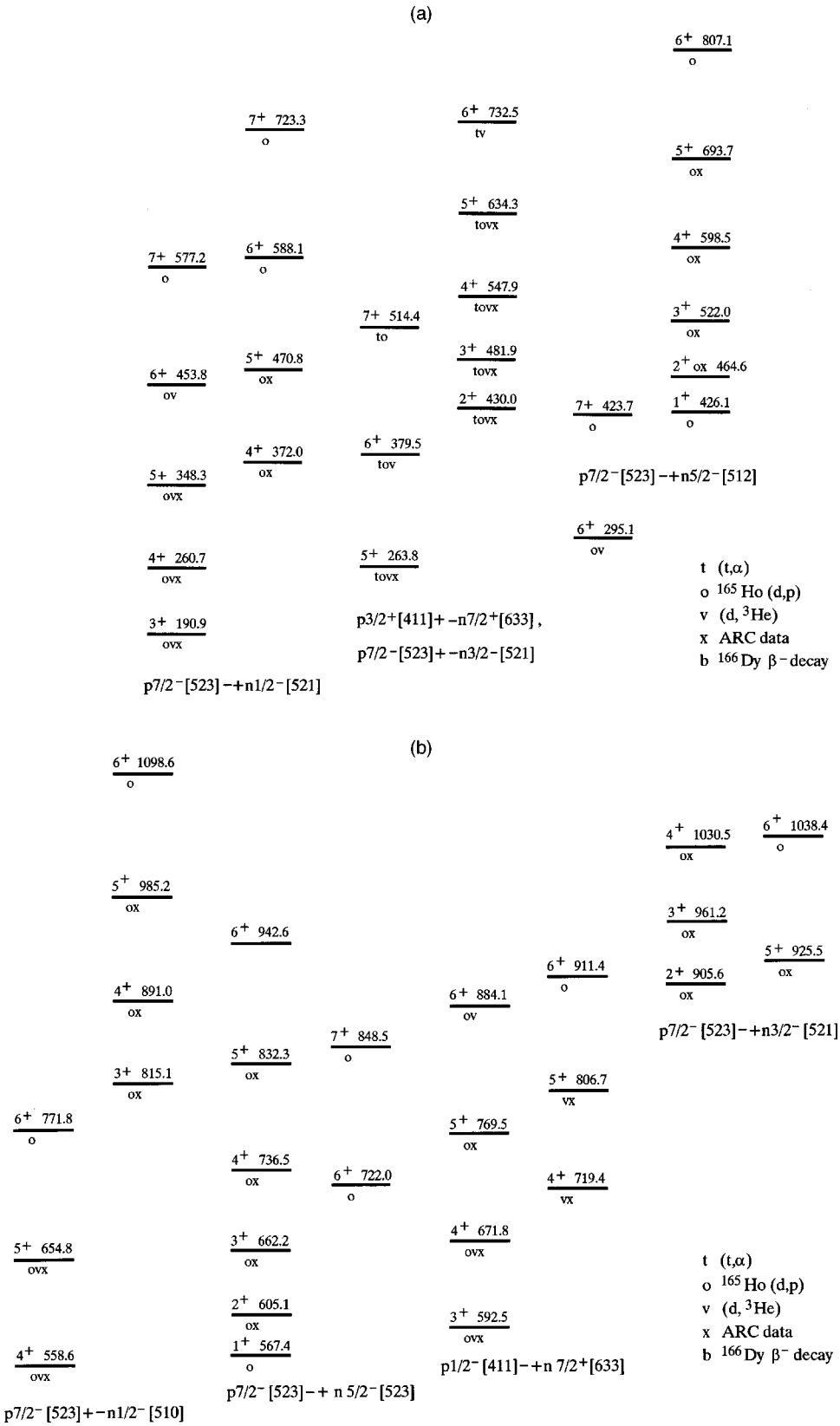

FIG. 10. Positive parity levels of ^{166}Ho.

coincidence measurements. Experimental multipolarities of Ref. [15], few in number, are included. The level energies (col. 2) were calculated by use of a least squares fit computer program (LEFIT by K. Schreckenbach).

As discussed in Sec. II A, the 2-keV ARC reaction is expected to populate all levels with $I^{\pi}=2^{+}$, 3^{+}, 4^{+}, and 5^{+} via intense *E1* transitions. In a similar manner, but with somewhat less intensity, *M1* transitions from the capture

TABLE VIII. Experimental and calculated bandhead energies, rotational parameters, and matrix elements in ^{166}Ho.

Bandhead energies (keV)				Rotational parameters (keV)				Matrix elements (keV)	
Cnfg.[a]	E_{expt}	$E_{calc}I$[b]	$E_{calc}II$[c]	A_{expt}, $I(1)$, $I(2)$[d]		A_{mean}[e]	A_{calc}[b]	$E(GM)_{expt}$	$E(GM)_{calc}$
0^-AZ	0.0	46	0	9.040(1)0,2	8.860(1)1,3	8.64	7.87	+84.1	+101[f]
				9.016(1)2,4	8.817(1)3,5			+84.1	+236[g]
				8.970(1)4,6	8.766(1)5,7			+84.1	+160[h]
7^-AZ	6.0	0	13	8.235(1)7,8	8.291(6)8,9	8.64	7.87	+32.4(E_N)	+31[i]
				$A=8.026$	$B=0.0016$			+32.4(E_N)	−2.9[h]
3^+AY	190.9	128(50)	147	8.720(1)3,4	8.760(1)4,5	9.30	9.25	−171.9	−159[f]
				8.792(3)5,6	8.818(3)6,7			−171.9	−169[g]
				$A=8.650$	$B=0.0022$			−171.9	−106[h]
4^+AY	372.0	296(50)	305	9.886(1)4,5	9.772(1)5,6	9.30	9.25		
				9.654(1)6,7					
				$A=10.144$	$B=-0.0052$				
5^+BZ	263.8	295(51)	292	9.627(1)5,6	9.630(1)6,7	9.13	8.40	+193.6	+146[f]
$+5^+$AU				$A=9.694$	$B=-0.0007$			+193.6	+147[g]
2^+BZ	430.0	416(51)	502	8.636(1)2,3	8.260(1)3,4	9.13	8.40	+193.6	+129[h]
$+2^+$AU				8.639(1)4,5	8.185(1)5,6				
				$A=8.475$	$D=-0.0537$				
6^+AX	295.1	262(81)	362	9.183(1)6,7		9.40	9.66	+177.2	+103[g]
1^+AX	426.1	333(81)	420	9.617(2)1,2	9.581(1)2,3	9.40	9.66	+177.2	+141[h]
				9.558(1)3,4	9.519(1)4,5				
				9.450(13)5,6					
				$A=9.646$	$B=-0.0036$				
1^-BY	373.2	460(101)	369	10.715(2)1,2	9.953(1)2,3	10.92	9.99	−254.4	−81[h]
				10.890(1)3,4	9.523(1)4,5				
				10.875(18)5,6					
				$A=10.410$	$D=0.152$				
2^-BY	638.2	590(101)	531	11.120(2)2,3	11.004(3)3,4	10.92	9.99		
				$A=11.268$	$B=-0.0083$				
5^-AZg	431.2	527(4)	452	8.215(18)5,6	8.177(4)6,7	8.55	7.67	+138.2	
				$A=8.197$	$D=0.0029$				
2^-AZg	543.7	624(4)	527	8.891(1)2,3	8.874(1)3,4	8.55	7.67		
				8.957(1)4,5					
				$A=8.883$	$D=-0.0024$				
5^-DZ		538(27)					7.57		
2^-DZ		636(27)					7.57		
4^+AT	558.6	666(97)	538	9.622(1)4,5	9.747(7)5,6	9.56	9.56	+266.0	+149[h]
				$A=9.338$	$B=0.0057$				
3^+AT	815.1	777(97)	864	9.490(2)3,4	9.416(4)4,5	9.56	9.56		
				$A=9.455(18)$	$D=0.0081$				
1^+AV	567.7	533(67)	585	9.458(1)1,3	9.385(1)2,4	9.25	9.19	−108.5	−154[f]
				9.446(1)3,5	9.369(1)4,6			−108.5	−322[g]
				$A=9.427$	$D=-0.0314$				
6^+AV	722.0	733(67)	888	9.035(18)6,7		9.25	9.19		
4^-BX		576(132)					10.46		
1^-BX		665(132)					10.46		
3^+CZ	592.5	392(18)	650	9.911(2)3,4	9.780(2)4,5	9.32	8.63	−117.6	−144[f]
				9.542(2)5,6				−117.6	−98[h]
				$A=10.145$	$B=-0.0073$				
4^+CZ	719.4	544(18)	801	8.724(18)4,5	8.727(15)6,7	9.32	8.63	−117.6	−150[g]
				$A=8.718$	$B=0.0001$				
1^-CY	595.8	585(68)	621	8.797(1)1,3	8.117(6)2,4	9.95	10.31	+128.0	+94[f]
				$A=8.581$	$D=-0.216$			+128.0	+198[g]

TABLE VIII. (*Continued*).

Cnfg.[a]	Bandhead energies (keV) E_{expt}	$E_{calc}I$[b]	$E_{calc}II$[c]	Rotational parameters (keV) A_{expt}, $I(1)$, $I(2)$[d]		A_{mean}[e]	A_{calc}[b]	Matrix elements (keV) $E(GM)_{expt}$	$E(GM)_{calc}$
0^-CY	659.0	669(68)	570	11.110(5)0,2	10.657(2)1,3	9.95	10.31	+128.0	+113[h]
				10.192(11)2,4				+47.1(E_N)	+31[i]
								+47.1(E_N)	+14.7[h]
2^-CX		668(100)					10.83		
3^-CX	760.4	799(100)		9.670(1)3,4	9.731(2)4,5	9.67	10.83		
$+3^-$EZ				$A=9.561$	$B=0.0034$				
1^+DY		693(77)					8.84		
2^+DY		822(77)					8.84		
3^-EZ		693					7.15		
4^-EZ		777					7.15		
0^+FZ		800(129)					8.30		
7^+FZ		933(129)					8.30		
6^-AS		802					7.68		
1^-AS		887					7.68		
4^+DX		806(108)					9.22		
1^+DX		898(108)					9.22		
3^+BW		844(55)					8.17		
0^+BW		939(55)					8.17		
1^-BV		861(118)					9.92		
1^+EY		877(118)					8.27		
2^+	905.6		955	9.27(3)2,3	8.66(4)3,4	9.34			
				$A=10.065$	$B=-0.0440$				
5^+	925.5		952	9.408(17)5,6		9.34			
0^+EY		918(50)					8.27		
2^+EX		935(81)					8.60		
1^+CW		940(22)					8.39		

[a]See Table VII for key to ''AZ'' notation.

[b]Values calculated with semiempirical model (Sec. IV). The uncertainties shown in parentheses are derived from the spread in experimental values taken from two neighboring odd-mass nuclei.

[c]Values calculated with quasiparticle-phonon model (Sec. V).

[d]Values of the rotational parameter calculated with the formula $A_{expt}=[E(2)-E(1)]/I(2)[I(2)+1]-I(1)[I(1)+1]$. For level energies $E(i)$ in the bands, see Table II. For A_{expt}, uncertainties in the last digits are in parentheses. The paired coefficients A,B or A,D are derived from the three lowest level energies using the formulas $E(I)=AI(I+1)+BI^2(I+1)^2$ or $E(I)=AI(I+1)+D(-1)^I I(I+1)$.

[e]Listed in this column is the mean of the first rotational parameter listed for each band of the GM pair.

[f]Calculated values taken from Ref. [4].

[g]Calculated values taken from Ref. [69].

[h]Calculated values taken from Ref. [6].

[i]Calculated values taken from Ref. [5].

states will populate all levels with $I^\pi=2^-$, 3^-, 4^-, and 5^-. In fact, this is exactly the case experimentally for the ^{166}Ho ARC data with just a few exceptions. Among the 23 rotational bands identified, there are 61 levels with $I=2$, 3, 4, or 5. All but two of these levels have been observed in the ARC spectra.

Since the averaging over many resonances that is the essence of the ARC technique means that all levels with appropriate spins and parity are populated, we can compare the number of observed levels with model predictions. Considering just the more prominent peaks in the ARC spectra, those that involve positive-parity levels with $I=2-5$, we postulate that all such levels within the first 1 MeV of excitation are represented in Table I. We observe 27 levels in the range of excitation energy 0–906 keV, while our semiempirical model predicts the existence of 41 such levels. Whereas some of the peaks reported in Table I may be due to multiplets with similar energies, it is likely that most of this discrepancy is caused by certain levels occurring at higher excitation energies than predicted.

For those levels populated by the ^{165}Ho$(d,p)^{166}$Ho reaction, the proton orbital, which is unchanged in the reaction, will be that of the target isotope, namely $p7/2^-[523](A)$. In an analogous manner, in the ^{167}Er$(t,\alpha)^{166}$Ho and ^{167}Er$(d,^3$He$)^{166}$Ho reactions the neutron orbital for the levels being populated will be that of the target, namely $n7/2^+[633](Z)$. The specificity of these single-particle transfer reactions is of great value in making configuration assign-

TABLE IX. Structure and energies of the intrinsic states in ^{166}Ho.

The structure of the intrinsic state $\lvert\psi_{\varrho\gamma}(K^{\pi})\rangle$		Intrinsic energy (theory) $\eta_{\varrho K\gamma}-\eta_{\varrho_0 K_0\gamma_0}$ [keV]	The first level of rotational band theory [keV]	The first level of rotational band experiment [keV]
$0^-(p7/2[523]-n7/2[633])$	95%	0.0	0.0	0.0
$\{(p7/2[523]-n3/2[651]-Q_{22}^+\}$	5%	$\Delta E^{(N)}=32.6$ keV		
$7^-(p7/2[523]+n7/2[633])$	83%			
$\{(p7/2[523]+n3/2[521]+Q_{32}^+\}$	4%			
$\{(p3/2[411]+n7/2[633]+Q_{32}^+\}$	4%			
$\{(p7/2[523]+n3/2[651]+Q_{22}^+\}$	3%			
$\{(p3/2[541]+n7/2[633]+Q_{22}^+\}$	2%			
$\{(p3/2[521]+n7/2[633]+Q_{22}^+\}$	1%	−50.4	13.2	5.9
$1^-(p3/2[411]-n1/2[521])$	94%			
$\{(p3/2[411]+n1/2[521]-Q_{22}^+\}$	1%			
$\{(p3/2[411]-n5/2[642]+Q_{32}^+\}$	1%			
$\{(p3/2[411]+n3/2[651]-Q_{32}^+\}$	1%	360.0	369.0	373.1
$2^-(p3/2[411]+n1/2[521])$	95%			
$\{(p7/2[523]+n1/2[521]-Q_{32}^+\}$	2%			
$\{(p3/2[541]+n1/2[521]+Q_{30}^+\}$	1%	513.2	531.2	638.2
$5^-(p7/2[523]+n3/2[651])$	81%			
$(p3/2[541]+n7/2[633])$	12%			
$\{(p7/2[523]+n7/2[633]-Q_{22}^+\}$	6%	407.5	452.5	431.2
$2^-(p7/2[523]-n3/2[651])$	62%			
$(p3/2[541]-n7/2[633])$	5%			
$\{(p7/2[523]-n7/2[633]+Q_{22}^+\}$	26%			
$\{(p7/2[523]+n1/2[660]-Q_{22}^+\}$	7%	509.1	527.1	543.7
$1^-(p1/2[411]+n1/2[521])$	97%			
$\{(p3/2[411]-n1/2[521]-Q_{22}^+\}$	1%			
$\{(p5/2[412]-n1/2[521]+Q_{20}^+\}$	1%	612.3	621.3	595.8
$0^-(p1/2[411]-n1/2[521])$	96%			
$\{(p3/2[411]+n1/2[521]-Q_{22}^+\}$	2%	570.2		
$\{(p1/2[411]+n3/2[521]-Q_{22}^+\}$	1%	$\Delta E^{(N)}=-40.2$ keV	570.2	658.9
$3^+(p7/2[523]-n1/2[521])$	60%			
$(p1/2[411]-n7/2[633])$	31%			
$\{(p3/2[411]+n7/2[633]-Q_{22}^+\}$	2%			
$\{(p3/2[541]+n7/2[633]-Q_{32}^+\}$	1%	120.2	147.2	190.9
$4^+(p7/2[523]+n1/2[521])$	70%			
$(p1/2[411]+n7/2[633])$	10%			
$\{(p7/2[523]-n3/2[521]+Q_{22}^+\}$	8%			
$\{(p7/2[523]+n5/2[512]-Q_{22}^+\}$	6%	269.2	305.2	371.9
$5^+(p7/2[523]+n3/2[521])$	30%			
$(p3/2[411]+n7/2[633])$	60%			
$\{(p7/2[523]+n7/2[633]-Q_{32}^+\}$	5%			
$\{(p7/2[523]-n1/2[521]+Q_{22}^+\}$	2%	247.1	292.1	263.8
$2^+(p7/2[523]-n3/2[521])$	39%			
$(p3/2[411]-n7/2[633])$	50%			
$\{(p7/2[523]-n7/2[633]+Q_{32}^+\}$	4%			
$\{(p7/2[523]+n1/2[521]-Q_{22}^+\}$	3%	474.1	592.1	430.0

TABLE IX. (*Continued*).

The structure of the intrinsic state $\lvert\psi_{\varrho\gamma}(K^\pi)\rangle$		Intrinsic energy (theory) $\eta_{\varrho K\gamma}-\eta_{\varrho_0 K_0\gamma_0}$ [keV]	The first level of rotational band theory [keV]	The first level of rotational band experiment [keV]
$6^+(p7/2[523]+n5/2[512])$	80%			
$(p7/2[523]+n5/2[523])$	10%			
$\{(p7/2[523]+n1/2[510]+Q_{22}^+\}$	5%			
$\{(p7/2[523]+n9/2[514]-Q_{22}^+\}$	4%			
$\{(p7/2[523]+n1/2[400]+Q_{32}^+\}$	1%	308.3	362.3	295.1
$1^+(p7/2[523]-n5/2[512])$	76%			
$(p7/2[523]-n5/2[523])$	10%			
$\{(p7/2[523]-n9/2[514]+Q_{22}^+\}$	4%			
$\{(p7/2[523]-n1/2[400]-Q_{32}^+\}$	4%			
$\{(p7/2[523]-n9/2[624]+Q_{32}^+\}$	1%	398.9	407.9	426.1
$4^+(p7/2[523]+n1/2[510])$	70%			
$(p1/2[411]+n7/2[633])$	1%			
$\{(p7/2[523]-n3/2[521]+Q_{22}^+\}$	19%			
$\{(p7/2[523]-n3/2[512]+Q_{22}^+\}$	6%			
$\{(p7/2[523]+n5/2[523]-Q_{22}^+\}$	2%	501.6	537.6	558.6
$3^+(p7/2[523]-n1/2[510])$	74%			
$(p1/2[411]-n7/2[633])$	2%			
$(p7/2[523]-n1/2[521])$	1%			
$\{(p3/2[411]+n7/2[633]-Q_{22}^+\}$	1%	836.9	863.9	815.1
$1^+(p7/2[523]-n5/2[523])$	88%			
$(p7/2[523]-n5/2[512])$	9%			
$\{(p7/2[523]-n1/2[521])-Q_{22}^+\}$	3%			
$\{(p7/2[523]-n9/2[514]+Q_{22}^+\}$	1%	576.2	585.2	567.7
$6^+(p7/2[523]+n5/2[523])$	79%			
$(p7/2[523]+n5/2[512])$	8%			
$\{(p7/2[523]+n1/2[510])+Q_{22}^+\}$	3%			
$\{(p3/2[541]+n5/2[523]+Q_{22}^+\}$	3%	834.2	888.2	722.0
$3^+(p1/2[411]-n7/2[633])$	69%			
$(p7/2[523]-n1/2[521])$	15%			
$(p7/2[523]-n1/2[510])$	15%			
$\{(p7/2[523]-n1/2[521]+Q_{20}^+\}$	5%	613.2	640.1	592.5
$4^+(p1/2[411]+n7/2[633])$	85%			
$(p7/2[523]+n1/2[510])$	2%			
$(p7/2[523]+n1/2[521])$	13%			
$\{(p7/2[523]+n1/2[521]+Q_{20}^+\}$	1%	747.1	783.1	719.3
$2^-(p3/2[541]-n7/2[633])$	72%			
$\{(p7/2[523]-n7/2[633])+Q_{22}^+\}$	9%			
$\{(p1/2[550]+n7/2[633])-Q_{22}^+\}$	7%			
$\{(p3/2[541]-n3/2[651]+Q_{22}^+\}$	6%	573.4	591.4	
$5^-(p3/2[541]+n7/2[633])$	75%			
$\{(p7/2[523]+n7/2[633])-Q_{22}^+\}$	9%			
$\{(p1/2[541]-n7/2[633])-Q_{22}^+\}$	7%			
$\{(p3/2[541]+n3/2[651]+Q_{22}^+\}$	4%	680.3	752.3	721.8

TABLE IX. (*Continued*).

The structure of the intrinsic state $\lvert\psi_{\varrho\gamma}(K^\pi)\rangle$		Intrinsic energy (theory) $\eta_{\varrho K\gamma}-\eta_{\varrho_0 K_0\gamma_0}$ [keV]	The first level of rotational band theory [keV]	The first level of rotational band experiment [keV]
$2^+(p3/2[411]-n7/2[633])$	13%			
$\{(p7/2[523]-n3/2[521])$	62%			
$\{(p3/2[411]-n3/2[651])+Q_{22}^+\}$	4%	951.2	969.2	905.6
$5^+(p3/2[411]+n7/2[633])$	12%			
$(p7/2[523]+n3/2[521])$	62%			
$\{(p3/2[411]+n3/2[651])+Q_{22}^+\}$	6%	920.4	956.4	925.5
$0^+(p7/2[404]-n7/2[633])$	74%			
$\{(p7/2[404]-n3/2[651])-Q_{22}^+\}$	15%			
$\{(p7/2[404]-n11/2[505])-Q_{32}^+\}$	4%	879.4		
$\{(p3/2[402]-n7/2[633]-Q_{22}^+\}$	3%	$\Delta E^{(N)}=57.2$ keV	879.4	
$7^+(p7/2[404]+n7/2[633])$	76%			
$\{(p7/2[404]+n3/2[651])+Q_{22}^+\}$	14%			
$\{(p7/2[404]+n11/2[505])-Q_{32}^+\}$	4%			
$\{(p3/2[404]+n7/2[633])+Q_{22}^+\}$	2%	985.3	1048.3	

ments in the complicated level scheme of ^{166}Ho, particularly for the more strongly populated levels. For various reasons, weak populations can exist for bands which do not satisfy the above ''selection rule,'' so caution must be used in interpreting small peaks with intensities only a few percent of those for the largest peaks in the spectrum. For example, both of the target nuclides ^{165}Ho and ^{167}Er have ground state orbitals originating from high-j shell model states, and are expected to contain Coriolis-admixed components of other Nilsson orbitals from the same shells (possibly at the level of up to a few percent). Thus, e.g., states involving the $5/2^-[532]$ proton might be seen weakly in the (d,p) reaction, although these would not be expected at very low excitation energies. In addition, there are often multistep processes in the reaction mechanism, which can redistribute strength among members of a band, and thus may have a significant effect on the intensities of weakly populated members. However, the most obvious cases where bands are populated, even though their labeled assignments (e.g., in Figs. 9 and 10) do not satisfy the ''selection rules,'' are due to configuration mixings. For example, the $K^\pi=3^+$ band at 190 keV is labeled in Fig. 10 as $p7/2^-[523]-n1/2^-[521]$ and the one at 592 keV is labeled $p1/2^+[411]-n7/2^+[633]$. This would imply the former should be populated only in the (d,p) reaction and the latter only in the $(d,^3\mathrm{He})$ reaction. However, Tables III and IV show that both bands are observed with both reactions, which is attributed to mixing of the configurations. Table IX shows the QPM predictions for these admixtures.

The experimental results, and the QPM predictions, indicate that most, if not all, of the bands in ^{166}Ho are mixtures of two-quasiparticle configurations. It is therefore important to stress that the two-quasiparticle descriptions used in the following discussion, and in Figs. 9 and 10, are merely convenient labels, indicating what are believed to be major components in the bands. This can be seen clearly in Tables X and XI, where the single-nucleon transfer strengths for some bands have only a small fraction of that expected for the two-quasiparticle state used as a label.

In previous studies of ^{166}Ho, the experimentally determined levels have been assigned spins and parities and have been arranged in rotational bands [19]. The earliest interpretation of ^{166}Ho level structure was derived from three papers published in the period 1965–1970 [9,11,13]. From the data in these publications, we have adopted what we consider a reliable set of 12 rotational bands comprised of approximately 45 levels. Among these, we find the most accurately determined energy levels among nine bands with bandhead energies $E<820$ keV and K-quantum numbers in the range $0\leqslant K\leqslant 4$. Their bandhead energies, K-quantum numbers, and parities are the following: 0 keV 0^-, 191 keV 3^+, 372 keV 4^+, 426 keV 1^+, 430 keV 2^+, 568 keV 1^+, 592 keV 3^+, 719 keV 4^+, and 815 keV 3^+. Our experimental results are in agreement with this basic band structure, i.e., we agree with the level energies, assigned spins, parities, and K quantum numbers for 40 levels in all, as listed in Ref. [19]. In many instances, the placement of gamma transitions has been altered, as compared with their arrangement in previous publications, due to the strong evidence we obtained from $\gamma\gamma$-coincidence measurements. For several of these bands, we have been able to add an additional, higher spin member based upon both deexciting γ-ray transitions and transfer reaction data. Some configuration assignments have been modified or added to bands in this group.

Three additional bands with $K\geqslant 5$ and bandhead energies <300 keV have been reported previously [19]. For these (6

TABLE X. Experimental and calculated (d,p) cross sections.

I^π	E_{lev}[a] (keV)	$\Theta_{lab}=15°$ I_{expt}(rel)	$\Theta_{lab}=15°$ I_{calc}(rel)	$\Theta_{lab}=30°$ I_{expt}(rel)	$\Theta_{lab}=30°$ I_{calc}(rel)	$\Theta_{lab}=45°$ I_{expt}(rel)	$\Theta_{lab}=45°$ I_{calc}(rel)
$K^\pi=0^-$ 0 keV band and calculation for pure $p7/2^-[523]-n7/2^+[633]$ AZ band							
0^-	0						
1^-	82	1.2(4)	0.8		1.6		1.2
2^-	54	2.4(6)	2.6		4.9	3.3(7)	3.6
3^-	171	3.2(8)	4.6	9.0(11)	8.2	5.2(8)	6.8
4^-	180	5.8(11)	7.1	12.9 (18)	11.0	9.8(9)	11.3
5^-	330	3.4(10)	9.1	9.2(18)	12.7	22.5(30)	15.2
6^-	378		8.5		11.2		14.4
7^-	558		5.3		6.8		9.0
$Sum_{obs.\ levs.}$		16.0	24.2	31.0	31.9	40.9	36.9
$Sum_{expt}/Sum_{calc}=0.95$ cf. QPM prediction of 95%							
$K^\pi=7^-$ 6 keV band and calculation for pure $p7/2^-[523]+n7/2^+[633]$ AZ band							
7^-	6	5.0(7)	6.5	17.0(41)	11.7	6.1(8)	9.5
8^-	138	8.4(11)	13.8	21.1(18)	22.1	20.7(18)	21.8
9^-	287	7.4(28)	12.8	8.7(18)	16.4	12.9(32)	21.9
10^-			7.2		9.2		12.3
$Sum_{J=7-9}$		20.8	33.1	46.9	50.2	39.6	53.2
$Sum_{expt}/Sum_{calc}=0.79$ cf. QPM prediction of 83%							
$K^\pi=3^+$ 190 keV band and calculation for pure $p7/2^-[523]-n1/2^-[521]$ AY band							
3^+	191	373(11)	780	267(60)	401	126(4)	293
4^+	261	152(6)	208	122(9)	185	80(7)	109
5^+	348	41(2)	60	58(4)	103	65(4)	55
6^+	454	19(5)	22	36(3)	43	28(2)	26
7^+	577	2.3(18)	5	7.5(13)	9	6.2(9)	7
Sum_{band}		587	1074	490	741	305	490
$Sum_{expt}/Sum_{calc}=0.60$ cf. QPM prediction of 60%							
$K^\pi=4^+$ 372 keV band and calculation for pure $p7/2^-[523]+n1/2^-[521]$ AY band							
4^+	372	540(8)	907	400(9)	485	213(4)	356
5^+	471	111(7)	119	135(6)	164	72(3)	86
6^+	588	45(4)	45	62(6)	87	42(3)	48
7^+	723		12		22		15
$Sum_{J=4-6}$		697	1070	598	736	327	490
$Sum_{expt}/Sum_{calc}=0.71$ cf. QPM prediction of 70%							
$K^\pi=6^+$ 295 keV band and calculation for pure $p7/2^-[523]+n5/2^-[512]$ AX band							
6^+	295	92(5)	147	137(6)	292	69(4)	144
7^+	424	120(7)	152	144(7)	299	70(4)	152
Sum_{band}		212	298	281	591	139	296
$Sum_{expt}/Sum_{calc}=0.53$ cf. QPM prediction of 80%							
$K^\pi=1^+$ 426 keV band and calculation for pure $p7/2^-[523]-n5/2^-[512]$ AX band							
1^+	426	15(6)	25	49(6)	50	35(4)	24
2^+	465	56(5)	76	109(6)	149	54(3)	74
3^+	522	84(4)	98	139(5)	192	80(3)	96
4^+	598	64(3)	73	86(4)	140	64(3)	73
5^+	694	22(2)	32	30(2)	62	23(3)	34
6^+	807	10(2)	8	10(1)	16	7(1)	10
7^+			1		2		2
$Sum_{J=1-6}$		251	312	424	609	263	311
$Sum_{expt}/Sum_{calc}=0.76$ cf. QPM prediction of 76%							

TABLE X. (*Continued*).

I^π	E_{lev}[a] (keV)	$\Theta_{lab}=15°$ I_{expt}(rel)	$\Theta_{lab}=15°$ I_{calc}(rel)	$\Theta_{lab}=30°$ I_{expt}(rel)	$\Theta_{lab}=30°$ I_{calc}(rel)	$\Theta_{lab}=45°$ I_{expt}(rel)	$\Theta_{lab}=45°$ I_{calc}(rel)
	$K^\pi=4^+$ 559 keV band and calculation for pure $p7/2^-[523]+n1/2^-[510]$ AT band						
4^+	559	114(4)	977	86(4)	598	62(3)	387
5^+	655	74(4)	478	73(5)	382	46(2)	228
6^+	772	21(2)	46	32(2)	89	18(1)	45
Sum_{band}		208	1501	191	1069	126	660
	$Sum_{expt}/Sum_{calc}=0.16$ cf. QPM prediction of 70%						
	$K^\pi=3^+$ 815 keV band and calculation for pure $p7/2^-[523]-n1/2^-[510]$ AT band						
3^+	815	213(5)	812	133(4)	507	99(5)	334
4^+	891	140(5)	537	126(10)	411	82(3)	253
5^+	985	46(3)	147	49(5)	165	38(2)	92
6^+	1099		22		41		22
$Sum_{J=3-5}$		398	1496	309	1083	218	679
	$Sum_{expt}/Sum_{calc}=0.28$ cf. QPM prediction of 74%						
	$K^\pi=1^+$ 568 keV band and calculation for pure $p7/2^-[523]-n5/2^-[523]$ AV band						
1^+	568	7.4(13)	6	12(2)	12	10.9(11)	6
2^+	605	15(2)	10	19(2)	19	15(2)	10
3^+	662	11(2)	11	22(5)	21	15(2)	14
4^+	736	20(2)	9	28(5)	16	20(1)	13
5^+	832	3.9(8)	5	4.6(11)	9	5.9(11)	9
6^+	943		2		3		4
$Sum_{J=1-5}$		56	40	85	77	67	52
	$Sum_{expt}/Sum_{calc}=1.23$ cf. QPM prediction of 88%						
	$K^\pi=6^+$ 722 keV band and calculation for pure $p7/2^-[523]+n5/2^-[523]$ AV band						
6^+	722		24		46		26
7^+	848	5.1(18)	16	13.7(18)	30	7.7(9)	24
$Sum_{J=7}$		5	16	14	30	8	24
	$Sum_{expt}/Sum_{calc}=0.38$ cf. QPM prediction of 79%						
	$K^\pi=2^+$ 906 keV band and calculation for pure $p7/2^-[523]-n3/2^-[521]$ AU band						
2^+	906	36(3)	44	54(4)	31	23(1)	20
3^+	961		35	26(2)	43	11.6(12)	24
4^+	1030	16.1(14)	28	14.3(13)	46	8.8(10)	25
5^+	1115	4.5(11)	17		30	2.8(8)	18
$Sum_{obs.levs.}$		56	89	94	120	47	86
	$Sum_{expt}/Sum_{calc}=0.67$ cf. QPM prediction of 62%						
	$K^\pi=5^+$ 926 keV band and calculation for pure $p7/2^-[523]+n3/2^-[521]$ AU band						
5^+	926		79	46(4)	67	22(1)	41
6^+	1038	13.3(14)	34	19.8(18)	63	12 (1)	34
$Sum_{obs.levs.}$		13	34	66	129	34	74
	$Sum_{expt}/Sum_{calc}=0.48$ cf. QPM prediction of 62%						
	$K\pi=3^+$ 592 keV band and calculation for pure $p7/2^-[523]-n1/2^-[521]$ AY band						
3^+	592	74(2)	785	58(1)	423	35(1)	317
4^+	672	12(1)	213	23(2)	196	13(1)	118
5^+	770		64		110		59
6^+	884		24		45	3,6(8)	28
$Sum_{obs.levs.}$		87	998	80	619	52	463
	$Sum_{expt}/Sum_{calc}=0.11$ cf. QPM prediction of 18%						

TABLE X. (*Continued*).

I^π	E_{lev}[a] (keV)	$\Theta_{lab}=15°$ I_{expt}(rel)	$\Theta_{lab}=15°$ I_{calc}(rel)	$\Theta_{lab}=30°$ I_{expt}(rel)	$\Theta_{lab}=30°$ I_{calc}(rel)	$\Theta_{lab}=45°$ I_{expt}(rel)	$\Theta_{lab}=45°$ I_{calc}(rel)
		$K\pi=5^+$ 264 keV, $p7/2^-[523]+n3/2^-[521]$ AU component					
5^+	264	21(5)	76	39(6)	61	23(6)	36
6^+	380	88(4)	29	110(5)	57	77(3)	30
7^+	514	54(3)	15	84(4)	28	48(3)	16
Sum_{band}		163	120	233	146	148	82
		$Sum_{expt}/Sum_{calc}=1.56$ cf. QPM prediction of 30%					
		$K\pi=5^+$ 264 keV, $p7/2^-[523]+n5/2^-[512]$ $K^\pi=6^+$ component					
5^+	264			Calc. for $K=6$ only			
6^+	380	88(4)	147	110(5)	292	77(3)	144
7^+	514	54(3)	152	84(4)	299	48(3)	152
$Sum_{J=6-7}$		142	298	194	591	125	296
		$Sum_{expt}/Sum_{calc}=0.39$					
		$K^\pi=2^+$ 430 keV band, $p7/2^-[523]-n3/2^-[521]$ component					
2^+	430	29(4)	43	22(3)	29	15.6(18)	18
3^+	482		33		40	4.6(14)	22
4^+	548	83(4)	25	58(3)	42	38(2)	23
5^+	634	45(3)	15	37(4)	28	22(2)	16
$Sum_{obs.levs.}$		157	83	117	99	80	79
		$Sum_{expt}/Sum_{calc}=1.36$ cf. QPM prediction of 42%					
		$K^\pi=2^+$ 430 keV band, $p7/2^-[523]-n5/2^-[512]$ $K^\pi=1^+$ component					
2^+	430	29(4)	76	22(3)	149	15.6(18)	74
3^+	482		98		192	4.6(14)	96
4^+	548	83(4)	73	58(3)	140	38(2)	73
5^+	634	45(3)	32	37(4)	62	22(2)	34
$Sum_{obs.levs.}$		157	181	117	351	80	277
		$Sum_{expt}/Sum_{calc}=0.44$					
		$K^\pi=2^+$ 430 keV band, $p7/2^-[523]+n1/2^-[510]$ $K^\pi=4^+$ component					
2^+	430	29(4)		22(3)		15.6(18)	
3^+	482				Calc. is for $K=4$ only		
4^+	548	83(4)	977	58(3)	598	38(2)	387
5^+	634	45(3)	478	37(4)	382	22(2)	228
$Sum_{obs.levs.}$		157	1455	117	980	80	615
		$Sum_{expt}/Sum_{calc}=0.09$					

[a]Experimental E_{lev} and I_{expt}(rel) from Table III.

keV 7^-, 264 keV 5^+, and 295 keV 6^+), our experimental measurements have provided more precise level energies for higher rotational levels and new placements of depopulating γ transitions. The existence of these bands is just as reliably known as for the nine bands just discussed. In fact, the characterization of the three bands, in terms of 2QP components, is quite certain.

Of the 12 rotational bands we have cited as most reliable, all have positive-parity except for the two lowest lying bands. In their 1970 paper, Bollinger and Thomas [13], using their own data and drawing upon previous work [9,11], made accurate descriptions of all of these bands. Most of their proposals for negative-parity bands, however, have not proven to be correct, presumably due to the quality of the data at that time. Since then several papers have addressed the question of additional negative-parity bands in ^{166}Ho; these papers are listed in Sec. I. Ours is the first to discuss these negative-parity bands systematically and to account for almost all bands expected up to about 700 keV.

Finally, we present evidence for the existence of eleven additional bands, some of which have not been identified previously and others where either very limited information was known previously (e.g., the identity of 1 or 2 levels) or whose level structure has been significantly changed from previous interpretations. In the process of establishing these bands, several new levels have been identified. Comments on specific details in the interpretation of each configuration in ^{166}Ho are given in Sec. VI B that follows. The evidence for certain levels, previously proposed but with reservations as to their reliability, e.g., those at 740.9, 759.5, and 771.5 keV [3,25], is now judged to be insufficient to support their existence. In all of the bands determined experimentally in

TABLE XI. Experimental and calculated (d,^{3}He) cross sections.

I^π	E_{lev} (keV)	$\Theta_{lab}=30°$ I_{expt}(rel)	$\Theta_{lab}=30°$ I_{calc}(rel)	$\Theta_{lab}=40°$ I_{expt}(rel)	$\Theta_{lab}=40°$ I_{calc}(rel)	$\Theta_{lab}=50°$ I_{expt}(rel)	$\Theta_{lab}=50°$ I_{calc}(rel)
		$K^\pi=0^-$ 0 keV band and calculation for pure $p7/2^-[523]-n7/2^+[633]$ AZ band					
0^-	0		0.2		0.2		0.1
1^-	82		0.5		0.4	0.4(2)	0.3
2^-	54	1.1(5)	1.2	1.3(3)	1.1	1.5(3)	0.8
3^-	171	2.8(8)	2.9	3.1(6)	2.9	2.0(6)	2.1
4^-	180	7.8(11)	4.2	4.0(7)	4.4	4.5(6)	3.1
5^-	330	3.9(9)	3.8	2.2(6)	4.1	3.0(5)	2.8
6^-	378		2.2		2.3		1.6
7^-	558		0.8		0.8		0.6
$Sum_{obs.\ levs.}$		15.6	12.1	10.6	12.5	11.0	8.8
		$Sum_{expt}/Sum_{calc}=1.11$ cf. QPM prediction of 95%					
		$K^\pi=7^-$ 6 keV band and calculation for pure $p7/2^-[523]+n7/2^+[633]$ AZ band					
7^-	6	8.5(10)	4.1	4.8(6)	3.8	5.2(6)	2.8
8^-	138	10.0(11)	7.1	8.2(7)	7.5	9.6(7)	5.2
9^-	287	7.5(10)	4.9	5.1(7)	5.3	6.9(6)	3.7
$Sum_{J=7-9}$		26.0	16.1	18.1	16.6	21.7	11.7
		$Sum_{expt}/Sum_{calc}=1.48$ cf. QPM prediction of 83%					
		$K^\pi=3^+$ 190 keV band, assumed $p1/2^+[411]-n7/2^+[633]$ CZ component in assigned $p7/2^-[523]-n1/2^-[521]$ AY band					
3^+	190	3.9(9)	12.1	2.8(6)	8.4	3.8(5)	5.8
4^+	261		7.2		4.6		3.8
5^+	348	2.0(6)	2.2	1.2(3)	1.5		1.2
6^+	454						
7^+	577						
$Sum_{obs.\ levs.}$		5.9	14.3	4.0	9.9	3.8	5.8
		$Sum_{expt}/Sum_{calc}=0.46$ cf. QPM prediction of 31%					
		$K^\pi=5^+$ 263 keV band and calculation for pure $p3/2^+[411]+n7/2^+[633]$ BZ band					
5^+	264	33.0(18)	60.7	22.2(11)	37.1	16.2(13)	31.9
6^+	380	21.8(16)	40.3	12.4(9)	25.3	14.0(8)	21.6
7^+	514		1.1		1.2		0.7
$Sum_{J=5,6}$		54.8	101.0	34.6	62.4	30.2	53.5
		$Sum_{expt}/Sum_{calc}=0.55$ cf. QPM prediction of 60%					
		$K^\pi=2^+$ 430 keV band and calculation for pure $p3/2^+[411]-n7/2^+[633]$ BZ band					
2^+	430	17.0(15)	26.9	11.1(11)	16.5	9.0(8)	14.4
3^+	482	22.0(19)	35.6	12.1(11)	22.1	10.7(9)	19.2
4^+	548	8.3(11)	22.0	5.6(7)	14.1	4.7(6)	12.1
5^+	634	2.8(9)	7.2	2.4(6)	4.9	2.8(5)	4.1
6^+	733	2.1(8)	1.2	1.2(4)	1.0		0.7
7^+			0.1		0.1		0.1
$Sum_{J=2-4}$		47.3	84.5	28.8	52.7	24.4	45.7
		$Sum_{expt}/Sum_{calc}=0.55$ cf. QPM prediction of 50%					
		$K^\pi=3^+$ 592 keV band and calculation for pure $p1/2^+[411]-n7/2^+[633]$ CZ band					
3^+	592	3.6(8)	9.2	2.0(6)	6.5	1.5(3)	4.7
4^+	672	2.9(9)	5.5	1.6(4)	3.6	1.7(3)	3.1
5^+	770		1.7		1.2		1.0
6^+	884						
$Sum_{J=3,4}$		6.5	14.7	3.6	10.1	3.2	7.8
		$Sum_{expt}/Sum_{calc}=0.41$ cf. QPM prediction of 69%					

TABLE XI. (*Continued*).

I^π	E_{lev} (keV)	$\Theta_{lab}=30°$ I_{expt}(rel)	$\Theta_{lab}=30°$ I_{calc}(rel)	$\Theta_{lab}=40°$ I_{expt}(rel)	$\Theta_{lab}=40°$ I_{calc}(rel)	$\Theta_{lab}=50°$ I_{expt}(rel)	$\Theta_{lab}=50°$ I_{calc}(rel)
	$K^\pi=4^+$ 719 keV band and calculation for pure $p1/2^+[411]+n7/2^+[633]$ CZ band						
4^+	719	7.3(11)	11.0	3.8(6)	7.8	4.7(6)	5.7
5^+	807		4.9	2.0(6)	3.2		2.8
6^+	911		0.8		0.6		0.5
$Sum_{J=4}$		7.3	11.0	3.8	7.8	4.7	5.7
	$Sum_{expt}/Sum_{calc}=0.64$ cf. QPM prediction of 85%						

[a]Experimental E_{lev} and I_{expt}(rel) from Table IV.
[b]Adopted E_{lev} from Table II.

^{166}Ho, the rotational parameters are well-behaved. In many cases, the parameters show slight variability with increasing spin, either decreasing or increasing in a more or less linear fashion. In these bands, one can fit level energies using a power series in $I(I+1)$, i.e., using the formula $E(I)=E_0+AI(I+1)+BI^2(I+1)^2$. The coefficients A and B can be obtained if three or more energies are known. Others exhibit an odd-even alternation that is frequently encountered in odd-odd nuclei with lower K values, e.g., $K=1$ and $K=2$ [49]. The energy levels in these bands can be fit using the formula $E(I)=E_0+AI(I+1)+D(-1)^I I(I+1)$. The observed alternation can be understood in terms of the Coriolis mixing of these bands with $K=0$ bands that have appreciable Newby shifts, either directly or through intermediates. Once the coefficients in the above formulas have been determined, one can predict the energies of higher lying levels, $E(4)$ and above. For those bands in ^{166}Ho where more than three level energies are known, we find the first rotational formula given above has the better predictive power for two of our $K=3$ (3^+AY) and $K=4$ (4^+AY) bands, as well as for the 1^+AX band. The remaining bands, three with $K=1$, two with $K=2$, and one with $K=3$, are best fit using the second rotational formula with its term whose sign alternates with increasing spin. We list the values derived for the rotational parameters for various bands in Table VIII.

Most of the experimental values show good agreement with rotational parameters modeled using our simple, semiempirical model. With this model, one derives a single value for the rotational parameters of a pair of GM partner bands. In the special case of GM partners where $\Delta K=1$, the bands may interact through Coriolis mixing, principally with each other. If this is the case, the observed rotational parameters will be displaced from some mean value, with the higher energy band exhibiting a larger parameter and the lower band exhibiting a correspondingly smaller rotational parameter. As can be seen in Table VIII, this is indeed the case for the band pairs: 3^+,4^+AY, 1^-,2^-BY, and 1^-,0^-CY. On the other hand, the relative magnitudes of the parameters of the band pairs: 4^+,3^+AT and 3^+,4^+CZ are opposite to that expected from this simple model. This behavior may appear to be anomalous because the levels labeled with a single configuration may not have dominant components of the assigned configuration, as seen from the single-nucleon transfer reaction data (especially the AT pair). Other components in the bands could be undergoing significant mixing, causing the observed deviations.

B. Rotational bands

$K^\pi=0^-(p7/2^-[523]-n7/2^+[633])$; 0, 82, 54, 171, 180, 330, 378, and 558 keV (AZ)

Our $\gamma\gamma$-coincidence spectra confirm earlier results [19] regarding level depopulation (Table II). Although not observed directly, a 9.39-keV transition between 4^- 180.4 keV and 3^- 171.1 keV levels is expected since several $\gamma\gamma$ coincidences found in a 116 keV gate are possible only if this transition exists.

Evidence confirming the two-quasiparticle assignment for this band is obtained from the (d,p) and $(d,^3\mathrm{He})$ results. Populations of band members with spins $I=1$ through 5 in both the (d,p) and $(d,^3\mathrm{He})$ reactions, with summed intensities comparable to those expected for a pure $p7/2^-[523]-n7/2^+[633]$ two-quasiparticle state (Tables X and XI), indicate the proton occupies the $p7/2^-[523]$ orbital and the neutron occupies the $n7/2^+[633]$ orbital, as in the ^{165}Ho and ^{167}Er target ground states, respectively. There may also be weak populations of the 6^- and 7^- band members in both reactions, but these would be obscured by much stronger unresolved peaks.

$K^\pi=7^-(p7/2^-[523]+n7/2^+[633])$; 6, 138, and 287 keV (AZ)

In earlier transfer reaction data, the 7^-, 8^-, 9^- levels of this band were seen in the (d,p) and (t,α) spectra with errors of about 5 keV. These levels are observed with greater precision in our new reaction data; e.g., from our (d,p) data, the 7^- level has the energy 6.21(25) keV. A more precise energy for this level, 5.98(2) keV, was previously determined by Balodis *et al.* [15] from γ rays populating and depopulating the band. The present best value for this level energy is 5.971(12) keV. Our placement of a 280.99(10) keV transition permits a more precise definition of the $I=9$ level energy, 286.96(10) keV.

As for the $K^\pi=0^-$ band discussed above, the observation of levels in this $K^\pi=7^-$ band in both single-nucleon transfer reactions, with summed intensities comparable to those expected for a pure $p7/2^-[523]+n7/2^+[633]$ two-quasiparticle state (Tables X and XI), confirms the

previously-known two-quasiparticle assignment. The cross sections for this band and the one discussed above are relatively weak in both reactions because the populations are mostly high angular momentum transfers of $l=5$ and $l=6$. Often the populations of low-lying, high-j transfers are even greater than predicted for the pure configurations, due to Coriolis mixing with higher-lying bands involving other $1h_{11/2}$ or $1i_{13/2}$ orbitals. Such mixing effects have not been included in the calculated values here.

$K^\pi=1^-(p3/2^+[411]-n1/2^-[521])$; 373, 416, 476, 563, 658, and 789 keV (BY)

The bandhead level for the above configuration, a $K^\pi=1^-$ level at 373 keV, was identified in the earliest studies of ^{166}Ho [9]. It was thought by these authors to have negative parity and a spin of 0 or 1 with configuration $0,1^-(p1/2^+[411]\mp n1/2^-[521])$. Sheline *et al.* [21] proposed a $K^\pi=1^-$ band of five levels, beginning at 373 keV and with a $1^-(p3/2^+[411]-n1/2^-[521])$ configuration assignment. Their first three levels agree with our interpretation, but we differ as to the $I=4$ and 5 levels in the band. Balodis *et al.*, having proposed the present configuration for this band in 1973 [23], first published the above level sequence in 1988 [15].

Our $\gamma\gamma$-coincidence data have allowed the placement of several new depopulating transitions. These transitions are split between feeding levels in the $K^\pi=0^-$ ground-state band and feeding lower levels within the BY band itself. No other attractive possibilities exist for the deexcitation of this $K^\pi=1^-$ band. We present evidence for γ transitions depopulating the $I^\pi=6^-$ level in the band at 788.610(12) keV. The rotational parameters for the band, while close to the predicted value, show some slight alternation which can be attributed to Coriolis mixing with $K^\pi=0^-$ bands. The phase of this alternation is consistent with mixing between this $K^\pi=1^-$ band and either or both of the two $K^\pi=0^-$ bands reported at 0.0 and 659.0 keV.

Of the two different configurations assigned to this band by previous authors, $1^-(p3/2^+[411]-n1/2^-[521])$ (BY) and $1^-(p1/2^+[411]+n1/2^-[521])$ (CY), we prefer the former since this is predicted by the semi-empirical model. Moreover, the BZ doublet lies lower than the CZ doublet which is a good indication of relative excitation energies for the B and C proton states. No significant transfer reaction population has been detected, consistent with a BY (or CY) assignment. The two (d,p) peaks that might be assigned to levels here are easily explained by close-lying levels in bands with a $7/2^-[523]$ proton.

$K^\pi=2^-(p3/2^+[411]+n1/2^-[521])$; 638, 705, and 793 keV (BY)

The negative-parity levels listed above were first detected in the ARC measurements of Bollinger and Thomas [13]. Of the transitions that depopulate these levels, several are supported by our coincidence data (Table II). In the paper of Bollinger and Thomas, the 638-keV level was proposed as a $K^\pi=2^-$ bandhead, but with a different configuration, namely $2^-(p1/2[411]-n5/2[512])$. Additional levels in the band were assigned at energies of 693, 771, and 867 keV. From our experimental data, we are unable to corroborate the existence of 3^- and 4^- levels at 693 and 771 keV; we have identified a level at 868.27 keV that is assigned as the $I^\pi=4^-$ member of a different band.

This $K^\pi=2^-$ band, as presently constituted, is assigned the $2^-(p3/2^+[411]+n1/2^-[521])$ (BY) configuration. The observed rotational parameter for the band, $A=11.1$ keV, matches that of its 1^- BY GM partner. Our semiempirical model predicts this band will occur at 590 ± 100 keV. band. The QPM calculations (Table IX) predict minimal mixing for both BY bands, consistent with the experimental observation that these bands are not populated by single-nucleon transfer reactions. The GM splitting between the two BY bands is 265 keV, not including rotational corrections. While one might try to explain this large splitting by citing an interaction between the 544-keV and 638-keV bands, there is little evidence that these are mixing with each other. Our QPM calculations indicate mutual admixtures of $<1\%$. Whereas large $\Delta j=2$ transitions are observed between levels of the 544-keV band and the 0^- ground-state band, analogous transitions are not observed in the depopulation of the 638-keV band. Sheline *et al.* [21] assigned the bandhead for this configuration to a level at 562.94 keV; additional levels in the band were not identified. Our data show strong evidence for the existence of the level, but our interpretation places this as the $I=4$ level in a $1^-(p3/2^+[411]-n1/2^-[521])$ band.

$K^\pi=5^-\{(p7/2^-[523]+n7/2^+[633])-Q_{22}\}$; 431, 530, and 644 keV (AZg)

In each of the odd-A nuclei neighboring ^{166}Ho, there is experimental evidence for a relatively pure, low-lying, γ-vibrational state built upon the ground-state quasiparticle configuration. The ground-state configurations of these $A=165$ and 167 nuclei are $p7/2^-[523]$ and $n7/2^+[633]$. Thus, the γ-vibrational states have $I^\pi=3/2^+$ or $3/2^-$ and occur at excitation energies ranging from 515 keV to 570 keV. We should, therefore, expect to find analogous states in ^{166}Ho. Energetically, the lowest of these would be those built upon the two AZ rotational bands that occur at 0 keV ($K^\pi=0^-$) and 6 keV ($K^\pi=7^-$). Of this expected pair of vibrational states, the lower, a new $K^\pi=5^-$ band, is proposed to consist of the three levels listed above. The existence of the two lower levels in this band was reported previously [25]. Detection of the bandhead at 431.240(5) keV is made difficult by the presence of an interfering level at 430.0 keV that dominates in the ARC and (d,p) spectra. Nevertheless, our $\gamma\gamma$-coincidence data provide evidence for the existence of the 431.2-keV bandhead. The two higher levels listed above do not suffer any interference and are seen in the (d,p) spectra, although they are weak peaks. For both levels, several depopulating γ transitions allow determination of precise level energies. These transitions all feed high-spin, high-K levels in lower bands.

We assign the configuration $5^-\{(p7/2^-[523]+n7/2^+[633])-Q_{22}\}$ because it is expected to occur well below any other $K^\pi=5^-$ state, probably somewhere close to

the excitations found for the γ-vibrational states in the neighboring odd-A nuclei, $\sim$550 keV. Other 5^- configurations, e.g. two-quasiparticle states such as $(p7/2^-[523]+n3/2^+[651])$ AW or $(p3/2^-[541]+n7/2^+[633])$ DZ, are expected to occur at energies above 800 keV and ranging well beyond 1 MeV [62]. There can be some mixing of these two-quasiparticle states into the 5^- γ-vibrational state, but this is expected to be a minor effect because the states are somewhat far apart in energy and the experimental data do not reveal any significant strength in single-nucleon transfer reactions. On the other hand, our QPM calculations suggest the major strength of a 5^- state occurring at 450 keV lies in the AW configuration (81%) with only a minor amount of vibrational nature (6% AZg). The observed rotational parameters of the 5^- vibrational band match the observed values of the 7^- AZ band which is to be expected for a vibrational state in an odd-odd nucleus.

$K^\pi=2^-\{(7/2^-[523]-n7/2^+[633])+Q_{22}\}$; 544, 597, 668, and 758 keV (AZg)

The four levels listed above have been detected previously in thermal neutron and resonance neutron capture measurements. Their existence as members of a single rotational band was first proposed by Balodis *et al.* [15] who suggested that the band has a large γ-vibrational component built upon the 0^- ground-state band. There is no evidence that any of these levels are observed in the single-nucleon transfer reactions, but for several members it is possible that weak populations could be obscured by strong peaks from unresolved levels.

The band is considered to have a $2^-\{(p7/2^-[523]-n7/2^+[633])+Q_{22}\}$ configuration. Consistent with this postulation, a large fraction of the γ-ray depopulation of each level in the band feeds levels of the $K^\pi=0^-$ band, the base configuration for this vibrational mode. The observed rotational parameters agree with those of the $K=5^-$GM partner of this band and with those of the ground state band (AZ) upon which the γ vibration is based. As with the previous band, the predominantly vibrational character of this band that has been demonstrated experimentally is at odds with our QPM calculation where a $K^\pi=2^-$ band occurring at 530 keV is suggested to have 62% quasiparticle AW character with a minor γ-vibrational component, 26% AZg.

$K^\pi=1^-(p1/2^+[411]+n1/2^-[521])$; 596, 628, 684, and 742 keV (CY)

Of the four levels assigned to this band, the upper three have been identified previously [13]. The bandhead at 595.841(5) keV, a level whose existence is supported by four depopulating transitions, was first assigned to the configuration listed above by Balodis [25]. Several new depopulating transitions are assigned to the upper levels. The present arrangement of levels in a $K^\pi=1^-$ band was also first proposed by Balodis [25]. The ARC data confirm the existence of the $I=2$, 3, and 4 levels. There is no evidence for significant population of any of these levels in the single-nucleon transfer reactions, but for some members any weak population would be obscured by large peaks for unresolved levels. The details of depopulation of the levels are somewhat mixed, but the overall pattern is to feed two low-K bands, 1^-BY and 2^+BZ. The rotational parameters exhibit an odd-even alternation that is characteristic of Coriolis mixing with $K=0$ bands. Using an alternate-sign rotational formula appropriate to a perturbed $K=1$ band, we obtain $A=8.581$ keV and $D=-0.216$ keV. The band is assigned a $1^-(p1/2[411]+n1/2[521])$ configuration which is predicted to occur at 585 keV by our semiempirical model. This same band has been identified in ^{170}Tm where it also exhibits a negative value for the D coefficient [63]. This observation helps to distinguish the present 1^-CY band from the 1^-BY band at 373 keV that has a positive D coefficient.

Sheline *et al.* [21] have proposed this 1^-CY configuration exists in ^{166}Ho at 350.61 keV; they have identified five band members. There are several criticisms that can be made of this assignment. (1) No ARC peak appears in the spectra for the proposed 2^-1CY level at 390.09 keV. (2) The γ rays assigned to these levels are, for the most part, extremely weak. The putative bandhead at 350.6 keV has a counterpart in the $I^\pi=1^-$ level at 373.2 keV. Both levels are fed predominantly by a cascade mechanism which provides statistical averaging so that two $K^\pi=1^-$ bandheads will exhibit comparable strength in the summed intensities of their depopulating transitions. But, experimentally we see that the total intensity out of the 373-keV bandhead is 2.0 (in arbitrary units) whereas the bandhead proposed by Sheline *et al.* is depopulated by transitions totaling only 0.16 units. Thus, we consider the evidence for the proposed band at 350.6 keV as questionable and we do not include it in our version of the excited levels of ^{166}Ho.

$K^\pi=0^-(p1/2^+[411]-n1/2^-[521])$; 659, 775, 726, 881, and 868 keV (CY)

The levels listed here are assigned to a new, $K^\pi=0^-$ band, previously unidentified in ^{166}Ho. All of these levels are new, although previous authors placed levels close to the energies of the three uppermost levels reported here. Level depopulation tends to favor feeding of levels in low-K bands, e.g., 1^-BY and 0^-AZ, as well as the structurally similar 1^-CY band. The ARC data confirm the existence of the $I=2$, 3, and 4 levels. There is no evidence that any of these levels are populated in single-nucleon transfer reactions. Evidence of the $I=0^-$ bandhead at 658.99(3) keV is sparse; its existence must be considered tentative. The rotational parameters derived from $(\Delta I=2)$ level spacings begin at 11.11 keV and decrease appreciably with higher spin; they match the predicted value of 10.31 keV reasonably well. The experimental Newby shift for this band is +47.1 keV, as compared with a predicted value of +31 keV [5].

Sheline *et al.* [21] have proposed this $K^\pi=0^-$CY configuration exists in ^{166}Ho at 525.37 keV $(I=0)$; they identified six members of the band. The energy spacings between various band members are quite regular and are compelling evidence for the band's existence, if taken alone. Nevertheless, the patterns of de-excitation proposed for various band members are startlingly different, so much so that one must assign members of the ensemble to at least two distinct con-

figurations. The $I=0,1,2,4$ levels all deexcite to negative parity levels. The $I=3$ and 5 levels both de-excite to positive parity levels (with one exception of one transition). This is an unphysical situation if one tries to assign all levels to the same band. Thus, the evidence for a $K^{\pi}=0^{-}$ band at 525.37 keV is questionable and we do not include it in our version of the excited levels of ^{166}Ho. However, we do recognize that certain pieces of experimental data (e.g., ARC spectra) point to levels with energies close to those proposed by Sheline *et al.* for this band. Generally, we have identified a different set of depopulating transitions that serve to define a precise energy for each level. We assign levels in our work at energies close to those claimed for the $I=2,3,4,5$ levels in the 0^{-}CY band, but with different spins and configuration assignments (and, in one case, different parity).

$K^{\pi}=3^{-}(p1/2^{+}[411]+n5/2-[512])$; 760, 838, and 935 keV (tentative band) (CX)

The assignment of several depopulating transitions provides good evidence for a level at 760.375(7) keV, apparently the bandhead of a $K^{\pi}=3^{-}$ band. These transitions display patterns of decay to levels in the bands $0^{-}AZ$, $3^{+}AY$, and $2^{-}AZg$. The upper two levels, whose existence is more tentative, occur at energies that indicate a regular rotational spacing with $A\approx 9.7$ keV. There is no evidence that any of these levels are populated in single-nucleon transfer reactions. The most likely configuration for this band is $3^{-}(p1/2[411]+n5/2[512])$ (CX), based upon a predicted energy of 799 keV and a predicted rotational parameter $A=10.8$ keV. It is also possible that another configuration, $3^{-}(p1/2[541]-n7/2[633])$ (EZ) plays a role here.

$K^{\pi}=3^{+}(p7/2^{-}[523]-n1/2^{-}[521])$; 191, 261, 348, 454, and 577 keV (AY)

The depopulation scheme for levels in this band (Table II) is essentially identical with that determined in previous studies [19]. It has a very strong (d,p) population, as expected from its previous assignment as predominantly a $p7/2^{-}[523]-n1/2^{-}[521]$ two-quasiparticle state. The measured relative (d,p) intensities have been normalized to expected cross section values for this band, as explained in Table III. This band is also observed in the $(d,^{3}\mathrm{He})$ reaction, probably because of a minor $p1/2^{+}[411]+n7/2^{+}[633]$ admixture, but the cross sections expected for pickup of a $1/2^{+}[411]$ proton (from above the Fermi surface) are too small for reliable quantitative estimates of the admixture to be made.

$K^{\pi}=4^{+}(p7/2^{-}[523]+n1/2^{-}[521])$; 372, 471, 588, and 723 keV (AY)

Previous studies have established the three lowest levels in this band [19]. We have found evidence for a level at 723.256(18) keV that we assign to the $I=7$ member of the band. This band is very strongly populated in the (d,p) reaction, and includes the strongest peak in the spectrum of Fig. 6, thus supporting the existence and main structural component of the band. Table X shows that the summed (d,p) intensity for this band is in excellent agreement with that predicted.

$K^{\pi}=5^{+}(p3/2^{+}[411]+n7/2^{+}[633])$ and $(p7/2^{-}[523](p7/2^{-}[523]+n3/2^{-}[521])$; 264, 380, and 514 keV (BZ+AU)

This band has been characterized in previous studies [19]. The $I^{\pi}=5^{+}$ bandhead is well established by two depopulating transitions, one of which has $M2$ multipolarity and leads to the 7^{-} level at 6 keV, and by peaks observed in the spectra from ARC measurements and the (t,α) reaction. In 1978 Balodis [24] proposed the placement of a key transition, the 257.8-keV $M2$, that links this bandhead with the isomeric level at 6 keV. Schilling *et al.* [64] have set a limit of $t_{1/2}\leqslant 0.5$ ns for the half-life of this 5^{+} bandhead. However, the Weisskopf estimate for the partial half-life of the 257.8 keV $M2$ transition ($I_{\gamma}=0.26$) is about 350 ns. Assuming that the total depopulation intensity of the 263.8 keV 5^{+} level is about 5, we obtain $t_{1/2}=15$ ns. This value is at variance with the upper limit of Schilling *et al.* According to a private communication of these authors, their value could be incorrect due to the very weak γ-intensity of the transitions.

We propose new assignments of the γ rays depopulating the $I=6$ and 7 levels that allow determination of more precise level energies, 6^{+} 379.549(4) and 7^{+} 514.363(7) keV. These levels were also identified in previous (d,p) and (t,α) spectra [11,12]. Although the (d,p) peak for the 6^{+} member at 379.5 keV is not resolved from that for the 6^{-} level at 377.8 keV, the latter is expected to have an almost negligible fraction of the observed intensity (see Table X). The improved resolution of the current (d,p) measurements has allowed the $I^{\pi}=5^{+}$ member at 263.8 keV to be detected near the more strongly populated $I,K^{\pi}=4,3^{+}$ level at 260.7 keV. The levels assigned to this band were also identified in (t,α) spectra.

Motz *et al.* [9] concluded that this band is an admixture of two configurations, i.e., $p3/2^{+}[411]+n7/2^{+}[633]$, which is predicted to occur close to the bandhead energy of 263.8 keV, and $p7/2^{-}[523]+n3/2^{-}[521]$, which could contribute to the (d,p) population of the band. Additional strong experimental evidence for the first of these components has been provided by (t,α) data and discussed by Dewberry *et al.* [12], as well as by the present $(d,^{3}\mathrm{He})$ results. Although for each of these proton-pickup reactions the 5^{+} bandhead has the strongest peak in the spectra, the absolute (t,α) cross sections are only slightly greater than half the values expected for a pure $p3/2^{+}[411]+n7/2^{+}[633]$ configuration. This result is reproduced by the present QPM calculations (Table IX) which show a 60% admixture for this configuration and a 30% $p7/2^{-}[523]+n3/2^{-}[521]$ component. [The $(d,^{3}\mathrm{He})$ intensities in Table IV were normalized using this band and its GM partner.]

In spite of the good agreement for the component described above, the (d,p) data appear to indicate the situation is more complex. The comparison of observed and expected (d,p) intensities in Table X shows not only that the observed distribution of intensity among band members (fingerprint) does not resemble that expected for the $p7/2^{-}[523]$

$+n3/2^-[521]$ configuration, but that the observed strength is much larger than expected, especially for the spin 6 and 7 members. The calculated values are rather weak because the $3/2^-[521]$ orbital is below the Fermi surface. In searching for a possible explanation for the large (d,p) intensities one could consider a $p7/2^-[523]+n3/2^-[512]$ admixture, as the $3/2^-[512]$ orbital is above the Fermi surface and should have large cross sections. However, it would be expected at a much higher energy. Other possible sources to consider for the (d,p) strength observed in this $K^\pi=5^+$ band could be Coriolis mixing with $p7/2^-[523]+n1/2^-[521]$ and/or $p7/2^-[523]+n1/2^-[510]$ configurations. The latter two both have large predicted cross sections, but would have much stronger intensities for the spin 5 member than for the spin 6 and 7 ones, contrary to experiment. A much more satisfying explanation, and one involving some interesting physics, is that the strong populations observed for the spin 6 and 7 members arise from Coriolis mixing between the $p7/2^-[523]+n3/2^-[521]$ component and the nearby $K^\pi=6^+$, $p7/2^-[523]+n5/2^-[512]$ band at 295 keV, which is described in a following subsection. The $n3/2^-[521]$ and $n5/2^-[512]$ orbitals are coupled by a fairly large Coriolis matrix element, $\langle j_- \rangle$, of about 2.8 keV. Earlier Coriolis calculations [22] showed no appreciable mixing of the $K^\pi=6^+$ band with any other configurations, but in that case the $p7/2^-[523]+n3/2^-[521]$ state had been placed at a higher energy, near 1 MeV, on the basis of simple model expectations. Sample Coriolis calculations performed in a similar manner for the present study, but with the $p7/2^-[523]+n3/2^-[521]$ band placed at 264 keV, exhibit quite large mixing between these $K^\pi=5^+$ and $K^\pi=6^+$ bands. In the actual situation, there is not a pure $p7/2^-[523]+n3/2^-[521]$ two-quasiparticle state at 264 keV, but only a (minor) component of one. The reduced amount of mixing due to such a component was simulated by reducing the value of the attenuation coefficient by which the Coriolis matrix elements were multiplied. Calculations performed using the standard formalism [65] for ordinary two-quasiparticle bands showed significant mixing but very little transfer of (d,p) strength between the bands because there was constructive interference for the (already large) $K^\pi=6^+$ intensities and destructive interference for the (originally weak) $K^\pi=5^+$ ones. However, the QPM prediction showed that the phase of the $p7/2^-[523]+n3/2^-[521]$ component at 264 keV is of opposite sign to that of the pure two-quasiparticle state (e.g., as predicted with the residual interaction switched off), and therefore opposite to that used in the Coriolis mixing calculation mentioned above. With the phase of this component reversed, typical predictions have 30% to 50% of the strengths for the $K^\pi=6^+$ band transferred to the $K^\pi=5^+$ one. This reproduces the observations shown in Table X, where the 6^+ and 7^+ members of the $K^\pi=5^+$ band have about 39% of the total cross section expected for the corresponding members of a pure $K^\pi=6^+$, $p7/2^-[523]+n5/2^-[512]$ band. (The same spin members of the $K^\pi=6^+$ band, discussed below, have about 53%.) This implies that the 264 keV band has three significant two-quasiparticle components, instead of the two in previous interpretations.

$K^\pi=2^+$(p3/2$^+$[411]−n7/2$^+$[633] and (p7/2$^-$[523](p7/2−[523] −n3/2$^-$[521]); 430, 482, 548, 634, and 733 keV (BZ+AU)

Evidence for the first four levels in this band has been established previously [19]. From our $\gamma\gamma$-coincidence data, we find good agreement with the transition-placement data for these levels. We have identified the 6^+ rotational level in this band for the first time at 732.549(14) keV, based upon depopulating transitions and observation in the $(d,^3\mathrm{He})$ and (t,α) spectra.

Evidence for configuration mixing in this band is provided by the observation of peaks in three direct-reaction spectra, those of the (d,p), $(d,^3\mathrm{He})$, and (t,α) reactions. As for the $K^\pi=5^+$ GM partner of this band, described above, the proton pickup reactions are consistent with a $p3/2^+[411]-n7/2^+[633]$ admixture of slightly more than 50% in this band. Also, as for the 5^+ band, the QPM calculations of Table IX predict a mixed configuration for this 2^+ band, including admixtures of 50% $p3/2^+[411]-n7/2^+[633]$ and 39% $p7/2^-[523]-n3/2^-[521]$. However, a quantitative examination of the (d,p) data shows that this $K^\pi=2^+$ band must also contain other admixtures than these. The comparison of observed and expected intensities seen in Table X shows a very anomalous pattern. The 2^+ bandhead is populated significantly, having intensities that could be compatible with a $p7/2^-[523]-n3/2^-[521]$ bandhead. The 3^+ level is populated so weakly that it was observed at only one of the three angles, even though it is in a clear region of the spectrum. The 4^+ member is populated very strongly and the 5^+ one quite significantly. There is no pure two-quasiparticle configuration predicted to have such a fingerprint pattern, and the total strength is far too large for any reasonable $p7/2^-[523]-n3/2^-[521]$ admixture. It seems very likely that the large strength for the 4^+ level (which is at 548 keV) arises from some type of mixing with the close-lying 4^+ level at 559 keV, which is tentatively assigned below as the $p7/2^-[523]+n1/2^-[510]$ bandhead. The populations of these two levels in the (d,p) reaction are similar to each other, and in the $(d,^3\mathrm{He})$ reaction they are almost identical to each other, consistent with a very strong mixing of their wave functions. The 5^+ members of these bands, at 634 keV and 655 keV, are also both observed in both reactions, consistent with appreciable mixing for these levels as well. It thus appears that the large unexpected (d,p) strength observed in this $K^\pi=2^+$ band is likely some of the ''missing'' strength from the $p7/2^-[523]+n1/2^-[510]$ band at 559 keV. The exact nature of the mixing is less clear, as significant amounts of strength appear to have been transferred between bands with $\Delta K=2$. If this occurred via the Coriolis interaction the process could have involved one or more of the $K^\pi=3^+$ bands as intermediaries.

Analogous to the situation for the GM partner described in the previous subsection, it is likely that the $p7/2^-[523]-n3/2^-[521]$ component in the 430 keV band mixes by Coriolis coupling with the $K^\pi=1^+$, $p7/2^-[523]$

$-n5/2^-[512]$ band at 426 keV described below. In this case, with the phase of the $p7/2^-[523]-n3/2^-[521]$ component opposite to that of the pure two-quasiparticle state, as predicted by the QPM, the sample Coriolis calculation shows there is no significant transfer of (d,p) strength between these two bands. (This is consistent with the observation that the $K^\pi=1^+$ band appears with the full strength expected for the pure two-quasiparticle state.) To summarize, there are probably four different two-quasiparticle configurations that have appreciable components in the 430 keV band; the major $p3/2^+[411]-n7/2^+[633]$ one responsible for the (t,α) and $(d,^3\mathrm{He})$ populations, the $p7/2^-[523]-n3/2^-[521]$ one introduced by the residual interaction as calculated in the QPM, a $p7/2^-[523]+n1/2^-[510]$ one for spin $I\geqslant 4$ members due to mixing with the very close-lying $K^\pi=4^+$ band [needed to explain the (d,p) intensities for the 4^+ member], and the $p7/2^-[523]-n5/2^-[512]$ admixture predicted by Coriolis calculations.

$K^\pi=6^+(p7/2^-[523]+n5/2^-[512])$; 295 and 424 keV (AX)

The 7^+ rotational level in this band, previously known only very approximately, has been established with an energy of 423.654(10) keV using our (d,p) reaction results and depopulating transitions. The rotational parameter for this band, $A=9.18$ keV, shows better agreement than previously with the modeled value in Table VIII, 9.66 keV, and with that of its $\Omega_p\pm\Omega_n$ doublet counterpart, 9.62 keV. The (d,p) intensity and its distribution provide strong evidence that the dominant component of this band is the $6^+(p7/2[523]+n5/2[512])$ configuration but, as mentioned above, there seems to be significant loss of strength by Coriolis mixing to the $K^\pi=5^+$ band at 263 keV.

$K^\pi=1^+(p7/2^-[523]-n5/2^-[512])$; 426, 465, 522, 599, 694, and 807 keV (AX)

The basic level structure of this band was determined in previous studies where level energies were reported for five members of the band [9,19]. From our $\gamma\gamma$-coincidence measurements we find good agreement with the transition placement data for the three lowest energy levels. We report several new depopulating transitions that are assigned to the $I=4$ and 5 levels. Thus, we have determined more precise energies for these levels, namely 4^+ 598.511(6) keV and 5^+ 693.701(6) keV. Although a level at 693.385(2) keV was deduced in previous work using the Ritz combination principle (see the 1992 Nuclear Data Sheets summary [19]), it was not assigned to this band. We find evidence for a level with a significantly different energy ($\Delta E=316$ eV) and assign this to the $I=5$ member of the band. All six levels listed above were detected in our (d,p) measurements where improved resolution has allowed resolution of peaks at 426.04 and 464.50 keV. Both peaks appeared in previous measurements as part of unresolved doublets.

Sood and Burke [22] have presented a detailed analysis of (d,p) intensities and beta decay into ^{166}Ho. They concluded that the largest component of this band at 426 keV has the configuration $(p7/2^-[523]-n5/2^-[512])$, contrary to some previous assignments. Our new (d,p) results including the angular dependence of intensity (Table X) support this interpretation. By default, the 1^+ band at 568 keV is assigned the configuration $(p7/2^-[523]-n5/2^-[523])$. Each band contains about 10% of the other due to $\Delta K=0$ mixing. As mentioned earlier, the 426 keV $K^\pi=1^+$ band also has appreciable Coriolis mixing with the $p7/2^-[523]-n3/2^-[521]$ component of the $K^\pi=2^+$ 430 keV band, but there is very little transfer of (d,p) strength between these bands. The summed (d,p) strength (Table X) agrees well with the value predicted for the pure two-quasiparticle state. (This is unlike the situation for the $K^\pi=5^+$ and $K^\pi=6^+$ GM partners of these bands, for which there was significant transfer of strength.) The overall behavior of the Coriolis mixing for these four bands nicely explains the observation that the summed intensity for the $K^\pi=1^+$ band is about 50% larger than that for its $K^\pi=6^+$ GM partner. (Without significant mixings a band is expected to have a single-nucleon transfer strength similar to that of its GM partner.) It should be noted that these assignments are in agreement with both our simple semi-empirical model and our QPM calculations.

$K^\pi=4^+(7/2^-[523]+1/2^-[510])$; 559, 655, and 772 keV (AT)

The lower two levels listed above were first identified as $I^\pi=4^+$ and 5^+ levels and were assigned to the above-listed configuration by Bollinger and Thomas [13]. Our $\gamma\gamma$-coincidence data are consistent with the previously assigned depopulating transitions; we add several more. These lower two levels appear in both (d,p)- and $(d,^3\mathrm{He})$-reaction data. We propose a new level, $I^\pi=6^+$, at 771.77(8) keV, based upon three depopulating transitions observed in the $\gamma\gamma$-coincidence data. Resolution of this level from an $I^\pi=5^+$ level at 769.5 keV was facilitated by coincident-γ observations.

The pattern of transitions depopulating levels in this band includes much strength feeding levels with $(p7/2^-[523]\pm n1/2^-[521])$ (AY) configurations, consistent with a simple $n1/2^-[510]$ to $n1/2^-[521]$ transformation, as well as some intraband transitions. However, from Table X it is seen that the observed (d,p) strength is only about 16% of that expected for a pure $p7/2^-[523]+n1/2^-[510]$ two-quasiparticle state, indicating the assigned label may not represent the major component of this band. It was mentioned above that levels of the $K^\pi=2^+$, 430-keV band were very close in energy to corresponding spin members of this band, and appeared to have acquired some of the ''missing'' $p7/2^-[523]+n1/2^-[510]$ strength. However, even for the strongly populated spin 4 member this would account for only another 9% of the expected strength. The most likely reason for the small summed $p7/2^-[523]+n1/2^-[510]$ strength in this band is that there is probably a great deal of additional mixing. Studies of odd-mass Dy, Er, and Yb nuclides [66–68] with (d,p) reactions have shown that the $1/2^-[510]$ band appears systematically at lower energies and with smaller cross sections than expected for the pure Nilsson orbital, and this has been ascribed to mixing with phonons based on lower-lying states. In particular, for ^{165}Dy and ^{167}Er, isotones of ^{166}Ho, there is only about 25% to 30%

of the full single-particle (d,p) strength for the $1/2^-[510]$ orbital found at the excitation energies listed for this state in Table VII [66,67]. (These weaker strengths were in approximate agreement with QPM calculations for the odd-mass nuclei at that time.) Therefore, it is not surprising to find the total (d,p) strength for transfer of a $1/2^-[510]$ neutron is reduced to a similar small fraction in this study. In the following subsection it will be seen that the $K^\pi = 3^+ (p7/2^-[523] - n1/2^-[510])$ GM partner to this band also has a small summed strength (about 28% of that expected for the pure configuration). It therefore seems likely that the QPM estimates of 70% and 74% in Table IX for the $p7/2^-[523] \pm n1/2^-[510]$ configurations in the 559 and 815 keV bands are overestimates. It is also likely that some strength could be lost to other bands by Coriolis mixing, but it is believed the main reason for the reduced strength is provided by the above explanation.

The 4^+ bandhead at 559 keV is populated appreciably in the $(d,{}^3\mathrm{He})$ spectrum, most likely due to mixing with the 4^+ level at 548 keV, from which it gains some of the $p3/2^+[411] - n7/2^+[633]$ strength. The weak population of the 5^+ member at 655 keV can also be explained by this component. The only component in Table IX predicted to be observed in the proton pickup reaction is a 1% admixture of the $p1/2^+[411] + n7/2^+[633]$ configuration, but it would have expected intensities much smaller than those observed and its contribution to the strengths is probably negligible compared to those from mixing with the $K^\pi = 2^+$ band.

$K^\pi = 3^+ (p7/2^-[523] - n1/2^-[510])$; 815, 891, 985, and 1099 (AT)

In previous studies [13], the lowest three levels in this band were identified in precise ARC measurements and were assigned to the configuration listed above. Our $\gamma\gamma$-coincidence data confirm the large number of transitions assigned to the level at 815.1 keV, as well as the depopulation of the 891.0-keV level. We provide depopulating transitions for the $I^\pi = 5^+$ level at 985.15(4) keV. Consistent with the assigned configuration, 3^+AT, the depopulation pattern of the 815-keV level includes considerable decay to levels in (AY) bands and apparently significant amounts of decay to the 3^+CZ band and to the 2^+BZ band. All of the levels in this 3^+AT band appear in the (d,p) spectra; the 6^+ member is a level at 1098.61(21) keV, newly identified in these spectra. As mentioned in the discussion of the GM partner band in the previous subsection, the observed total (d,p) intensity is only about 28% of that expected for the pure $p7/2^-[523] - n1/2^-[510]$ band (Table X), indicating considerable mixing with other configurations.

$K^\pi = 1^+ (p7/2^-[523] - n5/2^-[523])$; 568, 605, 662, 736, 832, and 943 (AV)

The five lowest levels in this band were identified previously [13,19] and were assigned as members of a $K^\pi = 1^+$ band. They are all populated in the (d,p) spectra; three of these are new observations. Most of the depopulating transitions from the two lowest levels were assigned previously. From our $\gamma\gamma$-coincidence data, we have placed several new transitions that show decay from the higher band levels. We have added a new level to this band, an $I^\pi = 6^+$ level at 942.605(13) keV.

The configuration of this band has already been mentioned in an earlier section of this paper dealing with the 1^+AX band at 426.0 keV. Our QPM calculations find some mixing, 9%, of the 1^+AX configuration in the present band. Thus, one would expect the transitions that depopulate the present band to feed levels in the 1^+AX band. This is indeed the case; in addition, several intraband transitions are also present. Table X shows that the total (d,p) intensity observed is somewhat greater than expected for a pure $p7/2^-[523] - n5/2^-[523]$ configuration. This is probably because of the small $p7/2^-[523] - n5/2^-[512]$ admixture, which has much larger cross sections since it is dominated by transfers of lower l value.

$K^\pi = 6^+ (p7/2^-[523] + n5/2^-[523])$; 722 and 848 (AV)

We assign the levels listed above to a new band with a previously unidentified configuration. The existence of these levels is supported by our $\gamma\gamma$-coincidence data. The 848-keV level is also observed in the (d,p) reaction. The 722.0-keV level is not resolved from another strong contributor in the (d,p) spectrum, a 7^+ level at 723.2 keV. This 6^+ band is predicted to occur at 733 keV by our semiempirical model. The observed rotational parameter, 9.04 keV, matches that of its $K^\pi = 1^+$ GM counterpart at 567.6 keV, 9.46 keV. The summed (d,p) intensity observed is less than half that expected for the pure configuration.

$K^\pi = 3^+ (p1/2^+[411] - 7/2^+[633])$; 592, 672, 770, and 884 keV (CZ)

On the basis of their ARC data, Bollinger and Thomas [13] assigned the three lowest levels of this band to the configuration listed above. Our $\gamma\gamma$-coincidence data support the existence of these levels, as well as being consistent with the assigned spins and K quantum numbers for this band. The 6^+ rotational level in this band has been established for the first time at 884.055(14) keV on the basis of deexciting transitions, largely intraband, and observation in spectra from transfer reactions. It would be expected that the assigned configuration should be populated in the proton pickup reactions, although relatively weakly because the $1/2^+[411]$ orbital is above the Fermi surface. Table XI shows that the summed $(d,{}^3\mathrm{He})$ intensity observed is about 40% of the value expected for the pure two-quasiparticle state. This is consistent with the (t,α) data of Ref. [12], in which it is seen that the cross section for the 592 keV bandhead is 13 μb/sr, about 45% of the predicted value of 29 μb/sr for this state. These results are somewhat smaller than the predicted value of 69% for the 3^+ CZ component (Table IX). There appears to be configuration mixing with the $K^\pi = 3^+$ AY band at 190 keV, as mentioned in an earlier subsection for that band. The (d,p) intensities for the 592 keV band could be explained by a 3^+ AY admixture of less than 10% (Table X). However, the situation is probably more complex. Table IX shows predicted components of 15% AY and 15% AT in this band. The (d,p) transition amplitudes for these components would

combine coherently, so it is not possible to extract admixtures from the observed intensities. Deexciting transitions feed levels in the 3^+AY and 2^+BZ bands.

Dewberry *et al.* [12] reached a different conclusion regarding the identification of this 3^+CZ configuration. On the basis of cross sections they have measured for the (t,α) reaction, deduced l transfers from angular distributions, and an application of the Ritz combination principle, they as signed the 3^+3CZ bandhead to a level at 721.07 keV and placed three rotational levels above this bandhead. The upper levels are connected by various intraband transitions, but no γ rays are assigned to the upper levels that would feed levels below the bandhead. The placement of many low-energy transitions high in the decay scheme raises some questions as to the validity of these assignments [12], but we cannot disprove their thesis. Our version of the levels that make up the 3^+3CZ band is supported, at least partially, by coincidence relationships. We also note that Dewberry *et al.* have observed in their (t,α) spectrum the 592-keV level that we claim as the bandhead level of our 3^+3CZ band and have assigned three depopulating transitions; they identified this level as having $I^\pi=3^+$, but left it unassigned with respect to configuration.

$K^\pi=4^+(p1/2^+[411]+n7/2^+[633])$; 719, 807, and 911 keV (CZ)

Bollinger and Thomas [13] identified the two lowest levels in this band, and our $\gamma\gamma$-coincidence data support these assignments. We tentatively propose the 6^+ rotational member is at 911.40(4) keV, on the basis of a very weak peak in the (d,p) spectrum and an intraband γ transition. The 4^+ bandhead is populated in the $(d,^3\mathrm{He})$ and (t,α) reactions with $\sim$64% and $\sim$80%, respectively, of the intensity expected for the pure two-quasiparticle configuration (Table XI and Ref. [12]). It is not certain whether the 719 and 807 keV levels are populated in the (d,p) reaction because there are weak peaks for other unresolved levels near these energies. These results suggest there is a dominant CZ component in this band, consistent with the QPM prediction of an 85% component for this configuration.

Dewberry *et al.* [12], in their analysis of the (t,α) data, assigned three levels to a rotational band at 891.7 keV with the 4^+CZ configuration, thus differing with the conclusions of Bollinger and Thomas [13] and Sood *et al.* [20] as to the location of this configuration. As they did in their definition of the 3^+CZ band, Dewberry *et al.* used the Ritz combination principle to locate depopulating γ transitions that define these level energies more precisely. We believe it is unlikely that so many transitions of low to moderate energy (71–323 keV) can occur at high excitation energies in ^{166}Ho and still be detected in the *singles* (n,γ) spectrum. We prefer the interpretations put forth previously [13,20] that places these bands at slightly lower excitation energies. The two lower levels assigned here are supported by our measured coincidence relationships. Since there is disagreement in interpreting the (t,α) data, care has been taken to account for these revised assignments in discussing cross sections for specific configurations in the above paragraphs.

$K^\pi=2^+$; 906, 961, and 1030 keV (tentative band)

The levels listed above have been identified in previous studies where the more conclusive evidence for their existence came from ARC data and (d,p) spectra. The present $\gamma\gamma$-coincidence data confirm their existence, but they do not support the previously assigned depopulating transitions. One of the difficulties in defining these higher levels in ^{166}Ho is that the γ-transition energies in question have rather large uncertainties. In the SACP measurement (Table II), two levels with energies 1029.6 and 1030.6 keV are found, with depopulation to the $I^\pi=1^-$ to 5^- levels of the ground state band and to the levels 3^+ 190.9 keV and 4^+ 260.6 keV. It seems very likely that two close-lying levels exist here with spin and parity 2^- and 4^+. Consistent with this hypothesis, the ARC data (Table I) indicate the existence of a 3^+ or 4^+ level at 1032.1(4) keV.

In Table IX this tentative band is associated with one from the QPM calculations that has a large (62%) $K^\pi=2^+AU$ $(p7/2^-[523]-n3/2^-[521])$ component. In Table X it is seen that the medium-intensity (d,p) cross sections are consistent with this proposed band having a $\sim$67% $(p7/2^-[523]-n3/2^-[521])$ component in this band, and this ought to have been observed in the proton pickup spectra with a strength about one-quarter of that for the $K^\pi=2^+$ band at 430 keV. The $(d,^3\mathrm{He})$ cross sections become weaker at excitation energies this high because the ejectile energy is near the Coulomb barrier, but this problem does not exist for the (t,α) measurements. The expected fingerprint pattern has large intensities for each of the spin 2, 3, and 4 members and, although the (t,α) spectrum [12] has a peak at 915 keV which could to some extent obscure the 906-keV bandhead, there are no large cross sections at 961 or 1030 keV (see Table II of Ref. [12]). Therefore, the data do not support the presence of this minor component.

$K^\pi=5^+$; 926, 1038 keV (tentative band)

This band, which may be the GM counterpart of the 2^+ band just discussed, is proposed for the first time. The 925-keV level is observed in the ARC, (d,p), and $\gamma\gamma$-coincidence spectra. The (d,p) data also include a 1038.4-keV level that is assigned to the 6^+ level of the band. The rotational parameter defined by these two levels, 9.41 keV, is consistent with that of its GM counterpart, 9.27 keV and with a calculated value, 9.87 keV. In Table IX the QPM calculated structure of this band includes a 62% component of the $K^\pi=5^+(p7/2^-[523]+n3/2^-[521])$ configuration, and Table X shows that the (d,p) cross sections are consistent with a $\sim$48% admixture of such a band. There is also a significant (13%) BZ component predicted in this band by the QPM, which should be observable in the (t,α) spectrum, as for the GM partner discussed in the previous subsection. The (t,α) results are not as definitive in this case; there is a peak reported at 1037(7) keV which could correspond to the proposed 6^+ member, but the reported uncertainty on the 915(3) keV peak would have to be stretched for it to correspond to the proposed 5^+ bandhead at 926 keV. Thus, the existence and nature of these suggested bands should be considered as tentative.

C. *n-p* interaction matrix elements

From the band structure of ^{166}Ho just discussed, one can determine values for several matrix elements that arise from the *n-p* interaction in ^{166}Ho, ten Gallagher-Moszkowski splittings and two Newby shifts. These values are listed in column 8 of Table VIII. The GM matrix elements reported here have not been corrected for perturbations in band energies due to Coriolis mixing which occurs most significantly for configurations that include high-*j* orbitals, e.g., $n7/2^+[633]$ and $p7/2^-[523]$.

The experimental Newby shifts (rotational bands 0^-AZ and 0^-CY) show good correspondence with theoretical values calculated by Frisk [5] and less agreement with the calculations of Nosek *et al.* [6]. Among the E_{GM} values, there are four where each pair of bands was known previously and where there is agreement as to the energies of the constituent bands and the GM matrix elements. These include the following configurations: AZ, AY, (BZ+AU), and AT. For another set of four matrix elements, there are differences among various authors regarding the energies of the constituent bands in a given pair that result in differences in E_{GM} values. These differences, which involve the configurations AX, BY, CY, and CZ, have been discussed in the individual subsections of Sec. VI B in this paper. In the case of the AX configuration, it is now generally accepted that the $K^\pi=1^+$ member of this band pair exists at 426.1 keV [22]. The appropriate value for E_{GM}(AX) is +177.2 keV. In Ref. [8], the band energies listed in their Table III for this configuration reflect this view, but the matrix element listed in their Table I is 316.8 keV, a value inconsistent with the foregoing discussion.

Our experimental value for E_{GM}(AV), −108.5 keV, is new. A value of $E_{\mathrm{GM}}=-146.0$ keV for this same configuration in ^{164}Ho was known previously [4,6]. Our determination of a GM matrix element for the (AZ+γ vibration), +138.2 keV, is also new. The question of what effect some γ vibrational character in the state would have on the *n-p* interaction matrix element can be asked. While one might expect the interaction matrix element to become smaller in magnitude, this is not the case here, since the low-lying AZ bands yield a value of $E_{\mathrm{GM}}(AZ)=+84.1$ keV.

The experimental GM matrix elements can be compared with theoretical calculations of these quantities made by various authors. The best fit is obtained from the calculations of Boisson *et al.* [4] where six matrix elements can be compared (see Table VIII) with experiment. The root-mean-squared deviation for this set is 14 keV, which shows markedly better agreement than for the calculations of Nosek *et al.* [6] (8 E_{GM}'s, rms deviation = 31 keV) or those of Hoff [69] (6 E_{GM}'s, rms deviation = 48 keV). Despite this good showing by Boisson *et al.* [4] for the matrix elements in ^{166}Ho, the predictive power of their set of E_{GM} calculations over a wider range of nuclei has been shown to be rather poor [70].

VII. CONCLUSION

The level scheme of ^{166}Ho was studied using new, more precise and more sensitive experimental methods. Because we have made comprehensive $\gamma\gamma$-coincidence measurements, many γ-transitions are now unambiguously placed in the γ-decay scheme. The deduced γ-branching ratios provided information on the various mixing mechanisms in this nucleus. New average resonance neutron capture results provide spin and parity values for levels up to 985 keV. The (d,p) and $(d,^3\mathrm{He})$ reactions, which were measured with high sensitivity and very good resolution, gave the best signatures for the single-particle structure of the nucleus. Levels with higher spins were predominantly seen in the transfer reactions. The high quality of the new experimental data helped to define excited levels in ^{166}Ho in spite of the large and increasing level density in this odd-odd nucleus. Results of the present investigation, as well as those of previous studies, permit the identification of 91 levels up to 1100 keV. Of these, 32 levels are newly identified. The levels are grouped in 23 rotational bands, among them 6 new ones. Consequently, a total of 10 Gallagher-Moszkowski splittings and 2 Newby shifts could be determined. In many cases we have extended previously known rotational bands by identifying new, higher spin levels.

It is often of interest to estimate what portion of the experimental level scheme represents a complete description of the nuclear excitations within a given nucleus. We use the predictions of our semiempirical model to guide such an estimate. Referring to the first twelve rotational bands listed in Table VIII, one can see that each of the experimentally determined configurations has been assigned to a calculated band excitation. Beginning at 575 keV, certain calculated configurations appear that have not yet been identified in ^{166}Ho, e.g., $K^\pi=4^-,1^-$BX; $3^-,4^-$EZ; etc. In the first 815 keV of excitation, we assign 21 predicted configurations to experimental bandheads. This leaves 7 unassigned configurations in this same energy range, 6 with negative parity and 1 with positive parity. This bias in favor of determining the location of positive-parity bands can be ascribed to the power of the ARC technique where positive-parity levels are favored.

Important progress in the interpretation of this level scheme has been achieved with new improved quasiparticle-phonon model calculations where residual interactions and γ, β, and octupole phonons were taken into account. The largest calculated γ-vibration mixing was found for the 2^- band predicted at 525 keV. In this case the configuration was calculated to consist of 26% of the $\{(p7/2^-[523]-n7/2^+[633])+Q_{22}\}$ configuration and 7% of the $\{(p7/2^-[523]+n1/2[660])-Q_{22}\}$ configuration. Other low-lying levels had generally only small collective components. From the experiment, it follows that the 2^- γ-vibrational band built on the ground state has the bandhead energy at 543.6 keV and is depopulated by strong $E2$ transitions to the ground state band. This band was not populated in transfer reactions. Apparently the collective component of this 2^- band is larger than predicted by the calculations. The 5^- γ-vibration built on the other member of this GM pair appears at an energy of 431.2 keV. In this case the collective component is larger than calculated also, even though the bandhead seems to have been observed in the (d,p) reaction. It appears that the agreement between the experiment and the

new calculations of both vibrational bands is much better than in previous theoretical results [26].

For most of the lower-lying bands the summed intensities in the single-nucleon transfer experiments were in good qualitative agreement with the expectations based on the microscopic compositions predicted by the QPM. Above about 1/2 MeV excitation there was often less strength observed in the experiments than calculated, possibly indicating a greater degree of mixing than considered. It should also be noted that even for the lower bands the distributions of intensities within bands (fingerprints) were often in poorer agreement with predictions than is usually found in such experiments on other well-deformed nuclei. This may be due (at least partly) to Coriolis mixing, which has not been considered in calculating the strengths.

The mixing of rotational band configurations has been deduced not only from the comparison of calculated and experimental transfer reaction cross sections and level depopulations, but also from rotational parameters. As the result of Coriolis ($\Delta K=1$) and residual ($\Delta K=0$) interactions, several negative parity bands are mixed, e.g., the 0^- ground state, the 1^- band at 373.0 keV, the 1^- band at 595.8 kev and the 0^- band at 658.9 keV. Only the odd-spin members of the ground-state band are strongly populated from γ decay of levels in the 373-keV 1^- band due to the above-mentioned mixing. The 2^+ band at 430.0 keV, the 3^+ band at 190.9 keV and the 4^+ band at 371.9 keV also show strong Coriolis mixing. Additional positive parity bands, especially the $(p1/2^+[411]\pm n7/2^-[633])$ and $(p7/2^-[523]\pm n1/2^-[510])$ contribute to this mixing, for which evidence is provided by both the reaction cross sections and the γ decay. This is in essential agreement with the new QPM calculations.

In summary, it can be stated that due to the improved experimental results and the more elaborate QPM calculations, our investigation constitutes a large step forward in our understanding of ^{166}Ho and more generally of odd-odd deformed nuclei.

Although a much better understanding of the ^{166}Ho nuclear structure has been obtained, there are some interesting aspects of various bands which are not yet fully understood, primarily concerning configuration (and other) mixing of bands. In order to refine our knowledge of the interactions involved, several suggestions can be made for extensions in both the experimental and theoretical portions of the study. There are two experiments that could be performed with currently-existing technology that stand good chances of improving the data base significantly. ^{166}Ho is one of the nuclides for which the GAMS spectrometers at ILL, Grenoble, have not been used to study secondary γ rays from the (n,γ) reaction [8,70]. The excellent resolution and precision of these instruments could well lead to significant improvements and/or extensions to the level scheme. Another project which should provide worthwhile information for understanding the band mixings would be to perform a (d,p) experiment with a complete angular distribution — e.g., at least 20 or 25 angles between reaction angles of 5° and 60°. If this were done with the very good resolution achieved in the present experiment it would be possible to extract spectroscopic strengths for competing l-values populating many of the levels. Results from both the (d,p) and (d,t) reactions have proven very useful in identifying components of two-quasiparticle configurations present in complex bands in other nuclides (e.g., ^{172}Yb [71] and ^{190,192}Ir [72,73]). It would be also important to determine absolute values for the cross sections, so that more meaningful comparisons with predicted values could be made without the uncertainty involved in choosing normalizations. On the theoretical side there are also important improvements which could be made in the model used for this study. The calculations should be extended to include predicted single-nucleon transfer cross sections or spectroscopic strengths for the mixed configurations. The comparisons in Tables X and XI considered only one component at a time in each band, and did not include possible interference effects between different configurations. Such effects are not likely to be large for most of the cases described above [an exception is the (d,p) population of the 592 keV band], but in an improved study which examined finer details these should be included. Another improvement, which is probably of greater importance for many bands, is that Coriolis mixing should be taken into account for both the level energies and the single-nucleon transfer cross sections. This is not an easy task because of the complicated wave functions of the mixed configurations in most of the bands. It is likely that some or all of these improvements will be necessary before one can achieve a detailed understanding of the structures of ^{166}Ho levels appreciably better than the one presented here.

ACKNOWLEDGMENTS

The authors from the Nuclear Research Center Salaspils, Latvia, thank the Volkswagenstiftung, Hannover, Germany, and the Latvian Scientific Council (Contract No. 96.0413) and thank their colleagues from the technical staff of the Salaspils reactor. M.B. wishes to thank Professor R.K. Sheline for fruitful discussions regarding the level scheme of ^{166}Ho. This work was supported, in part, by the Deutsche Forschungsgemeinschaft, Bonn (Eg 25/4, 436 LET 17/3/97) and the Beschleunigerlaboratorium der Universität und Technischen Universität München. Target preparation by P. Maier-Komor and K. Nacke is appreciated. This work was performed, in part, under the auspices of the U.S. Department of Energy by the Lawrence Livermore National Laboratory under Contract No. W-7405-ENG-48, by the Brookhaven National Laboratory under Contract No. DE-AC02-98-CH10886, and by Yale University under Contract No. DE-FG02-91-ER40609. This work was supported, in part, by the Grant Agency of the Czech Republic under Contract No. 202/97/K038. S.T.B., V.A.K., and A.M.S. would like to thank Dr. W.I. Furman for his help in organizing the measurement of high-energy-low-energy cascades in ^{166}Ho. D.G.B. acknowledges financial support from the Natural Sciences and Engineering Research Council of Canada. J.K. and A.M. would like to express gratitude for financial support by the Grant Agency of Czech Republic under Contract No. 202/96/1744.

[1] G.J. Gallagher and S.A. Moszkowski, Phys. Rev. **111**, 1282 (1958).
[2] N.D. Newby, Phys. Rev. **125**, 2063 (1962).
[3] D.M. Headly, R.K. Sheline, P.C. Sood, R.W. Hoff, I. Hřivnáčová, J. Kvasil, D. Nosek, A.K. Jain, and D.G. Burke, At. Data Nucl. Data Tables **69**, 239 (1998).
[4] J.P. Boisson, R. Piepenbring, and W. Ogle, Phys. Rep., Phys. Lett. **26C**, 99 (1976).
[5] H. Frisk, Z. Phys. A **330**, 241 (1988).
[6] D. Nosek, J. Kvasil, R.K. Sheline, P.C. Sood, and J. Noskova, Int. J. Mod. Phys. E **3**, 967 (1994).
[7] R.W. Hoff, A.K. Jain, J. Kvasil, R.K. Sheline, and R.W. Hoff, in *Exotic Nuclear Spectroscopy*, edited by W.C. McHarris (Plenum, New York, 1990), p. 413.
[8] A.K. Jain, R.K. Sheline, D.M. Headly, P.C. Sood, D.G. Burke, I. Hřivnáčová, J. Kvasil, D. Nosek, and R.W. Hoff, Rev. Mod. Phys. **70**, 843 (1998).
[9] H.T. Motz, E.T. Jurney, O.W.B. Schult, H.R. Koch, U. Gruber, B.P. Maier, H. Baader, G.L. Struble, J. Kern, R.K. Sheline, T. von Egidy, Th. Elze, E. Bieber, and A. Bäcklin, Phys. Rev. **155**, 1265 (1967).
[10] T.J. Kennett, M.A. Islam, and W.V. Prestwich, Phys. Rev. C **30**, 1840 (1984).
[11] G.L. Struble, J. Kern, and R.K. Sheline, Phys. Rev. **137**, B772 (1965).
[12] R.A. Dewberry, R.K. Sheline, R.G. Lanier, and R. Lasijo, Z. Phys. A **307**, 351 (1982).
[13] L.M. Bollinger and G.E. Thomas, Phys. Rev. C **2**, 1951 (1970).
[14] J.J. Bosman and H. Postma, Nucl. Phys. **A320**, 260 (1979).
[15] M.K. Balodis, A.V. Afanasjev, P.T. Prokofjevs, and J.J. Tambergs, Izv. Akad. Nauk SSSR, Ser. Fiz. **52**, 2117 (1988).
[16] R.G. Helmer and S.B. Burson, Phys. Rev. **119**, 788 (1960).
[17] V. Brabec, O. Bergman, Y. Grunditz, E. Aasa, and S.E. Karlsson, Ark. Fys. **26**, 511 (1964).
[18] S. Bjornholm, J. Borggreen, H.J. Frahm, N.J.S. Hansen, and O. Schult, Phys. Rev. **140**, B816 (1965).
[19] E.N. Shurshikov and N.V. Timofeeva, Nucl. Data Sheets **67**, 45 (1992).
[20] P.E. Sood, R.K. Sheline, and R.S. Ray, Phys. Rev. C **35**, 1922 (1987).
[21] R.K. Sheline, P.C. Sood, Baluba Mutshil, Butsana bu Nianga, and Lufungula Nkwambiaya, Phys. Rev. C **40**, 1065 (1989).
[22] P.E. Sood and D.G. Burke, Phys. Rev. C **51**, 2226 (1995).
[23] M.K. Balodis, J. Alksnis, and J.J. Tambergs, ''13th Symposium on Nuclear Spectroscopy and Nuclear Theory,'' Dubna (1973), Report No. JINR D6-7094 (1973), p. 116.
[24] M.K. Balodis, Latv. PSR ZA Vestis, fiz. tehn. zin. ser. **3**, 6 (1978).
[25] M.K. Balodis, J. Berzins, V. Bondarenko, P. Prokofjevs, and A.V. Afanasjev, in *Capture Gamma-Ray Spectroscopy and Related Topics*, edited by J. Kern (World Scientific, Singapore, 1994), p. 268.
[26] J. Kvasil, R.K. Sheline, V.O. Nesterenko, I. Hřivnáčová, and D. Nosek, Z. Phys. A **343**, 145 (1992).
[27] R.C. Greenwood and R.E. Chrien, Nucl. Instrum. Methods **138**, 125 (1976).
[28] M.L. Stelts and R.E. Chrien, Nucl. Instrum. Methods **155**, 253 (1978).
[29] A.H. Wapstra and G. Audi, Nucl. Phys. **A432**, 1 (1985).
[30] R.E. Chrien, in *Capture Gamma-Ray Spectroscopy and Related Topics*, Proceedings of the Fifth International Symposium, edited by S. Raman, AIP Conf. Proc. 125 (AIP, New York, 1984), p. 342.
[31] J. Honzátko, K. Konečný, I. Tomandl, J. Vacík, F. Bečvář, and P. Cejnar, Nucl. Instrum. Methods Phys. Res. A **376**, 434 (1996).
[32] S.T. Boneva, E.V. Vasilieva, Yu.P. Popov, A.M. Sukhovoj, and V.A. Khitrov, Fiz. Elem. Chastits At. Yadra **22**, 479 (1991) [Sov. J. Part. Nucl. **22**, 232 (1991)].
[33] A.M. Sukhovoj and A.M. Khitrov, Instrum. Exp. Tech. (USSR) **27**, 1071 (1984).
[34] M. Löffler, H.J. Scheerer, and H.K. Vonach, Nucl. Instrum. Methods **111**, 1 (1973).
[35] J. Ott, H. Angerer, T. von Egidy, R. Georgii, and W. Schauer, Nucl. Instrum. Methods Phys. Res. A **367**, 280 (1995).
[36] B. Elbek and P.O. Tjøm, in *Advances in Nuclear Physics*, edited by M. Baranger and E. Vogt (Plenum, New York, 1969), Vol. 3, p. 259.
[37] D.G. Burke, G. Kajrys, and D. Beachey, Nucl. Phys. **A492**, 68 (1989).
[38] D.G. Burke, P.C. Sood, P.E. Garrett, Tao Qu, R.K. Sheline, and R.W. Hoff, Phys. Rev. C **47**, 131 (1993).
[39] P.D. Kunz, Computer program DWUCK4, University of Colorado, 1993.
[40] C.M. Perey and F.G. Perey, Phys. Rev. **132**, 755 (1963).
[41] F.D. Becchetti and G.W. Greenlees, Phys. Rev. **182**, 1190 (1969).
[42] M.T. Lu and W.P. Alford, Phys. Rev. C **3**, 1243 (1971).
[43] I.-L. Lamm, Nucl. Phys. **A125**, 504 (1969).
[44] R.W. Hoff, S. Drissi, J. Kern, W. Strassmann, H.G. Börner, K. Schreckenbach, G. Barreau, W.D. Ruhter, L.G. Mann, D.H. White, J.H. Landrum, R.J. Dupzyk, R.F. Casten, W.R. Kane, and D.D. Warner, Phys. Rev. C **41**, 484 (1990).
[45] V.G. Soloviev, Phys. Lett. **21**, 320 (1966).
[46] N.I. Pyatov, Izv. Akad. Nauk SSSR, Ser. Fiz. **27**, 1436 (1963) (in Russian).
[47] L. Benour, J. Libert, M. Meyer, and P. Quentin, Nucl. Phys. **A465**, 35 (1987).
[48] A.V. Afanasjev and I. Ragnarsson, Phys. Rev. C **51**, 1259 (1995).
[49] A.K. Jain, J. Kvasil, R.K. Sheline, and R.W. Hoff, Phys. Rev. C **40**, 432 (1989).
[50] P.C. Sood, D.M. Headly, and R.K. Sheline, At. Data Nucl. Data Tables **47**, 89 (1991).
[51] V.G. Soloviev, V.O. Nesterenko, and S.I. Bastrukov, Z. Phys. A **309**, 353 (1983).
[52] A.V. Afanasjev, T.V. Guseva, and Yu.Yu. Tamberg, Izv. Akad. Nauk SSSR, Ser. Fiz. **52**, 130 (1988).
[53] A.B. Balantekin, I. Bars, and F. Iachello, Phys. Rev. Lett. **47**, 19 (1981).
[54] W.T. Chow, W.C. McHarris, and O. Sholten, Phys. Rev. C **37**, 2834 (1981).
[55] V. Paar, Nucl. Phys. **A331**, 16 (1979).
[56] S. Brant, V. Paar, D. Vretenar, G. Alaga, H. Seyfarth, O. Schult, and M. Bogdanovic, Phys. Lett. B **195**, 111 (1987).
[57] I. Hřivnáčová, J. Kvasil, D. Nosek, and R.K. Sheline, Phys. Scr. **T56**, 256 (1995).

[58] V.G. Soloviev, *Theory of Complex Nuclei* (Nauka, Moscow, 1971) (transl. Pergamon, Oxford, 1976).
[59] S.G. Nilsson, C.F. Tsang, A. Solczenski, Z. Szymanski, S. Wycech, C. Gustavson, I.-L. Lamm, P. Möller, and B. Nilsson, Nucl. Phys. **A131**, 1 (1969).
[60] J. Kvasil, N. Lo Iudice, V.O. Nesterenko, and M. Kopal, Phys. Rev. C **58**, 209 (1998).
[61] C.J. Gallagher and V.G. Soloviev, K. Dan. Vidensk. Selsk. Mat. Fys. Skr. **2**, No. 2 (1962).
[62] A.K. Jain, R.K. Sheline, P.C. Sood, and Kiran Jain, Rev. Mod. Phys. **62**, 393 (1990).
[63] R.W. Hoff, H.G. Börner, K. Schreckenbach, G.G. Colvin, F. Hoyler, W. Schauer, T. von Egidy, R. Georgii, J. Ott, S. Schründer, R.F. Casten, R.L. Gill, M. Balodis, P. Prokofjevs, L. Simonova, J. Kern, V.A. Khitrov, A.M. Sukhovoj, O. Bersillon, S. Joly, G. Graw, D. Hofer, and B. Valnion, Phys. Rev. C **54**, 78 (1996).
[64] K.D. Schilling, L. Kaubler, W. Andrejscheff, T.M. Muminov, V.G. Kalinnikov, N.Z. Marupov, F.R. May, and W. Seidel, Nucl. Phys. **A299**, 189 (1978).
[65] H.D. Jones, N. Onishi, T. Hess, and R.K. Sheline, Phys. Rev. C **3**, 529 (1971).
[66] T. Grotdal, K. Nybø, and B. Elbek, K. Dan. Vidensk. Selsk. Mat. Fys. Medd. **37**, 12 (1970).
[67] P.O. Tjøm and B. Elbek, K. Dan. Vidensk. Selsk. Mat. Fys. Medd. **37**, 7 (1969).
[68] D.G. Burke, B. Zeidman, B. Elbek, B. Herskind, and M. Olesen, K. Dan. Vidensk. Selsk. Mat. Fys. Medd. **35**, 2 (1966).
[69] R.W. Hoff, in *Proceedings of the IV International Conference on Selected Topics in Nuclear Structure*, edited by V.G. Soloviev (Dubna, Russia, 1994), p. 183.
[70] R.W. Hoff, in *Capture Gamma-Ray Spectroscopy and Related Topics*, edited by J. Kern (World Scientific, Singapore, 1994), p. 132.
[71] D.G. Burke, V.G. Soloviev, A.V. Sushkov, and N.Yu. Shirikova, Nucl. Phys. **A656**, 287 (1999).
[72] P.E. Garrett and D.G. Burke, Nucl. Phys. **A581**, 267 (1995).
[73] P.E. Garrett and D.G. Burke, Nucl. Phys. **A568**, 445 (1994).
[74] W. Michaelis, F. Weller, H. Schmidt, G. Markus, and U. Fanger, Nucl. Phys. **A119**, 609 (1968).
[75] S. Daava, T.I. Kracikova, M. Finger, J. Kvasil, V.I. Fominykh, and W.D. Hamilton, J. Phys. G **8**, 1585 (1982).
[76] V.G. Soloviev, V.O. Nesterenko, and S.I. Bastrukov, Z. Phys. A **309**, 353 (1983).